[Corrected Copy]

Study Of Dynamical Aspects Of Some Class Of ODEs And PDEs

Thesis submitted for the degree of
Doctor of Philosophy (Science)
in
Physics (Theoretical)

by

ANKAN PANDEY

Department of Physics
University of Calcutta

2021

Dedicated to

Family and Friends

Acknowledgement

I wish to express my sincere thanks to my supervisor, Prof. Partha Guha for his supervision and guidance during my Ph.D. I have learnt a lot from him and I am really thankful for his valuable inputs and insights without which this thesis would not have been possible. I would also like thank the library services for nice collection of books, computer section for various computational help, cleaning staff, as without a clean environment research couldn't be done peacefully.

I would also like to acknowledge prof. Jayant K Bhatttacharya, prof. Deb Shankar Ray, prof. Gautam Gangopadhyay, prof. A Ghose-Choudhury, prof. Rajib Mitra for their help and deep insights which directly or indirectly influence my understanding of the subject.

I should also acknowledge various seminars I attended and would emphasise on the role they play in cultivating a robust research environment.

I also want to thank Ashutosh, Arup, Ravi, Ransell, Shaili, Dhani, Chandrayee, Poonam, Ritam, Anirban, Sandip, Shishir and Balwant for contributing towards making these years at S. N. Bose memorable.

Finally, I would like to express my love and gratitude to my family. I am grateful to my parents, brother for their unconditional love, support and respect for my decisions and choices.

Ankan Pandey

List Of Publications

1. **Ankan Pandey**, A Ghose-Choudhury, and Partha Guha. Chiellini integrability and quadratically damped oscillators. *International Journal of Non-Linear Mechanics*, 92:153-159, 2017.

2. **Ankan Pandey**, A Ghose Choudhury, and Partha Guha. Quadratically damped oscillators with non-linear restoring force. *arXiv preprint arXiv:1610.07821*, 2016.

3. **Ankan Pandey**. Forced coupled duffing oscillators with nonlinear damping: Resonance and antiresonance. *arXiv preprint arXiv:1909.11390*, 2019.

4. **Ankan Pandey**, Mainak Mitra, A Ghose-Choudhury, and Partha Guha. On coupled delayed van der pol-duffing oscillators. *Journal of Applied Nonlinear Dynamics*, 9(4), 2020.

5. A Ghose-Choudhury, Aritra Ghosh, Partha Guha, and **Ankan Pandey**. On purely nonlinear oscillators generalizing an isotonic potential. *International Journal of Non-Linear Mechanics, 106:55-59*, 2018.

List of Figures

1.1 Illustration of nonlinear systems. 4

2.1 Description of linear stability analysis. 15

3.1 Phase plots showing the existence of a center for two different combinations of $f(x)$ and $g(x)$ for multiple initial conditions. 27

3.2 Phase plots for the system described by (3.12) and (3.13) when (a) $f(x) = 0.5$ and $g(x) = x$ showing the spiralling nature of the trajectory and (b) $f(x) = 3x$ and $g(x) = x + x^3$ for which the orbits are closed. 29

3.3 Plots of the potentials $V^{\pm}(x)$ for the system in (3.12) and (3.13) when $f(x) = 0.5$ and $g(x) = x$ in (a, b) and when $f(x) = 3x$ and $g(x) = x + x^3$ in (c, d). 30

3.4 Contour plots of Hamiltonian of (3.12), (3.13) defined (3.14) for different combinations of $f(x)$ and $g(x)$. 31

3.5 Phase space plots of the system (3.12) and (3.13) for higher degree polynomial $f(x)$ and $g(x)$: (a) when $f(x) = x^2, g(x) = x^5$ and (b) when $f(x) = x^3, g(x) = x^7$ showing the spiral nature of the trajectory for even f and the closed orbits for odd f. 31

4.1 Phase space plots for odd-power restoring force ($g(x) = x^3$) with a) odd damping coefficient, $f(x) = x$, showing closed orbits for different initial conditions, and b) even damping coefficient, $f(x) = 1$, showing damp orbit. 55

4.2 Energy variation with displacement for odd-power restoring forces, $g(x) = x^3$ with a) even damping coefficient, $f(x) = 1$), and b) odd damping coefficient, $f(x) = x$. 57

4.3 Phase-space plots for even-power restoring force, $g(x) = x^2$ with a) odd damping coefficient function, $f(x) = x$, showing center orbits, and b) even damping coefficient function, $f(x) = 1$, showing damped orbits. 57

4.4 Energy-displacement curve for even-power restoring force ($g(x) = x^2$) with a) even damping coefficient function ($f(x) = 1$), and b) odd damping coefficient function ($f(x) = x$). 59

5.1 Numerical simulation of Fractional Harmonic Oscillator (5.2) for $w = \sqrt{2}$ and $\gamma = \{1, 0.9, 0.45\}$. The figure shows contrasting behaviour of the oscillator for different order of derivatives: oscillation for $\gamma = 1.0$ (solid line); underdamped oscillation for $\gamma = 0.9$ (dashed line); overdamping for $\gamma = 0.45$ (dot dashed line). 74

5.2 Phase portrait of Fractional Van der Pol (5.7) for $w = 1.0$, $\alpha = 0.5$. The subplots a) $\epsilon = 1.5$, showing limit cycle corresponding to the unstable origin, and b) $\epsilon = 1.3$, showing stable origin. 76

5.3 Stability region of in-phase solution $u(t)$ in $\alpha - \gamma$ parameter space. The shaded parts are stable regions of the limit cycle for a) $b = -0.15$, and b) $b = 0$. Dashed line represents the condition $tr(M) = 0$ which denoted the critical line of Hopf bifurcation and solid lines represents $det(M) = 0$. . . 79

5.4 The plot shows the variation of delay with coupling coefficient for values $\omega = 1.0$, $k = 0.1$, with $n = \{1, 2, 3, 4\}$ for T_+ and $n = \{1, 2, 3\}$ for T_-. . . . 88

5.5 The plot shows time series of system (5.36,5.37) for parameters $\omega = 1.0$, $k = 0.1$, $\lambda = -0.1$, $\alpha = 1.5$ and $T = 2.7$, & $T = 7.2$ denoting the stability of origin and limit cycle, respectively. 89

6.1 Amplitude Frequency Response of amplitudes A (of oscillator-x)(in blue) and B (of oscillator-y)(in red). Three sub-plots are for different damping exponents: a) $p = 0$; b) $p = 1$; c) $p = 2$. Continuous line represents theoretical predictions and solid circles and triangles are data points of numerically calculated amplitudes of A and B, respectively. The parameter settings are: $d = 1$, $b = 1$, $\alpha = 4$, $F = 1$, $\epsilon = 0.1$. 100

6.2 The dependence of dips on coupling parameter α for damping exponents $p = 0, 1, 2$. Antiresonance values for a) oscillator-x (amplitude A); b) oscillator-y (amplitude B). The data points are numerically computed points and continuous lines are trend lines. Shows separation between the three exponents for small α and convergence for large α values. The parameter settings are: $d = 1$, $b = 1$, $\alpha = 4$, $F = 1$, $\epsilon = 0.1$. 101

6.3 The dependence of resonant frequencies on coupling parameter α for damping exponents $p = 0, 1, 2$. Resonance values for a) oscillator-x (amplitude A); b) oscillator-y (amplitude B). The data points are numerically computed points and continuous lines are trend lines. The two branches, below and above $\omega = 1$, belongs to two resonances for each oscillator. The parameter settings are: $d = 1$, $b = 1$, $\alpha = 4$, $F = 1$, $\epsilon = 0.1$. 102

6.4 The dependence of resonant peaks on coupling parameter α for damping exponents $p = 0, 1, 2$. Resonance values for a) oscillator-x (amplitude A); b) oscillator-y (amplitude B). The data points are numerically computed points and continuous lines are trend lines. The two branches, below and above $\omega = 1$, belongs to two resonances for each oscillator. The parameter settings are: $d = 1$, $b = 1$, $\alpha = 4$, $F = 1$, $\epsilon = 0.1$. 103

6.5 Stability analysis of amplitude-phase equation (6.6). The unstable values are shown in red and stable with blue. Each row corresponds to $p = 0$, $p = 1$, $p = 2$ and shows stability of amplitudes A and B. The parameter settings are: $d = 1$, $b = 1.5$, $\alpha = 4$, $F = 1$, $\epsilon = 0.1$. 104

6.6 Phase-frequency response of oscillator-x. a)The phase response of oscillator-x is given for all damping exponents. Amplitude response for $p = 1$ is given gray to correlate the response events. This response is given for $p = 2$. b) Phase response of oscillator-y for all the damping exponents. The parameter settings are: $d = 1$, $b = 1$, $\alpha = 4$, $F = 1$, $\epsilon = 0.1$. 104

6.7 Amplitude response of (6.10) for damping exponent $p = 0$. The plots are obtained using theoretical predictions. The subplots shows the response for different values of ω mentioned in the caption of each subplot. The two resonance corresponds to equilibriums X_0, and $X_\pm$. The parameter settings are: $a = 1.0$, $b = 1.0$, $d = 0.05$, $F = 0.01$, $\Omega = 10.0$ 110

6.8 Vibrational Resonance position variation with respect to ω for $p = 0$. The plot is obtained using theoretical predictions. The continuous curve shows the variation of resonance position corresponding to the equilibrium state X_0 and dashed curve shows the variation corresponding to the equilibrium states $X_\pm$. The parameter settings are: $a = 1.0$, $b = 1.0$, $d = 0.05$, $F = 0.01$, $\Omega = 10.0$ 111

6.9 Variation of resonance value with respect to ω for $p = 0$. The plot is obtained using theoretical predictions. The continuous curve shows the variation of resonance value corresponding to the equilibrium state X_0 and dashed curve shows the variation corresponding to the equilibrium states $X_\pm$. The parameter settings are: $a = 1.0$, $b = 1.0$, $d = 0.05$, $F = 0.01$, $\Omega = 10.0$ 111

6.10 Amplitude response of (6.10) for damping exponent $p = 1$. The plots are obtained using theoretical predictions. The subplots shows the response for different values of ω mentioned in the caption of each subplot. The two resonance corresponds to equilibriums X_0, and $X_\pm$. The parameter settings are: $a = 1.0$, $b = 1.0$, $d = 0.05$, $F = 0.01$, $\Omega = 10.0$ 112

6.11 Vibrational Resonance position variation with respect to ω for $p = 1$. The plot is obtained using theoretical predictions. The continuous curve shows the variation of resonance position corresponding to the equilibrium state X_0 and dashed curve shows the variation corresponding to the equilibrium states $X_\pm$. The parameter settings are: $a = 1.0$, $b = 1.0$, $d = 0.05$, $F = 0.01$, $\Omega = 10.0$ 113

6.12 Variation of resonance value with respect to ω for $p = 1$. The plot is obtained using theoretical predictions. The continuous curve shows the variation of resonance value corresponding to the equilibrium state X_0 and dashed curve shows the variation corresponding to the equilibrium states $X_\pm$. The parameter settings are: $a = 1.0$, $b = 1.0$, $d = 0.05$, $F = 0.01$, $\Omega = 10.0$ 113

List of Tables

3.1 Values for the amplitudes in each half cycle when $f(x) = 0.5$ and $g(x) = x$ for the system described by (3.1) and (3.2). 29

3.2 Time periods and the corresponding changes in the energy in each cycle when $f(x) = 0.5$. 34

3.3 Time periods of the cycles when $f(x) = 3x$ for different initial conditions. . 34

4.1 Change in Hamiltonian and Energy in each complete cycle in example 1 $(f(x) = 1,\ g(x) = x^3)$. 60

4.2 Change in Hamiltonian and energy in each complete cycle in example 2 $(f(x) = x,\ g(x) = x^3)$. 60

6.1 List of corrections. 119

Contents

Table of Contents vi

List of Figures xi

List of Tables xiii

1 Introduction 1

1.1 Basic Outline of Nonlinearities 4

2 Background and Methods 13

2.1 Basic Concepts of Dynamical Systems 13

2.2 Analytical Methods for NODE 16

2.3 Numerical Methods for NODE 18

3 Nonlinear Damping 23

3.1 Chiellini Integrability and Quadratically Damped Oscillators 23

3.2 The Hamiltonian in presence of quadratic velocity 25

3.3 Quadratic damping 27

3.3.1 Closed and Damped Orbits 28

3.3.2 Analytic results based on Chiellini integrability condition 32

3.3.3 Analysis of the period function 33

3.3.4 Analytic Solutions 34

3.4 Conclusion 35

A Lambert W Functions 41

A.1 Introduction 41

4 Strongly Nonlinear Oscillators 43

4.1 Nonlinear Oscillator: $\ddot{x} + c_\alpha^2 sgn(x)|x|^\alpha = 0$ . . . 44
4.1.1 Time period using Symmetrization Procedure . . . 45
4.2 On Generalised Isotonic Potential . . . 47
4.2.1 Isotonic Potential: A brief recap and time-period calculation . . . 47
4.2.2 Generalised Isotonic potential . . . 50
4.2.3 Conclusion . . . 54
4.3 Oscillators with non-negative real-power restoring force and quadratic damping . . . 54
4.3.1 The Hamiltonian structure of the system . . . 59
4.3.2 Conclusion . . . 60
4.4 Summary . . . 61

B Ateb Functions **67**

5 History Dependent Nonlinearities **71**
5.1 Fractional Dynamical System . . . 71
5.1.1 Fractional Oscillators . . . 73
5.1.2 Conclusion . . . 79
5.2 Delay Dynamical System . . . 80
5.2.1 Delay Coupled van der pol-Duffing (VDP-D) Oscillators . . . 81
5.3 Summary . . . 89

6 Damped Forced Nonlinear Oscillators **97**
6.1 Forced Coupled Duffing Oscillators with Nonlinear Damping: Resonance and Antiresonance . . . 97
6.1.1 Periodically driven coupled Duffing oscillator . . . 98
6.1.2 Discussion and Conclusion . . . 102
6.2 Nonlinear Systems Under Multiple Forcing - Vibrational Resonance . . . 103
6.2.1 The System . . . 105
6.2.2 Theoretical Analysis . . . 105
6.2.3 Conclusion . . . 112
6.3 Summary . . . 113

Chapter 1

Introduction

Dynamical systems are, basically, systems whose state evolve with time (or with some other parameter). Examples of such systems include regular motion of our daily life like motion of cars or other vehicles, motion of human body. It cut across the scales and defines the dynamics from the movement of huge planets, stars, and other celestial bodies which defines the "daily", to the dynamics in the realm of small particles where classical laws no longer holds. In applications it blurs the boundary between physics and other subjects while modelling various phenomenons. This can be seen in the oscillating chemical reactions, or in the stripe patterns of zebra, or in periodic patterns in economics. This way dynamical system approach provides a mechanical description of various processes while exposing the complex nature behind it. This physical description maps the complexity of such phenomenons to a subtle picture from a physical perspective. For such reasons and for the purpose of this thesis I will consider a physical approach for explaining various systems and their dynamics.

Dynamical systems comprises of a dynamical unit, state space of the dynamical unit, and a time parameter. The dynamical unit could be physical objects like electrons, atoms, cells, cars, celestial bodies etc., or abstract quantities like temperature, density, qubits, intensity of waves etc. The state space is a set of values that the dynamical unit can acquire during the evolution. This can be a continuous space such as in the dynamics of vehicle where the vehicle can have any position and velocity in a range, or it can be discrete like in the case of qubits or a motion of a particle in a lattice. The evolution refers to change in state of the system and is with respect to time, in general, however, this could be any independent variable of the system. For example, the evolution of density with respect to the temperature can be considered as a dynamical system as well. This evolution can also be continuous or discrete depending on how one is registering a change. A continuous change is more intuitive and is visible more often. Examples of continuous changes can be motion of planets, movement of particles etc,. Discrete changes are not so subtle, however, they have applications in many systems. A most common occurrence is in the stroboscopic study of any continuous system where the changes in the state of continuous system at particular time instances are analyzed. Apart from this, they are quite apparent in the stock prices which are recorded in discrete time.

The concepts and methods of dynamical system has evolved through time. Humans from prehistoric times have a keen sense observing different motions which are because of evolutionary needs, such as hunting, or some other reasons. This curiosity led humans to discover various machines with simple dynamics like cart wheel etc,. But this idea of mechanics was still lacking the mathematical formulation to theorize various methods. This formulation was first done by the great Newton in the form of Newtonian mechanics. Newtonian mechanics, basically, tells that the acceleration of any body is proportional to the applied force on that body using second order differential equation. This laid the founding stone of the subject of Dynamical Systems.

But, what does this mathematical formulation of dynamics looks like? In general, the governing equations of dynamical systems can be represented by either differential equations defining the dynamics of continuous independent variables or difference equations or iterative maps where the dynamics is observed over discrete independent variables, [1, 2]. Both the types have been rigorously studied since the emergence of dynamical system and tons of volumes have been dedicated to discuss the methods and applications of such equations. For difference equations the dynamical unit evolves in discrete time steps where the next state of the unit is defined according to some function. A very popular example of such equation is logistic map where the iterative steps are in terms of logistic function of current state. Such equations have applications in population dynamics and a typical equation to study *chaos*, [2]. Differential equations, on the other hand, deals with dynamics over continuous time steps as in the Newtonian dynamics. Dynamics in science and engineering often require continuous variables whose variations are studied over continuous time steps, [2, 3, 4, 5]. Hence, differential equations are the most common employee in such applications some of which may be discussed in the course of this thesis. It needs to be stated that there are more applications than equations and often single dynamical equation is used to model multiple phenomenons. For example, duffing equation defined by George Duffing,[6], contains quadratic and cubic nonlinear (defined later) term and is used to approximate the motion of a pendulum as well as to model the stiffness of spring which does not obey Hooke's law, [7]. Moreover, it is also used to model many bistable systems in various biological and chemical models, and is often considered to study chaotic dynamics. Similarly, one can find logistic equation is various roles in different context, from population dynamics to tumor growth. Following this train of thoughts one tends to define a class of differential equations which defines multiple dynamical phenomenons. This class is not a mathematical construct, however, it is defined so as to classify certain mathematical quantities based on some criteria to understand the corresponding dynamics these quantities generate. To the extent of extracting and exploiting the dynamical features of such differential equations there are various methods, both analytic as well as numerical, which needs to be studied. These studies forms the subject matter of this thesis.

Now, to make sense it is important to answer two questions - what is this classification based on?, and What does one mean by dynamical aspects of differential equations? To address the first question, we need to consider the dynamical system from an operational perspective. In the operational picture, dynamical system, represented by differential equations, works as a process which takes some initial states as input then perform some mathematical operations and gives the output state in a given time interval. Now, to

define our classification criteria consider the relationship between the input states and the output states. There is a set of systems for which the output states are proportional to the input to the system. These are called linear systems. Equation of simple harmonic oscillator is the classical example of linear systems. For linear systems any changes in the input states is proportionally reflected in the output state. This generates a very monotonous dynamics. Many simple dynamics belongs to this set of dynamics like motion along a straight line with constant acceleration or small deformations of spring. However, these linear systems are not very efficient in modelling physical systems and are only a simplified approximations to physical phenomenons as the simple harmonic motion is only a linear approximation of the pendulum equation which is used to model the motion of a swinging pendulum. Physical systems are, in general, nonlinear in nature. In nonlinear systems the output state is a function of the input which may or may not be proportional to the input state. In pendulum equation the acceleration of the angular displacement depends on the sine of angular displacement which is the source of the nonlinearity.

Physical modelling of systems contains multiple components which plays different roles in the dynamics of the system. For example, the compression of springs results in a potential which when released apply force on the connected body. Similarly, the interaction of a system with the outside environment results in exchange of energy which gives rise to damping and forcing in the system dynamics. These different components are represented in the equation in different forms. These forms can be linear or nonlinear depending on the complexity of the system. Hence, there are, usually, multiple sources of nonlinearities in the system. In this thesis, a set of such nonlinearities are considered which will be the basis of the classification for various studies.

Now coming to the next question, the concept of dynamical aspects of differential equations has been part of tons of textbooks, and may be a title of few. A simple explanation would tell that it deals with the question of how the trajectories of the dynamical unit evolves with time?. However, since the advent of the subject the understanding of the subject has developed manifolds. From pioneers of dynamical systems, Poincarè, Lyapunov, Birkhoff, Smale etc., to later years developers, Nayfeh, Balachandran, Strogatz and many others, various theories have been developed which has enhanced the understanding about the subject. However, a brief introductory description of the dynamical aspects, which are more relevant to the cause of this thesis, are discussed in **chapter 2** and, as per requirement, in later chapters too.

Dynamical aspects varies for different types of dynamical systems. For linear systems, the dynamical aspects are simple, monotonous and isotropic in nature. This fails to encapsulate the complexity of a general physical phenomenon. Nonlinearity, from various sources and in different forms, incorporates such complexities in the system and assist in explaining the scientific nature of the phenomenon. To understand this, recall the operational picture of dynamical systems. In nonlinear systems, the mathematical operations involves many feedback loops which changes the effective inputs and corresponding outputs. This feature becomes visible in the perturbation analysis of differential equations in various case studies in this thesis. A brief introduction of basics of various perturbation theories employed in the work is given in **chapter 2**.

Differential equations can also be of multiple forms. This may depend on the number of independent variables with respect to which the differentiation is done. Equations with single independent variable are referred to as ordinary differential equations (ODEs). ODEs are defined for the dynamics of 1-dimensional systems and shall be part of major portion of the thesis. When there are more than one independent variables are involve, they are called partial differential equations (PDEs). They define dynamics when there is a dependence on more than on space variable, like in 2D systems, or when there is both spatial as well as time variations are involved. They have vast range of applications in reaction-diffusion systems, [8, 9], in hydrodynamic equations, [10, 11, 11, 12], thin films, [13, 14] and many more. They are not directly involved in any case studies, however, the methods and techniques used in the thesis are completely applicable to such equations. In practise, PDEs are converted to ODEs through a travelling wave transformation where the dynamics of the system is observed from the wave frame of reference.

Other forms of differential equations can be based on the way they are defined. An important class of differential equations employed in this thesis is fractional differential equations (FDEs). They are defined by relating the functions of dependent variables and their fractional derivatives. Fractional derivatives, in contrast to regular derivative where the order of derivatives are always integers, gives fractional order differentiation of the functions. They are discussed in more details in later parts of this chapter and in further in **chapter 5**.

1.1 Basic Outline of Nonlinearities

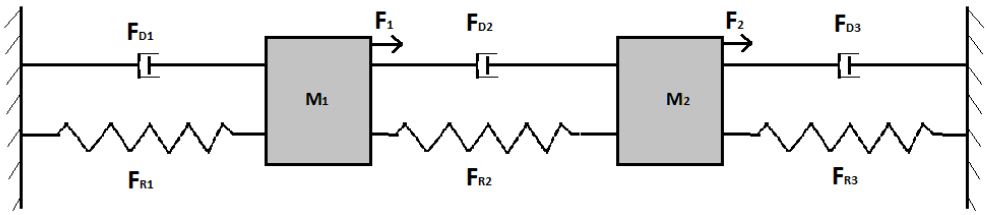

Figure 1.1: Illustration of nonlinear systems.

Differential equations gives a relation between a dependent variable and its derivatives. This relation could be linear or nonlinear based on the physics of the system. In physical modelling, the equations have certain structures or components which have there own origin and roles in governing the dynamics. Figure 1.1 shows a general illustration of nonlinear system. The illustration is done using a spring-mass system, however, such generalised illustrations could be done using electronic circuits, pendulum system, interacting particle system etc. The system shows two masses, M_1 & M_2, attached to a fixed support through different springs and dampers, and which are also connected to each other though another spring and a damper. Analysing each components of this system shall form the basis for the nonlinear systems considered in this thesis.

The equations of motion of the system in figure 1.1 are given as

$$\begin{aligned} M_1\ddot{x_1} + F_{D1} + F_{R1} &= F_{D2} + F_{R2} + F_1, \\ M_2\ddot{x_2} + F_{D3} + F_{R3} &= -F_{D2} - F_{R2} + F_2, \end{aligned} \tag{1.1}$$

where x_1, x_2 denote the displacement of M_1 and M_2, respectively, and the dots above them denote derivative with respect to time. In the equation F_{D1}, F_{D3} denote the damping in each connection, F_{R1}, F_{R3} denote the forces derived from an arbitrary potential acting on the respective masses, and F_1, F_2 are external forces applied on respective masses. Further, the masses coupled through F_{D2} and F_{R2}.

First consider a single spring-mass system without any coupling or external force. The corresponding dynamics have three important components - mass and acceleration, damper, and the potential force. The forces derived from potentials are functions of the variable alone and can be both- linear and nonlinear. The potential determines the constraint on the energy the system can stay upto. In the linear system this restoring force is proportional to the displacement which pull the mass towards the equilibrium at the bottom. In physics, this is called Hooke's law, [7]. It guides the relation between the stress and strain of spring as long as the deformation is small which varies for different materials. The modern theory of elasticity is an extension of Hooke's law in way of relating the stress-strain relationship of any material. As the displacement increases the molecular arrangement/alignment inside the material changes which makes the spring hard or soft, depending on the material. Hence, Hooke's law first-order linear approximation fails and the force becomes nonlinear in nature.

Linear systems, although an approximation, have diverse applications in science such as in acoustic, [15], material science, [16], seismology,[17], and others. In elastic materials such as alloys, [18, 19], aircraft materials, [20], polymers, [21], etc., the restoring forces are strongly nonlinear in nature. To analyze such systems the physical modelling is done by considering the restoring force of the form x^n, for arbitrary real n values, [22]. For such systems there are no general method to obtain exact solutions and as these are strongly nonlinear, the usual treatments, like linearisation or perturbation methods, are applicable. These kinds of potential functions are consider in **chapter 4** where some non-trivial methods are discussed for qualitative analysis of such systems.

Nonlinear restoring forces can have multiple steady states which often impacts the basins of attraction of each other. The dynamics in such settings results in non-trivial phenomenons. These nonlinearities could be both algebraic as well as transcendental in nature. Duffing potential, also Duffing oscillator, is one of the most important of and widely applied nonlinear restoring force. It has application across science and engineering problems like vibrating beams, [6], nano-rods, [6], nonlinear isolators, [23], material stiffness etc. The Duffing potential is given as, $V(x) = a\frac{x^2}{2} + b\frac{x^4}{4}$, where a and b are real parameters. Duffing oscillator can have three or a single steady state based on the parameters a, & b. It is known to show chaotic behaviour when under external force, [24], hardening and softening or mixed frequency response, [6], jump phenomenon, [6] etc. Given its utility, Duffing potential is going to be in many part of this theses.

It is often desirable in physical applications to have systems which can conserve its energy or atleast minimize its energy dissipation. Unfortunately, laws of nature are not interested in our desires and, in general, total conservation of energy is not possible (thermodynamic issues) and, hence, dissipation of energy becomes an intrinsic part of the system. With the development of various technologies systems are becoming more energy efficient. Similar advancements are also taking place in theoretical development of the dynamical system theory to cope with this problem. On the other hand, there are certain situations when dissipation is desirable to counter unwanted motion from outside, for example, to suppress the vibrations in skyscrapers caused by earthquakes or other ground shaking activities, [25].

The dissipation in physical systems results in the damping of the motion of its parts which ultimately halt the system and in a more complex scenario it may lead to more catastrophic consequences. The damping in system (1.1) is of general form and can be linear or nonlinear. Linear damping or viscous damping is often used in modelling for slow motions. Initially, linear damping was able to model the damping in physical systems. However, with various developments in the engineering science the demand to understand and model structural designs and other dynamic phenomenons coerced the practitioners to shift their attention to the damping nature of the system. Soon theorists starts to employ nonlinear sources to explain the complex behaviours in the vibration of the beams. This leads to the understanding that usual dynamics contains both linear as well as nonlinear component, however, nonlinear component is not much relevant for small amplitudes. But as the oscillation amplitude increases the role of nonlinear damping becomes significant. Analogous to the restoring force, linear damping is a simplified approximation and damping in physical scenarios are essentially nonlinear in nature. Such nonlinear form of damping finds space in many research studies such as in the rolling motion of ships, [26, 27, 28], NEMS and MEMS, [29, 30], in rotor dynamics, [31, 32], in building applications, [33, 34], and many other, [35, 36]. Apart from this, many experimental and numerical studies have been conducted to identify the damping structure of the system, [32, 33, 37, 38].

Nonlinear damping brings out many significant features which are not possible in linear settings. Linear damping in dynamical systems leads to dissipation of energy from the system in a an exponential manner and are inconsequential to any other events in the dynamics. Damping, however, is, in general, a function of the first derivative of the dependent variable, usually it is referred as *velocity*, so that it has opposite phase than the acceleration and the restoring forces which is a primary feature of the damping term. This requirement needs to be fulfilled by both linear as well as nonlinear damping sources. In addition to this, nonlinearity define ways the energy is distributed across the state space and rates with which dissipation occurs. A classic example would be of van der Pol equation, [39], a dissipative system, which shows existence of isolated periodic solution called *limit cycle*. Another form to represent nonlinearity in damping includes polynomials in velocity terms.

Damp systems are non-conservative in general which restricts the construction of hamiltonian structure, [40], for such systems. For linear systems, various approaches have been developed through some transformations or with any other, [41]. Although, the Hamiltonian in such systems are usually time dependent, and hence non-conservative in nature,

it allows further analysis associated with the hamiltonian structure. These structures, in case of nonlinear damping, are not easy to obtain. In **chapter 3**, this problem of hamiltonian is considered in the context of quadratic damping. Further, results of this analysis has been used in **chapter 4** to analyse the role of quadratic damping in a strongly nonlinear potential. Later, in **chapter 6** a generalised nonlinear damping in polynomial form is considered for its role in the dynamics of forced and coupled oscillators.

Next consider coupling of two systems as shown in figure 1.1 without any external forcing. In physical world, dynamical systems often occur as small individual systems coupled with each other. This arrangement could be found in power grid, [42], engineering systems, [43], and in various other scientific models. Coupled systems produce novel interaction which are not available in a single system. These interactions leads to various phenomenon exclusive to coupling effects such as amplitude death, [44], chimeras, [45], basin stability, [46], internal resonances, [47], etc,. Coupling also contributes towards complexity of such systems and may result in unfavourable outcomes sometimes. Hence the necessity to understand the structures of coupled systems, and development of abilities to harness beneficial applications from it.

In coupled systems there is usually a time lag between the motion of different systems. This also happens in systems with feedbacks at the system level. This lag commonly occurs in physical systems because of signal delays in the system. The concept of delay in the system is often used in physical models and has diverse applications such as in climate models, [48], semiconductor lasers, [49], population dynamics models, [50], in network dynamics, [45], etc,. The delay could be a constant or a variable. For constant delay, the system depends on the delayed term at a previous instant of time. In many applications delays are variable and are cumulated or distributed over the entire history of the system. A particular way to model weighted distributed dependence on the previous states of the system is through *fractional differential equations*. *Fractional differential equations* is a very old mathematical construct where fractional order derivatives are considered. These are found in systems with power law memory and have significant applications such as in dielectric modelling, [51, 52], viscoelasticity, [53, 54], relaxation processes, [55] and many more. Delays in the system are obligations of physics and it can have both advantageous and disadvantageous outcomes and hence the importance to study this concept. In **chapter 5** the basic understanding of analysis of such systems are considered.

Next, switching on the forcing in system (1.1) would further transform the dynamical properties of the system. Forcing in dynamical systems has been extensively studied concept since the inception of the subject, [56, 57]. External forces impacts a system through the energy it puts into the system. The two components with which the external forces manipulate the energy in the system are its amplitude and frequency. When the frequency of the force matches the natural frequency of the system, the energy gets completely absorbed and the system responds by an increase in the amplitude of the vibrations, limited only by the energy dissipation components of the system. This is a popular phenomenon of resonance which is quite evident in many physical systems. However, when the forcing is applied to a oscillator which is in turn coupled to another oscillator, the resultant vibrations destructively interacts with each other and gives minimum amplitude at the natural frequency of the system. This is called antiresonance. Such phenomenons de-

pends greatly on the systems ability to dissipate its energy and shown range of non-trivial behaviours. In **chapter 6**, we consider two case studies of damped forced nonlinear oscillators examining the competing roles of nonlinear damping and periodic forcing focussing on associated nonlinear phenomenons.

Bibliography

[1] Richard A Holmgren. *A first course in discrete dynamical systems*. Springer Science & Business Media, 2012.

[2] Steven H Strogatz. *Nonlinear dynamics and chaos with student solutions manual: With applications to physics, biology, chemistry, and engineering*. CRC press, 2018.

[3] Morris W Hirsch, Stephen Smale, and Robert L Devaney. *Differential equations, dynamical systems, and an introduction to chaos*. Academic press, 2012.

[4] Lawrence Perko. *Differential equations and dynamical systems*, volume 7. Springer Science & Business Media, 2013.

[5] James D Meiss. *Differential dynamical systems*. SIAM, 2007.

[6] Ivana Kovacic and Michael J Brennan. *The Duffing equation: nonlinear oscillators and their behaviour*. John Wiley & Sons, 2011.

[7] Robert Hooke. *Lectures de potentia restitutiva, or of spring explaining the power of springing bodies*. John Martyn, 2016.

[8] Bartosz A Grzybowski. *Chemistry in motion: reaction-diffusion systems for micro- and nanotechnology*. John Wiley & Sons, 2009.

[9] Andreas Liehr. *Dissipative solitons in reaction diffusion systems*, volume 70. Springer, 2013.

[10] Sergej B Kuksin. *Randomly forced nonlinear PDEs and statistical hydrodynamics in 2 space dimensions*, volume 3. European Mathematical Society, 2006.

[11] Massimiliano Berti. *Nonlinear oscillations of Hamiltonian PDEs*, volume 74. Springer Science & Business Media, 2007.

[12] Hans Triebel. *PDE Models for Chemotaxis and Hydrodynamics in Supercritical Function Spaces*. 2017.

[13] Dong Ni and Panagiotis D Christofides. Multivariable predictive control of thin film deposition using a stochastic pde model. *Industrial & Engineering Chemistry Research*, 44(8):2416–2427, 2005.

[14] Thomas P Witelski. Nonlinear dynamics of dewetting thin films [j]. *AIMS Mathematics*, 5(5):4229–4259, 2020.

[15] Timothy Leighton. *The acoustic bubble*. Academic press, 2012.

[16] Gyaneshwar P Srivastava. *The physics of phonons*. Routledge, 2019.

[17] Keith Edward Bullen, Keith A Bullen, Keith Edward Bullen, and Bruce A Bolt. *An introduction to the theory of seismology*. Cambridge university press, 1985.

[18] CC Lo and S Das Gupta. Bending of a nonlinear rectangular beam in large deflection. *Journal of Applied Mechanics*, 1978.

[19] Gilbert Lewis and Frank Monasa. Large deflections of cantilever beams of non-linear materials of the ludwick type subjected to an end moment. *International Journal of Non-Linear Mechanics*, 17(1):1–6, 1982.

[20] Stephen P Timoshenko and James M Gere. *Theory of elastic stability*. Courier Corporation, 2009.

[21] Ian M Ward and John Sweeney. *Mechanical properties of solid polymers*. John Wiley & Sons, 2012.

[22] Ronald E Mickens. Analysis of non-linear oscillators having non-polynomial elastic terms. *Journal of Sound Vibration*, 255:789–792, 2002.

[23] B Ravindra and AK Mallik. Hard duffing-type vibration isolator with combined coulomb and viscous damping. *International journal of non-linear mechanics*, 28(4):427–440, 1993.

[24] Stephen Wiggins. Chaos in the quasiperiodically forced duffing oscillator. *Physics Letters A*, 124(3):138–142, 1987.

[25] Charles H Dowding and CH Dowding. *Construction vibrations*, volume 81. Prentice Hall Upper Saddle River, NJ, 1996.

[26] M Taylan. The effect of nonlinear damping and restoring in ship rolling. *Ocean Engineering*, 27(9):921–932, 2000.

[27] M Taylan. Solution of the nonlinear roll model by a generalized asymptotic method. *Ocean Engineering*, 26(11):1169–1181, 1999.

[28] Robert V Wilson, Pablo M Carrica, and Fred Stern. Unsteady rans method for ship motions with application to roll for a surface combatant. *Computers & fluids*, 35(5):501–524, 2006.

[29] Stav Zaitsev, Oleg Shtempluck, Eyal Buks, and Oded Gottlieb. Nonlinear damping in a micromechanical oscillator. *Nonlinear Dynamics*, 67(1):859–883, 2012.

[30] Alexander Eichler, Joel Moser, Julien Chaste, Mariusz Zdrojek, I Wilson-Rae, and Adrian Bachtold. Nonlinear damping in mechanical resonators made from carbon nanotubes and graphene. *Nature nanotechnology*, 6(6):339–342, 2011.

[31] Clifford Smith and Norman Wereley. Linear and nonlinear damping identification in helicopter rotor systems. In *39th AIAA/ASME/ASCE/AHS/ASC Structures, Structural Dynamics, and Materials Conference and Exhibit*, page 2003, 1998.

[32] Clifford B Smith and Norman M Wereley. Nonlinear damping identification from transient data. *AIAA journal*, 37(12):1625–1632, 1999.

[33] GV Demarie and D Sabia. Non-linear damping and frequency identification in a progressively damaged rc element. *Experimental mechanics*, 51(2):229–245, 2011.

[34] MR Hajj, J Fung, AH Nayfeh, and SO'F Fahey. Damping identification using perturbation techniques and higher-order spectra. *Nonlinear Dynamics*, 23(2):189–203, 2000.

[35] SJ Elliott, M Ghandchi Tehrani, and RS Langley. Nonlinear damping and quasi-linear modelling. *Philosophical Transactions of the Royal Society A: Mathematical, Physical and Engineering Sciences*, 373(2051):20140402, 2015.

[36] Tareq Al-Hababi, Maosen Cao, Bassiouny Saleh, Nizar Faisal Alkayem, and Hao Xu. A critical review of nonlinear damping identification in structural dynamics: Methods, applications, and challenges. *Sensors*, 20(24):7303, 2020.

[37] N Harish Chandra and AS Sekhar. Nonlinear damping identification in rotors using wavelet transform. *Mechanism and Machine Theory*, 100:170–183, 2016.

[38] Mathieu Colin, Olivier Thomas, Sébastien Grondel, and Éric Cattan. Very large amplitude vibrations of flexible structures: Experimental identification and validation of a quadratic drag damping model. *Journal of Fluids and Structures*, 97:103056, 2020.

[39] Ronald E Mickens. *Oscillations in planar dynamic systems*, volume 37. World Scientific, 1996.

[40] John Guckenheimer. Hamiltonian dynamics.

[41] VK Chandrasekar, M Senthilvelan, and M Lakshmanan. On the lagrangian and hamiltonian description of the damped linear harmonic oscillator. *Journal of mathematical physics*, 48(3):032701, 2007.

[42] Adilson E Motter, Seth A Myers, Marian Anghel, and Takashi Nishikawa. Spontaneous synchrony in power-grid networks. *Nature Physics*, 9(3):191–197, 2013.

[43] Guanrong Chen. *Controlling chaos and bifurcations in engineering systems*. CRC press, 1999.

[44] Renato E Mirollo and Steven H Strogatz. Amplitude death in an array of limit-cycle oscillators. *Journal of Statistical Physics*, 60(1-2):245–262, 1990.

[45] YN Kyrychko, KB Blyuss, and E Schöll. Amplitude death in systems of coupled oscillators with distributed-delay coupling. *The European Physical Journal B*, 84(2):307–315, 2011.

[46] Sarbendu Rakshit, Bidesh K Bera, Soumen Majhi, Chittaranjan Hens, and Dibakar Ghosh. Basin stability measure of different steady states in coupled oscillators. *Scientific reports*, 7:45909, 2017.

[47] Franco Mangussi and Damián H Zanette. Internal resonance in a vibrating beam: a zoo of nonlinear resonance peaks. *PloS one*, 11(9):e0162365, 2016.

[48] Andrew Keane, Bernd Krauskopf, and Claire M Postlethwaite. Climate models with delay differential equations. *Chaos: An Interdisciplinary Journal of Nonlinear Science*, 27(11):114309, 2017.

[49] T Heil, I Fischer, W Elsäßer, and A Gavrielides. Dynamics of semiconductor lasers subject to delayed optical feedback: The short cavity regime. *Physical Review Letters*, 87(24):243901, 2001.

[50] Yang Kuang. *Delay differential equations: with applications in population dynamics*. Academic press, 1993.

[51] Vasily E Tarasov. Universal electromagnetic waves in dielectric. *Journal of Physics: condensed matter*, 20(17):175223, 2008.

[52] Vasily E Tarasov. Fractional integro-differential equations for electromagnetic waves in dielectric media. *Theoretical and Mathematical Physics*, 158(3):355–359, 2009.

[53] Ronald L Bagley and PJ Torvik. A theoretical basis for the application of fractional calculus to viscoelasticity. *Journal of Rheology*, 27(3):201–210, 1983.

[54] Francesco Mainardi. *Fractional calculus and waves in linear viscoelasticity: an introduction to mathematical models*. World Scientific, 2010.

[55] Francesco Mainardi and Rudolf Gorenflo. Time-fractional derivatives in relaxation processes: a tutorial survey. *arXiv preprint arXiv:0801.4914*, 2008.

[56] K Tomita. Periodically forced nonlinear oscillators. *Chaos*, 10:211–36, 1986.

[57] Lawrence N Virgin. *Introduction to experimental nonlinear dynamics: a case study in mechanical vibration*. Cambridge University Press, 2000.

Appendix A

Lambert W Functions

A.1 Introduction

The history of the Lambert W function goes back to Johann Lambert (1728-1777) and also legendary Leonhard Euler (1707-1783), they developed a series solutions for a trinomial series. Two century later this solution was named Lambert W function. It is defined as the inverse of the function $f(z) = ze^z$ satisfying $W(z)e^{W(z)} = z$.

The trinomial series $x = p + x^n$ which solved by Lambert was transformed by Euler into a symmetrized form

$$x^\alpha - x^\beta = (\alpha - \beta)ux^{\alpha-\beta},$$

where α, β, u are known. Suppose $\alpha = 1$, $\beta = n$, let $\bar{x} = \frac{1}{x}$, then Euler form equation can be recasted to Lambert form $\bar{x}^n - \bar{x} = p$, where $p = (1 - n)u$.

Given Euler's form and using l'Hôpital's rule we obtain $ux^\alpha = \ln x$. Let us change $x \to X$, then multiplying both sides by $e^{-\alpha X}$ we obtain $Xe^{-\alpha X} = u$. Suppose $\alpha X = Y$, then Y can be expressed in terms of Euler T-function, $Y = T(\alpha u)$. If $y = xe^{-x}$ then $x = T(y)$, like Lambert W function it satisfies $y = T(y)e^{-T(y)}$. One can readily see that $W(-y) = -T(y)$. The power series expansion shows

$$S(y) = \sum_{n=1}^{\infty} \frac{(\pm n)^{n-1}}{n!} y^n = y \pm y^2 + \frac{3}{2}y^3 - \pm\frac{8}{3}y^4 + \frac{125}{24}y^5 \pm \frac{54}{5}y^6 + \cdots,$$

where all positive terms yield T series and alternative signs yield W series.

Properties of Lambert W function : There are two real branches of W function, $W_0(x)$ and $W_{-1}(x)$. The branch point is at $x = -e^{-1}$:

$$W_0(-e^{-1}) = W_{-1}(-e^{-1}) = -1.$$

The domain for W_0 is $x \in [-e^{-1}, \infty)$ and domain for W_{-1} is $x \in [-e^{-1}, 0)$. Both branches are negative for $x < 0$, hence the Lambert W function is multivalued, and $W_{-1} \leq W_0$, we will choose the branch depending on the physical situation. In general, W_0 is frequently

used because of its regular behaviour $W_0(x \to 0) \sim x$, whereas $W_{-1}(x \to 0) \sim \ln(-x)$ diverges logarithmically.

Starting from $W(x)e^{W(x)} = x$, we obtain

$$W'e^{W(x)} + W(x)W'e^{W(x)} = 1,$$

which yields

$$W' = \frac{1}{1+W}e^{-W(x)} = \frac{W(x)}{(1+W)x}.$$

One can also show

$$\int W(x)dx = \int W(W+1)e^W\, dW = (W^2 - W + 1)e^W + C$$

$$= W.We^W - We^W + e^W + C = xW(x) - x + \frac{x}{W} + C = x(W(x) - 1 + \frac{1}{W}) + C,$$

where we have tacitly used $dx = dW(W+1)e^W$.

The sum rule is given by

$$W(x) + W(y) = W\big(xy(\frac{1}{W(x)} + \frac{1}{W(y)})\big).$$

This can be proved as follows:

$$W(x) + W(y) = W\big(W(x) + W(y)e^{W(x)+W(y)}\big) = W\big(W(x)e^{W(x)}e^{W(y)} + W(y)e^{W(y)}e^{W(x)}\big)$$

$$= W(xe^{W(y)} + ye^{W(x)}) = W(x\frac{W(y)e^{W(y)}}{W(y)} + y\frac{W(x)e^{W(x)}}{W(x)} = W\big(xy(\frac{1}{W(x)} + \frac{1}{W(y)})\big).$$

In fact, one can even prove also

$$W(x)W(y) = xye^{-W\left(xy(\frac{1}{W(x)}+\frac{1}{W(y)})\right)}.$$

There are numerous applications of these properties for the solutions of differential equations.

Chapter 2

Background and Methods

The discovery of differential equations and their applications to laws of motion and theory of gravity in the seventeenth century by Newton, Kepler and Leibniz, gave birth to the idea to study dynamics using mathematics. With this enlightenment differential equations began to be applied to every dynamical problems. Differential equations governs how an initial state of the system evolves over time. The trajectory of evolution of system over time is, in general, not possible to obtain in closed-function forms. This problem stalked the early practitioners of the subject for a long till Poincarè came to the picture. Poincarè using the geometric approach provided a new perspective to understand and analyse such problems. His approach focuses on the qualitative aspects of the dynamics rather than the, erstwhile, quantitative outlook. Instead of finding exact solutions to the governing equations, Poincarè explained the qualitative properties such as stability, frequency, asymptotic behaviours, and approximations. Later, many great dynamical theorists emerge like Lyapunov, Arnold, Birkhoff and others who contributed immensely to this field.

2.1 Basic Concepts of Dynamical Systems

To examine the dynamical aspects of differential equations, it is necessary to understand the mathematical constructs of the dynamical system theory. The theoretical development of dynamical systems and there are huge literature available for detailed explanation of the concepts, [1, 2, 3, 4, 5, 6, 7]. However, for the purpose of this theses, the basic concepts and definitions will be presented in this section.

Dynamical systems consists of a state space, a time set, and an evolution mapping. State space represents collection of state the system can be in. This space could be discrete like in a dynamics on a lattice, or continuous like a phase space of a pendulum. The dimensions of the state space are the degrees of freedom in which the system can change its state. This dimension could be finite, as in the case of ordinary differential equations in finite variables, or infinite, as for functional differential equations. Time set is a set of instants in the evolution of the system. It provides for an ordered record of the system evolution. This record could be discrete when the events occur at certain intervals, or

continuous when the records are kept in continuous manner. The third element is the evolution rule. It defines the ways through which the system transforms from one state to another state at any given time. If we denote state space by S, time set as T, then the evolution map, E, is given as $E : S \times T \to S$.

In this theses, however, we are interested in a continuous state space with a real time set. Such dynamical systems are usually referred to as *flows*. *Flows* are continuous dynamical systems over real time set on a continuously differentiable manifold. The corresponding evolution rules are given by differential equations and evolved states at any instant is the flow of the initial states for that time period. If $x(0)$ is the initial state, then state at time $t \in T$ is given as $\phi_t(x(0))$, where ϕ_t is the flow map.

In the state space there are certain points (states) which are invariant under a *flow*. In such states the system cease to evolve any further and stays in that state forever. These points are called *fixed points* of the flow. For the physical problems which the dynamical system are modelling, the *fixed points* are the equilibrium solutions (or points). These points can also be referred to as steady states or stationary points. For instance, in the dynamical picture of a simple pendulum the lowest and the highest points are *fixed points* and if the pendulum happens to have zero velocity at these points then it will cease to move and remain there as long as there are no external perturbations. For a qualitative analysis of the differential equations one studies about *fixed points* and in praxis the *fixed points* are shifted to origin by translating the system to make it easier to study as it eliminates the effects of any nonlinear terms.

For linear systems the state space is homogeneous with a single *fixed point*. This allows to obtain flow solutions in closed functional forms. However, nonlinear systems can have multiple *fixed points* which transforms the state space in a non-trivial manner. This morphing of state space makes it inhomogeneous, in the sense that the topology of state space varies across the space, which means the solution set of the system can change remarkably for even a minute change in the initial conditions. There are no accurate tools or methods to study such variation in the global setting. However, there is a mathematical scheme which allows to study such systems locally in a form of a simpler system - linear system. The scheme is called *linearisation* and it derive its validity from Hartman-Grobman theorem also known as linearisation theorem, [2, 6]. To understand the theorem first consider locality and linearisation.

Consider a nonlinear system given as

$$\dot{x} = F(x, \alpha), \tag{2.1}$$

where $x \in \mathbb{R}^n$ is the dependent n-dimensional variable and function of time t. The dots represent order of time derivative. $F(x,) \in \mathbb{R}^n$ is an arbitrary nonlinear function of x, and parameter $\alpha \in \mathbb{R}$. Further assume that the system has a *fixed point* at origin, $\mathcal{O}$, i.e, at $x = 0$, for simplification of the process. This simplification is not a special case as any equilibrium point can simply be translated to the origin through linear translation.

To analyse the local dynamics, the linear approximation of $F(x, \alpha)$ is obtained by calculating the *Jacobian* of F at $x = 0$. The *Jacobian* is a $n \times n$ matrix with elements given as, $J_{ij} = \frac{\partial F_i}{\partial x_j}$. For $n = 1$ the *Jacobian* is a regular derivative of F with respect to x. The

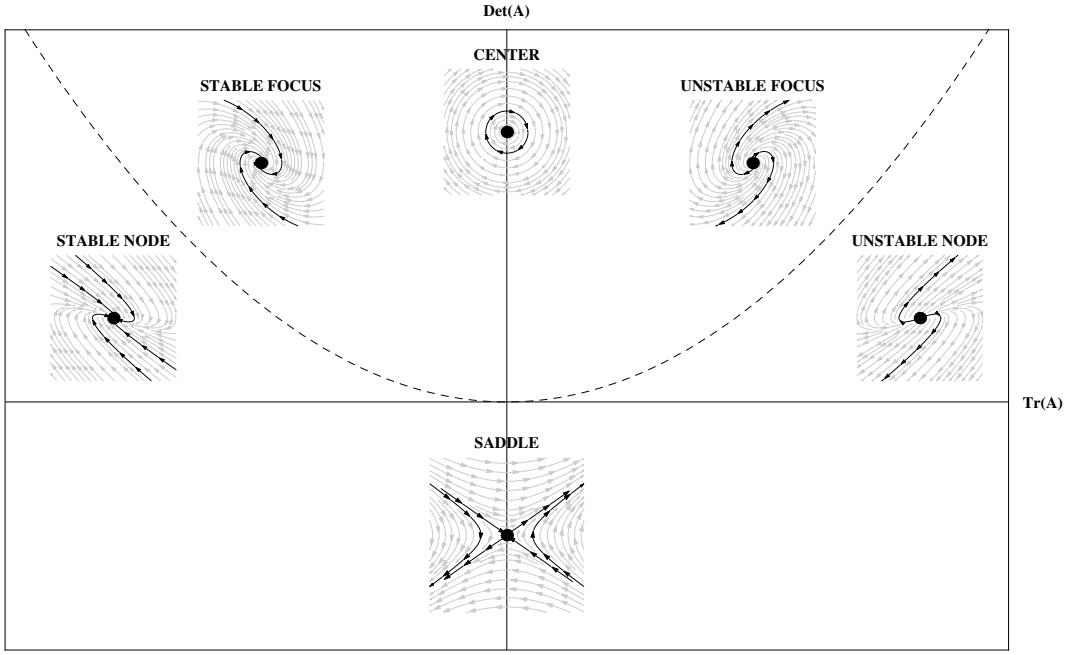

Figure 2.1: Description of linear stability analysis.

Jacobian defines the ways in which the function affects the neighbourhood of any point. Therefore, the *Jacobian* matrix, say A, of F determines the local dynamics around any *fixed point* , or in our case, the origin. The local dynamics is given by the equation

$$\dot{x} = A\,x. \tag{2.2}$$

Here x denotes the states of the local dynamics. Given the linearisation of the nonlinear equations, the Hartman-Grobman theorem states that for an hyperbolic equilibrium point, x^*, i.e, for those equilibrium points for which the *Jacobian* has eigenvalues with non-zero real parts, the dynamic flow of system (2.1) will be topological conjugate to the dynamical flow of (2.2) in some neighbourhood of x^*. A more well explained explanation and the proof could be found in several literature, [1, 2, 6]. This shows the effectiveness of linearisation in predicting the qualitative behaviour of the system near equilibrium points.

Linear Stability Analysis

The general form of linear system and the linearised nonlinear equations is given by (2.2). The matrix, A, could comprise of linear coefficients from linear dynamical system or coefficients from linearised nonlinear equations. In both cases, the eigensystem of A determines a lot of qualitative features of the dynamics. Based on the eigensystem of A, the solution of (2.2) can be a *center*, *focus*, *node*, or a *saddle*. Based on the trace and determinant of the matrix A, a description of solution set of (2.2) is given in figure 2.1. The stability of the point is determined by the real part of the eigenvalues. A fixed point is stable if the real part of the eigenvalues are negative and, unstable, if the real part is positive. In figure 2.1, the stable region is to the left of the y-axes. On the axis the

real is part is zero which corresponds to *center* type periodic orbits, and to the right it is unstable. Apart from this, the point can also be a *saddle* where it is stable along one direction and unstable along another.

In linear systems, the above mentioned solutions are the exhausted set of general solutions and are valid throughout the phase space. For nonlinear systems, there may be multiple fixed points in the phase space because of which the linearisation around a fixed point is valid in a limited region of the phase space. Hence, linearisation of nonlinear systems determines only local stability and not global stability. For instance, in undamped unforced Duffing oscillator equation the *center* orbits around the origin undergoes *heteroclinic* bifurcation as it encounters the other fixed points of the system and forms a *heteroclinic* orbit, [6, 8].

2.2 Analytical Methods for NODE

Modelling of physical systems helps to understand the working, as well as, in anticipation of unknown behaviours of the system. This demands an repository of analytical tools to extract various properties of the dynamics of the system. Various tools pertinent to this end are mainly of two types - analytical and numerical. Numerical tools and methods are very efficient, fast, and accurate. However, it has its limitations as well. The efficiency of numerical methods are bounded by the theoretical developments in various algorithms. The quickness of numerical schemes are also bounded by technological advancements in the computational power. To overcome the shortcomings, analytical methods are utilised in simplifying the equations and rationalise expressions before putting it through numerical schemes. In this section, we shall look into basic analytical treatments usually applied to nonlinear systems with special emphasis on methods relevant for the case studies adopted in this theses.

In linear systems, the local dynamics translates into the global behaviour and the solutions could be obtained in a closed form function - exponential. This property of linear systems aid in the construction of a general solution. Introduction of nonlinearity destroys this homogeneity of the phase space which, in general, prohibits to obtain a general solution for the system. Very often, novel functions are created to define the solutions in certain nonlinear equations, particular cases shall be presented in **chapters 3 & 4**.

The solution set of a NODE can have different type of solutions representing different dynamical behaviour. These solutions are majorly of two categories - transient states, and steady states. The steady states could be fixed points, periodic orbits, homoclinic and heteroclinic orbits. In this theses, we shall be interested in periodic solutions and its characteristics. Periodic orbits are those for which the orbits revisits a state (other than fixed points) after a finite time. Periodic solutions of dynamical systems can be of *centre* type or an isolated periodic orbit, called *limit cycle*. The *centre* type periodic orbits are densely packed periodic orbits such that there is a periodic orbit in the neighbourhood of every periodic orbit. These orbits are characteristics of conservative systems where each orbit corresponds to a certain energy level define through the integral of motion, [9, 10], most commonly the Hamiltonian, [9, 10, 11]. For such system, a closed-form exact solution

could be found through the Hamiltonian atleast upto quadrature. However, for nonlinear systems, the Hamiltonian is often very complex which restricts to get the solutions in a functional form, as will be shown in **chapters 3 & 4**.

For non-conservative systems or in broader category of non-integrable NODEs, there are not enough integrals of motions to obtain a general solution. These are usually damped, coupled, systems with delays or with fractional derivatives. Difficulties become grievous for non-autonomous systems, where there is an explicit time dependence. For remedy, various analytical methods have been developed to approximate the solutions, most prominent of which are perturbation methods, [1, 12]. Perturbation methods are applicable for weak nonlinearities where the effects of nonlinear terms are weakened by associating a small parameter with the term. Although, this restricts the application scope of these methods, it is still helpful in dealing with a wide class of nonlinearities and widely used in practise. Perturbation methods include Lindstedt-Poincarè method, [1, 13], Homotopy perturbation method, [14], Multi-scale perturbation methods, [5, 15], averaging method, [12] etc,. Apart from this, there are variational techniques such as Variational Iteration Method (VIM), [16], Ritz method, soliton solutions, etc,. Other non-perturbative methods include Adomian Decomposition method, [17], Harmonic Balance Method, modified Lindstedt-Poincarè, [18, 19], etc,. These non-perturbative methods are applicable for strong nonlinearity in equations.

To understand the concept of perturbation methods in NODEs a prerequisite is to comprehend the idea of how nonlinearity influences the dynamics across scale. This scale varies according to degree of relevance in terms of how far is the interested state from the perturbed state. For instance, the cubic nonlinearity in Duffing equation is not much relevant for the dynamics near the origin. However, nonlinearities does play influential role qualitatively which could be extracted through the perturbation scheme. The solution is constructed in the form of a power series in the small parameter and, as the parameter is assumed to be much less than one, the higher power terms become less relevant. These higher power terms are consider as corrections. Writing the solution in power series needs to address a major question of convergence of such series and its region of convergence. The vindication comes from a theorem by Kolmogorov, Arnold, and Moser called KAM theorem, [20, 21], named after each contributor. Without indulging in the technical details of the theorem, the theorem basically describes the persistence of the invariant tori of integrable systems under small weak nonlinear perturbations beyond which the system enters chaotic realm where the steady states collapse. Taking cue from this, in perturbation methods the dynamical system is considered as a perturbation of a simple system and the weak nonlinear terms are considered as perturbations, [22], which contributes to the correction terms. The simple systems could be linearised system, or an integrable system, or normal forms.

The main perturbation methods employed in this theses are - Lindstedt-Poincarè and multi-scale analysis method. In regular perturbation scheme, the solution and frequency are assumed to be in power series given in the form

$$\begin{aligned} x(t) &= x_0(t) + x_1(t)\epsilon + x_2(t)\epsilon^2 + ..., \\ \omega(t) &= \omega_0(t) + \omega_1(t)\epsilon + \omega_2(t)\epsilon^2 + ..., \end{aligned}$$

where $0 < \epsilon \ll 1$ is the small parameter and x_is and ω_is denote the state and frequency of dynamics at the corresponding ith scale. Next step is to substitute the above expansions in (2.1) and equate expressions for each order corresponding to the power of ϵ and solve them. The zeroth order equation is simple and can be solved in a straightforward manner in terms of regular trigonometric functions. However, higher order equations often have secular terms which leads to blow-up of the solution. In Lindstedt-Poincarè these secular terms are equated to zero and the respective solutions give correction terms for the frequency expression.

In multi-scale analysis, the dynamics is studied at multiple time scales. For this the natural time is split up into different scale rather than the frequency as

$$\tau = t_0 + t_1 + ...,$$

where τ is the new time and $t_i = t_0\,\epsilon^i$ corresponds time scale in each scale. The dynamical equation is then expanded, separated, and solved for each scale. The dynamics across multiple time scale is observable for damp oscillations where the oscillation is taking place at a faster scale and the damping at another slower scale. These two methods are well known in literature and a detailed introduction could be found in [1, 2, 5, 9]. The methods can be seen in practise in **chapters 5 & 6**.

2.3 Numerical Methods for NODE

Numerical methods for dynamical systems, particularly for NODEs, existed since the realisation of the subject and its development runs parallel with theoretical advancements. The pioneers of numerical analysis include *Euler, Newton, Lagrange, Gauss, Chebyshev, Fourier* and many others. However, the major impetus to the field was provided with the improvement of computational technology. Although, the basic idea of numerical algorithms remain in the discretisation and iterative calculations of differential equations, new algorithms are developed to incorporate the challenge of increasing complexity of nonlinearities in the system.

The class of case studies undertaken for this theses can be characterised as initial value problems (IVP). Prominent numerical algorithms for these problems are Runge-kutta methods, such as Euler method, [23, 24], and multi step methods such as Adams-Bashforth method, [23, 24]. The multi step methods are also referred as predictor-corrector methods where individual steps can be solved using any Runge-Kutta schemes. These methods can calculate the solution of the system based on either current state of the system, known as explicit methods, or through both current and later state, known as implicit methods. Apart from these methods, there are modified versions of these methods for specialised nonlinearities like in delay differential equations, [25], or for fractional differential equations, [26, 27]. These algorithms need to be implemented in any programming language such as Fortran, C++, Python, Matlab etc,. There are also dedicated packages, for executing various dynamical analysis functions, such as sciPy, numPy, pydelay, [28], in python, DDE-BIFTOOL, [29], in Matlab, XPPAUT, [30], Mathematica, [31] etc,. All the numerical analysis in this theses are done in Mathematica (mostly), Python, and Matlab.

Bibliography

[1] Dominic Jordan, Peter Smith, and Peter Smith. *Nonlinear ordinary differential equations: an introduction for scientists and engineers*, volume 10. Oxford University Press on Demand, 2007.

[2] Steven H Strogatz. *Nonlinear dynamics and chaos with student solutions manual: With applications to physics, biology, chemistry, and engineering*. CRC press, 2018.

[3] Martin Golubitsky, Ian Stewart, and David G Schaeffer. *Singularities and Groups in Bifurcation Theory: Volume II*, volume 69. Springer Science & Business Media, 2012.

[4] Ronald E Mickens. *Truly nonlinear oscillations: harmonic balance, parameter expansions, iteration, and averaging methods*. World Scientific, 2010.

[5] Ali H Nayfeh and Balakumar Balachandran. *Applied nonlinear dynamics: analytical, computational, and experimental methods*. John Wiley & Sons, 2008.

[6] Stephen Smale. Differentiable dynamical systems. *Bulletin of the American mathematical Society*, 73(6):747–817, 1967.

[7] John Guckenheimer and Philip Holmes. *Nonlinear oscillations, dynamical systems, and bifurcations of vector fields*, volume 42. Springer Science & Business Media, 2013.

[8] Yuri A Kuznetsov. *Elements of applied bifurcation theory*, volume 112. Springer Science & Business Media, 2013.

[9] Muthusamy Lakshmanan and Shanmuganathan Rajaseekar. *Nonlinear dynamics: integrability, chaos and patterns*. Springer Science & Business Media, 2012.

[10] Alain Goriely. *Integrability and nonintegrability of dynamical systems*, volume 19. World Scientific, 2001.

[11] Gaetano Vilasi. *Hamiltonian dynamics*. World Scientific, 2001.

[12] Vladimir I Arnold, VV Kozlov, and AI Neishtadt. *Dynamical systems III*. Springer, 1988.

[13] Henri Poincaré. *Les méthodes nouvelles de la mécanique céleste*, volume 3. Gauthier-Villars, 1899.

[14] Ji-Huan He. Homotopy perturbation method: a new nonlinear analytical technique. *Applied Mathematics and computation*, 135(1):73–79, 2003.

[15] M Pakdemirli, MMF Karahan, and H Boyacı. A new perturbation algorithm with better convergence properties: Multiple scales lindstedt poincaré method. *Mathematical and Computational Applications*, 14(1):31–44, 2009.

[16] Ji-Huan He. Variational iteration method–a kind of non-linear analytical technique: some examples. *International journal of non-linear mechanics*, 34(4):699–708, 1999.

[17] George Adomian. A review of the decomposition method in applied mathematics. *Journal of mathematical analysis and applications*, 135(2):501–544, 1988.

[18] Ji-Huan He. Modified lindstedt–poincare methods for some strongly non-linear oscillations: Part i: expansion of a constant. *International Journal of Non-Linear Mechanics*, 37(2):309–314, 2002.

[19] Ji-Huan He. Modified lindstedt–poincare methods for some strongly non-linear oscillations: part ii: a new transformation. *International Journal of Non-Linear Mechanics*, 37(2):315–320, 2002.

[20] Vladimir Igorevich Arnold. *Geometrical methods in the theory of ordinary differential equations*, volume 250. Springer Science & Business Media, 2012.

[21] Robert A Meyers. *Encyclopedia of complexity and systems science*. Springer, 2009.

[22] Henk W Broer and Heinz Hanßmann. Hamiltonian perturbation theory (and transition to chaos)., 2009.

[23] John Guckenheimer. Numerical analysis of dynamical systems. *Handbook of dynamical systems*, 2:345–390, 2002.

[24] Andrew Stuart and Anthony R Humphries. *Dynamical systems and numerical analysis*, volume 2. Cambridge University Press, 1998.

[25] Alfredo Bellen and Marino Zennaro. *Numerical methods for delay differential equations*. Oxford university press, 2013.

[26] Roberto Garrappa. Numerical solution of fractional differential equations: A survey and a software tutorial. *Mathematics*, 6(2):16, 2018.

[27] Joseph A Connolly and Neville J Ford. Comparison of numerical methods for fractional differential equations. *Communications on Pure & Applied Analysis*, 5(2):289, 2006.

[28] Valentin Flunkert and Eckehard Schoell. Pydelay-a python tool for solving delay differential equations. *arXiv preprint arXiv:0911.1633*, 2009.

[29] Koen Engelborghs, Tatyana Luzyanina, and Dirk Roose. Numerical bifurcation analysis of delay differential equations using dde-biftool. *ACM Transactions on Mathematical Software (TOMS)*, 28(1):1–21, 2002.

[30] Bard Ermentrout. *Simulating, analyzing, and animating dynamical systems: a guide to XPPAUT for researchers and students*. SIAM, 2002.

[31] Martha LL Abell and James P Braselton. *Differential equations with Mathematica*. Academic Press, 2016.

Chapter 3

Nonlinear Damping

In physical systems energy is not a constant or a conserve quantity and dissipation is a natural part of the system. The dissipation of energy leads to damping in the motion which may or may not be desirable. This damping of the motion is often treated as linear. However, this is an approximation which lose its relevance in high velocity flows. An accurate modelling of the damping can be done only in a nonlinear fashion and the structure of this nonlinearity varies from system to system.

The phenomenological modelling of damping is done in terms of velocity raised to some power, usually written in the form $v|v|^{p-1}$ where $p \in \mathbb{R}$, [1]. In most application, only the linear term, denoting viscous damping, is assumed. This linear assumption often proves to be too simplistic and fail to represent dissipation in the system. Such viscous damping is valid for low velocity oscillations in fluid mediums, [2]. For different scenarios separate damping exponent is considered or a combination of them. Among integer order damping exponent, the most commonly employed exponents are, $p = 0$, to model *Coulomb damping* or dry friction, [3]. This type of damping occurs when two machine parts rub against each other $p = 1$, for the linear case, and $p = 2$ case representing *Quadratic damping* which is encountered in flows with high Reynolds number, [4]. Damping of fractional orders as well as combinations of different damping mechanisms have been utilised in physical modeling as well, [5, 6].

In this chapter a generalised quadratically damped oscillator shall be analysed from a Hamiltonian point of view. Further, conditions will be obtained for closed and damped orbits. Moreover, an integrable structure of such damped systems shall be developed.

3.1 Chiellini Integrability and Quadratically Damped Oscillators

In recent times a number of articles have appeared in the literature which deal with the phenomenon of a linear oscillator subject to a quadratic damping force [7, 8, 9, 10, 11]. Most elementary textbooks deal with viscous damping for the obvious reason that it involves a linear dependence on the velocity of the oscillator and presents the simplest

situation where an exact analytical treatment is possible. In general this involves analysis of a second-order ordinary differential equation (ODE) of the Liénard type [12], namely $\ddot{x} + f(x)\dot{x} + g(x) = 0$, where it is assumed that f is a constant and the function $g = x$. As damping does not arise from a single physical phenomena and is itself of various kinds, e.g., material damping, structural damping, interfacial damping, aerodynamic and hydrological drag etc., therefore a different mathematical description is needed in each case. Systems like the simple harmonic oscillator and the viscously damped harmonic oscillator, both of which can be solved by elementary techniques, however, represent idealizations of real life phenomena because they ignore nonlinear aspects of the forcing term as well as the damping force.

For more realistic models applicable to problems involving hydrological drag and aerodynamics, which usually involve higher velocities, the damping force is found to be proportional to the square of the velocity. The same is also true when an immersed object moves through a fluid at relatively high Reynolds numbers [13]- the corresponding drag force is found to be proportional to the square of the velocity $v = sgn(\dot{x})\dot{x}^2$. In recent times oscillators with a non-negative real-power restoring force $F(x) = ksgn(x)|x|^{\alpha}$ and quadratic damping have also been studied by Kovacic and Rakaric [11].

The principal feature associated with quadratic damping is a discontinuous jump of the damping force in the equation of motion whenever the velocity vanishes such that the frictional force always opposes the motion. For oscillatory systems this occurs every half cycles and means that instead of a single equation of motion the latter splits into two parts depending on the sign of the velocity. Each equation has to solved separately and matched at the points where the velocity changes sign. In general solving such a system in presence of nonlinearity is a rather daunting task and only in rare cases is an exact solution to be expected. Numerical techniques on the other hand provide valuable information about the evolution of the system and its general nature.

From the mathematical point of view the construction of first integrals for systems involving a quadratic dependence on the velocity often provides interesting insights. Indeed constants of motion are the bedrock of many of the conservation principles at the heart of theoretical physics: the work-energy theorem applied to a conservative system, is perhaps the most striking and often quoted example, as it has evolved into the principle of conservation of energy.

In this work we examine the equation, $\ddot{x} + sgn(\dot{x})f(x)\dot{x}^2 + g(x) = 0$, in the light of several recent articles which have also dealt with the same equation[7, 8, 9]. This is a discontinuous generalization of an equation of the Liénard type involving a quadratic dependence on the velocity. In particular we show that by imposing the Chiellini condition of integrability on the functions f and g one can subsume many of the previous examples into a compact scheme. Incidentally the Chiellini condition is typically encountered in the context of integrability of the standard Liénard equation in course of its transformation to the first-order Abel equation of the first kind and also while finding a Lagrangian/Hamiltonian description of the Liénard equation [14, 15, 16]. However, its application in the case of quadratic damping appears to be new. We show how one can derive in a systematic manner the maximum amplitudes analytically in terms of the Lambert W function and also construct a formal solution up to quadrature.

The organization of the paper is as follows. In Section 2 we review the second-order ODE with a quadratic dependence on velocity in the context of its Lagrangian/Hamiltonian description. It is shown that such a system may be interpreted as one displaying a position dependent mass function. The trajectory is explicitly displayed by numerical investigations. In Section 3 we split the ODE into two parts as mentioned above depending on the sign of the velocity $\dot{x}$ and investigate the trajectories, maximum amplitudes as well as period of oscillations. In particular we show that the periods of the cycles and the corresponding maximum amplitudes are both determined exclusively by a potential function which involves the position dependent mass function. Furthermore by invoking the Chiellini integrability condition it is possible to write down analytic formulae for the maximum amplitudes in terms of the Lambert W function [17, 18], and also deduce the solution up to a quadrature.

The Lambert W function is defined as the inverse function of the mapping $x \mapsto xe^x$ and thus solves the equation $ye^y = x$. The solution is given in the form of the Lambert W function, $y = W(x)$, i.e. W satisfies $W(x)e^{W(x)} = x$. The equation always has an infinite number of solutions, most of which are complex, and W is multivalued. The examples presented here include those obtained earlier by Cveticanin [7, 8].

3.2 The Hamiltonian in presence of quadratic velocity

Consider a second-order ODE with a quadratic dependence on the velocity given by

$$\ddot{x} + f(x)\dot{x}^2 + g(x) = 0. \tag{3.1}$$

We assume $f(x)$ and $g(x)$ are such that $f(0) = g(0) = 0$ and $f(x)$ is integrable while $g'(0) > 0$. The functional form of $g(x) = g'(0)x + g_n(x)$ where $g_n(x)$ is analytic.

The Jacobi Last Multiplier (JLM) originally arose in the context of Jacobi's efforts to derive an additional first integral for a system of n first-order ODEs given $(n-2)$ conserved quantities [19, 20]. It also appears in the Lie theory of infinitesimal transformations [21, 22]. In addition the JLM plays a pivotal role in the context of the inverse problem of Lagrangian dynamics as it allows for the determination of the Lagrangian of a second-order ODE of the form, $\ddot{x} = \mathcal{F}(x, \dot{x})$, an aspect that has been extensively probed in [23, 24, 25, 26, 27, 28]. In this context the JLM may be defined as a solution of the equation,

$$\frac{d}{dt}\log M + \frac{\partial \mathcal{F}(x,\dot{x})}{\partial \dot{x}} = 0. \tag{3.2}$$

Therefore in case of (3.1) it follows that

$$M = \exp\left(2F(x)\right), \qquad \text{where} \qquad F(x) = \int_0^x f(s)ds. \tag{3.3}$$

The relationship between the JLM, M, and the Lagrangian is provided by, $M = \partial^2 L/\partial \dot{x}^2$, as a consequence of which the Lagrangian of (3.1) may be expressed as

$$L = \frac{1}{2} e^{2F(x)} \dot{x}^2 - V(x). \tag{3.4}$$

The potential $V(x)$ is determined by substituting (3.4) into the Euler-Lagrange equation

$$\frac{d}{dt}\left(\frac{\partial L}{\partial \dot{x}}\right) = \left(\frac{\partial L}{\partial x}\right),$$

and comparing the resulting equation with (3.1) which immediately shows that

$$V(x) = \int_0^x e^{2F(s)} g(s) ds. \tag{3.5}$$

Using a Legendre transformation we then obtain the Hamiltonian

$$H = \frac{1}{2} e^{2F(x)} \dot{x}^2 + \int_0^x e^{2F(s)} g(s) ds. \tag{3.6}$$

It is easily verified that H is a constant of motion and the expression for the conjugate momentum, $p = e^{2F(x)}\dot{x}$, suggests that, $M = e^{2F(x)}$, serves as a position dependent mass term. In fact equations with a quadratic velocity dependence of the type considered here naturally arise in the Newtonian formulation of the equation of motion of a particle with a variable mass. Clearly then, the trajectories for arbitrary initial conditions (x_0, y_0), where $y = \dot{x}$, are given by

$$\frac{1}{2} e^{2F(x)} y^2 + V(x) = \frac{1}{2} e^{2F(x)} y_0^2 + V(x_0). \tag{3.7}$$

In terms of the canonical momentum, $p = e^{2F(x)}\dot{x}$, the Hamiltonian H becomes

$$H = \frac{p^2}{2e^{2F(x)}} + V(x). \tag{3.8}$$

Defining a new set of canonical variables

$$P := \frac{p}{e^{F(x)}} \qquad \text{and} \qquad Q = \int_0^x e^{F(s)} ds = \Psi(x), \tag{3.9}$$

the Hamiltonian has the appearance

$$H = \frac{1}{2} P^2 + V(\Psi^{-1}(Q)) = \frac{1}{2} P^2 + U(Q), \qquad \text{where} \quad U = V \circ \Psi^{-1}, \tag{3.10}$$

and corresponds to that of a particle of unit mass provided $\Psi(x)$ is invertible.

Let us consider a simple example in which $f(x) =$ constant and $g(x) = x$. In particular suppose $f(x) = 1/2$, so that $F(x) = x/2$. Then the canonical momentum and coordinate are $P = e^{x/2}y$ and $Q = 2e^{x/2}$ respectively, and $V(x) = e^x(x-1)+1$. Thus in terms of the new coordinates the Hamiltonian has the following form

$$H = \frac{1}{2}P^2 + \frac{Q^2}{4}\ln(\frac{Q^2}{4} - 1). \tag{3.11}$$

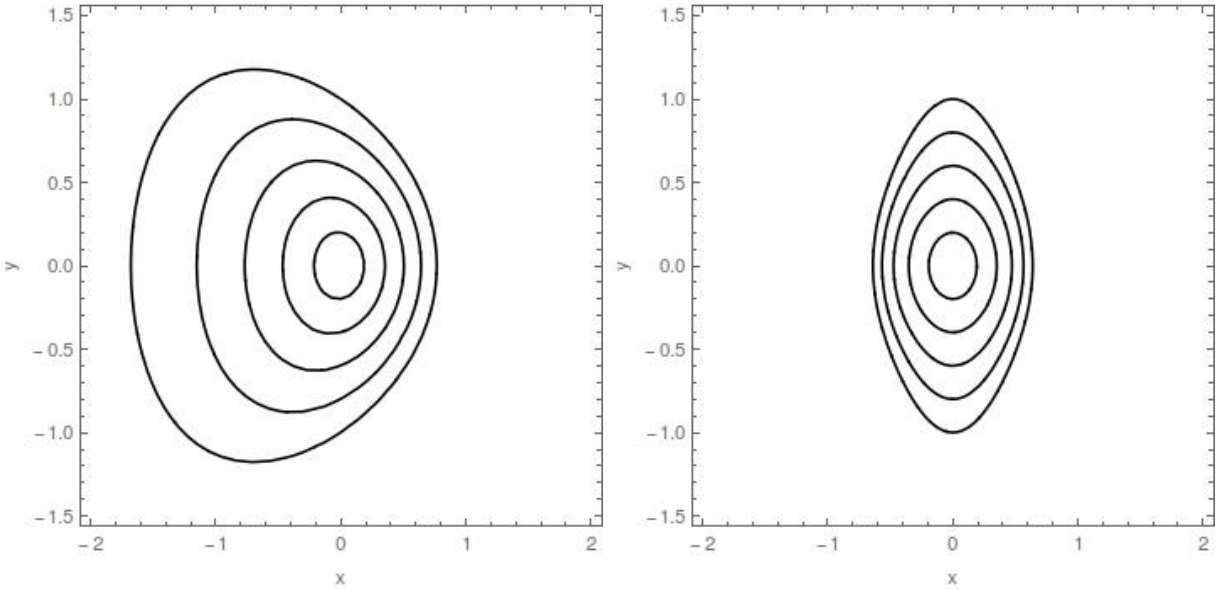

(a) $f(x) = 0.5$, $g(x) = x$ (b) $f(x) = 3x$, $g(x) = x + x^3$

Figure 3.1: Phase plots showing the existence of a center for two different combinations of $f(x)$ and $g(x)$ for multiple initial conditions.

Figure 3.1 shows some of the trajectories for the Hamiltonian in equation (3.7) with different initial conditions and it is clear from these figures that the origin $(0, 0)$ is a center.

Note that for suitable choices of the functions f and g, (3.1) often exhibits the property of isochronicity and this feature has been extensively studied in [29, 30, 31].

3.3 Quadratic damping

It is plain that (3.1) cannot describe a system with a quadratic damping as the term involving $\dot{x}^2$ does not change sign and oppose the motion when the velocity reverses its sign. To remedy this feature it is necessary to split (3.1) into two parts and write

$$\ddot{x} + f(x)\dot{x}^2 + g(x) = 0, \quad \dot{x} > 0, \tag{3.12}$$

$$\ddot{x} - f(x)\dot{x}^2 + g(x) = 0, \quad \dot{x} < 0. \tag{3.13}$$

Let us denote the Hamiltonian associated with these pieces by

$$H^{\pm} = \frac{1}{2}e^{\pm 2F(x)}y^2 + V^{\pm}(x) \tag{3.14}$$

with the superscript $\pm$ standing for $\dot{x} = y > (<)0$. Furthermore it will be assumed that the initial point (x_0, y_0) with $(y_0 > 0)$ is such that $V^+(x_0) = 0$ and $F(x_0) = 0$. Thus when motion commences from the initial point then the trajectory is defined by $H^+ = K_0^+ = y_0^2/2$ or in explicit form

$$\frac{1}{2}e^{+2F(x)}y^2 + V^+(x) = \frac{1}{2}y_0^2.$$

This trajectory first crosses the x-axis at say $x = x_1$ when the velocity $y = 0$. Consequently the point of intersection $x_1(> 0)$ which denotes the maximum amplitude is determined from the equation $V^+(x_1) = y_0^2/2$, i.e., from

$$\int_{x_0}^{x_1} e^{2F(s)}g(s)ds = \frac{1}{2}y_0^2. \tag{3.15}$$

Continuing the trajectory to below the x-axis means that it is now determined by the equation

$$H^- = \frac{1}{2}e^{-2F(x)}y^2 + V^-(x) = K_1^-$$

where the constant K_1^- is determined by the new initial condition $(x_1, 0)$ which represents the first turning point. This gives $K_1^- = V^-(x_1)$ so that beneath the x-axis the trajectory is given by

$$\frac{1}{2}e^{-2F(x)}y^2 + V^-(x) = V^-(x_1).$$

At the next turning point we have $(x = x_2, y = 0)$ and

$$V^-(x_2) = V^-(x_1), \quad (x_2 < 0) \tag{3.16}$$

which allows for the determination of x_2. After this we are again above the x-axis and the trajectory is given by $H^+ = K_2^+$ with $K_2^+ = V^+(x_2)$. Continuing in this manner we may summarize the points of intersections with the x-axis by stating that:
if i =odd then x_{i+1} is determined by

$$V^-(x_{i+1}) = V^-(x_i)$$

and if i =even then x_{i+1} is determined by

$$V^+(x_{i+1}) = V^+(x_i).$$

3.3.1 Closed and Damped Orbits

Systems given by (3.12) and (3.13) do not always show damped behaviour. The as their qualitative features depend on $f(x)$. We consider two cases: $f(x) = 0.5$ and $f(x) = 3x$

	Amplitudes ($\lvert x_n \rvert$)
x_1	0.7680390470134656
x_2	0.5049710640693359
x_3	0.37698121404812546
x_4	0.3009607508865283
x_5	0.2505262046138416
x_6	0.21459868739856763
x_7	0.18769746691321143
x_8	0.166796834446442
x_9	0.15008870326261628

Table 3.1: Values for the amplitudes in each half cycle when $f(x) = 0.5$ and $g(x) = x$ for the system described by (3.1) and (3.2).

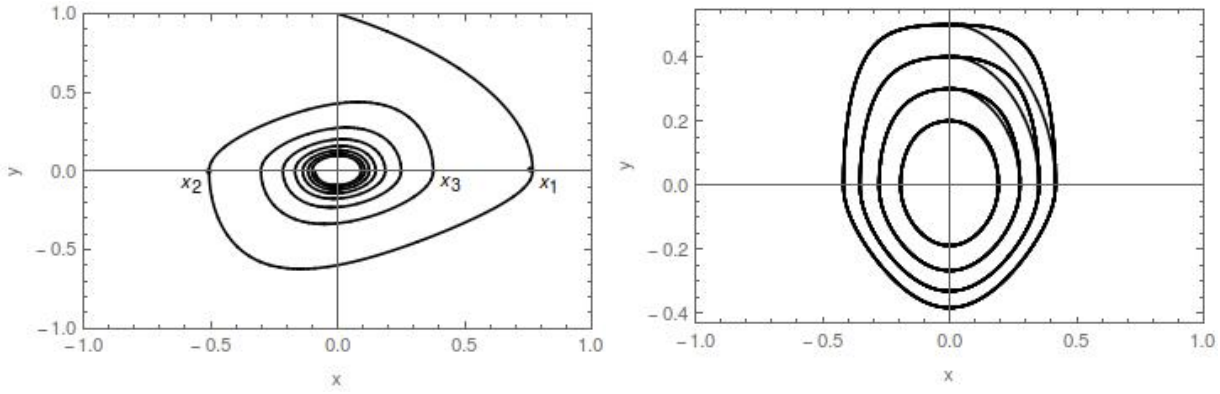

(a) (a) (b) (b)

Figure 3.2: Phase plots for the system described by (3.12) and (3.13) when (a) $f(x) = 0.5$ and $g(x) = x$ showing the spiralling nature of the trajectory and (b) $f(x) = 3x$ and $g(x) = x + x^3$ for which the orbits are closed.

with $g(x) = x$ and $g(x) = x + x^3$, respectively. Figure 3.2 shows the plot for both the cases in phase space. When $f(x) = 0.5$ the amplitude continuously diminishes and the trajectory is a spiral. Table 3.1 below gives the values of the amplitudes for each half of the cycle. In this case the damping force has the same sign as the linear damped oscillator in each of the four quadrants. Indeed whenever $f(x)$ is an even function this feature is present.

However when $f(x) = 3x$ one finds that the orbits are closed. Figures 3.2a and 3.2b shows the orbits for four initial conditions. In this case the damping force alternates in sign in each of the four quadrants – a feature shared by all odd functions $f(x)$.

In Figure 3.3 the potentials $V^{\pm}(x)$ are plotted for both the cases under study. From the figure, it is clear that there are initial conditions for which bounded solutions exists in both cases.

Now, consider the kinetic part. In our case the mass term is position dependent and it plays a key role in whether there is closed or damped orbit. The main idea is the mass term depends on $F(x)$ only. Consider figure 3.4 of contour plots of Hamiltonian in the

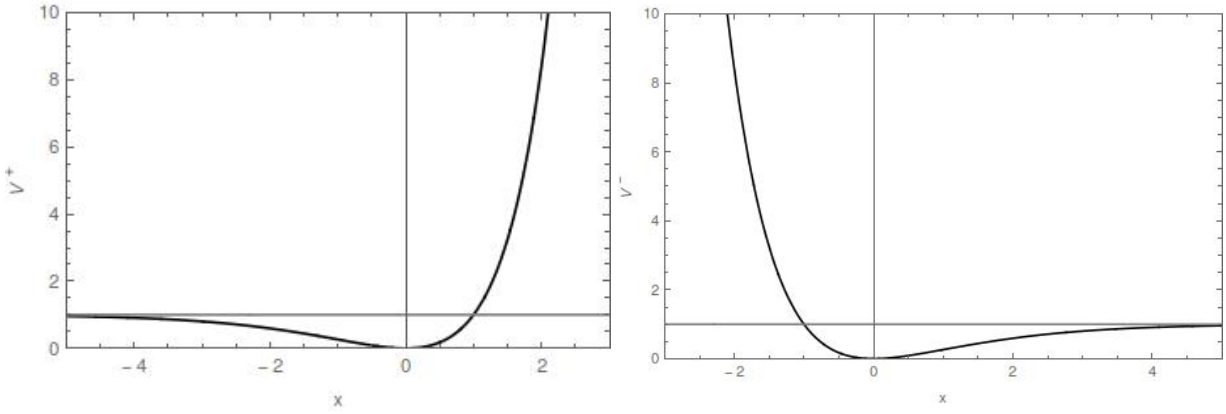

(a) $V^+(x)$

(b) $V^-(x)$

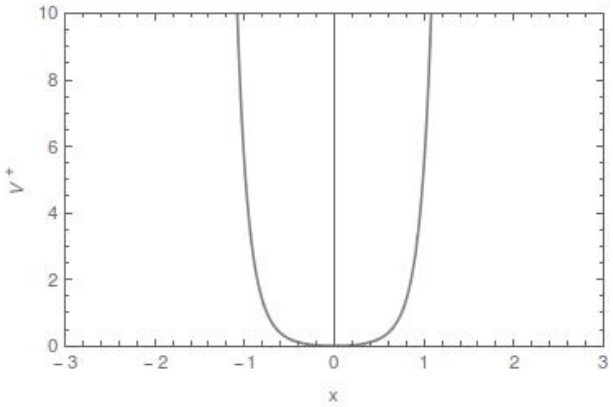

(c) $V^+(x)$

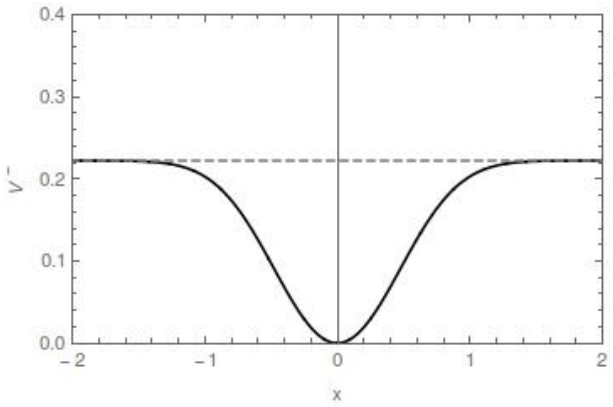

(d) $V^-(x)$

Figure 3.3: Plots of the potentials $V^{\pm}(x)$ for the system in (3.12) and (3.13) when $f(x) = 0.5$ and $g(x) = x$ in (a, b) and when $f(x) = 3x$ and $g(x) = x + x^3$ in (c, d).

two cases. In the first case, $f(x)$ is constant and so even and therefore $F(x)$ is odd. While in the second case, $f(x)$ is odd function and $F(x)$ is even and its evident from the plots that Hamiltonian is symmetric about the y-axis.

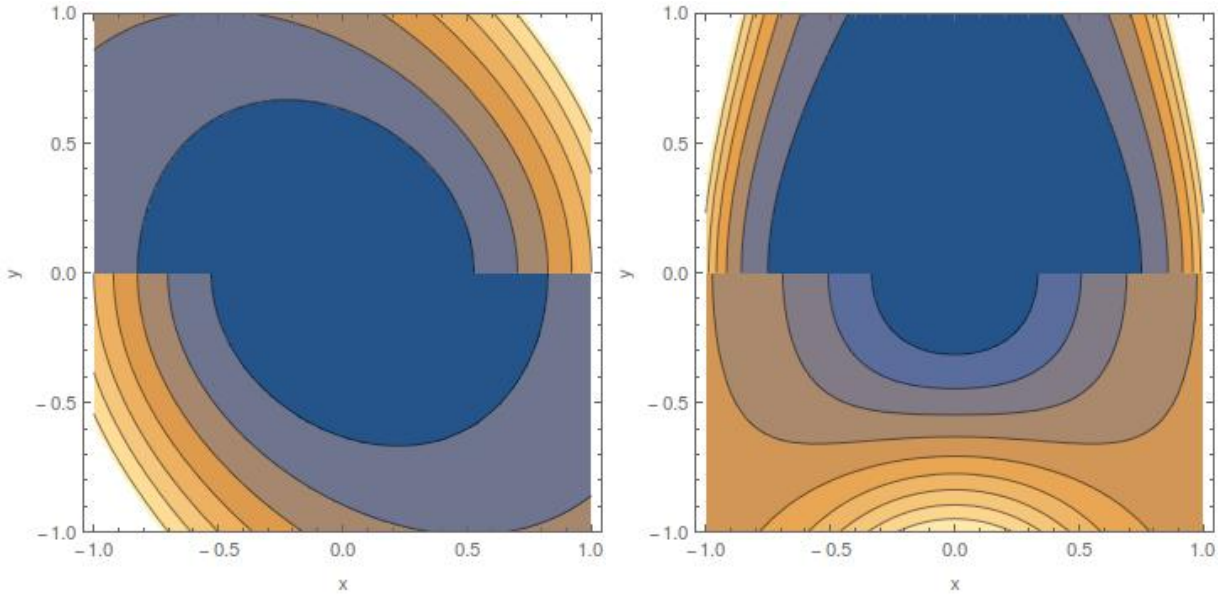

(a) $f(x) = 0.5$, and $g(x) = x$ (b) $f(x) = 3x$ and $g(x) = x + x^3$

Figure 3.4: Contour plots of Hamiltonian of (3.12), (3.13) defined (3.14) for different combinations of $f(x)$ and $g(x)$.

Figure 3.5 depicts the behaviour of higher degree functions.

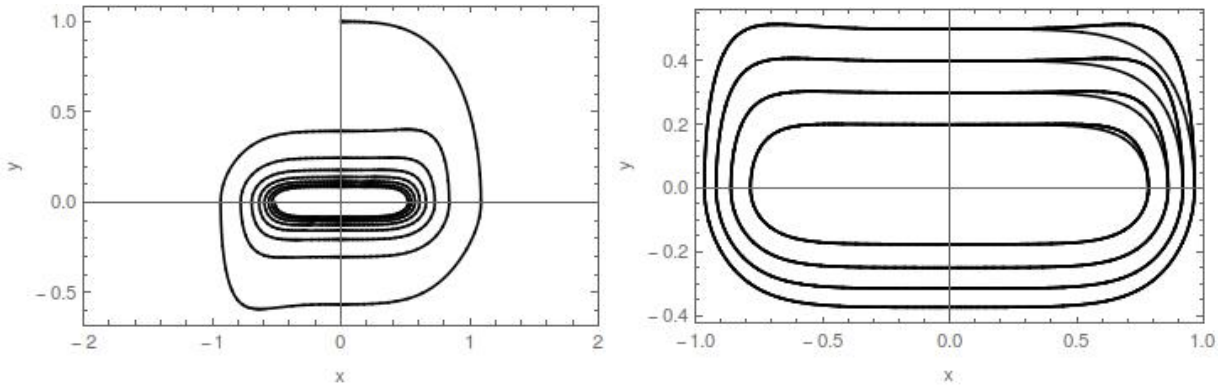

(a) (b)

Figure 3.5: Phase space plots of the system (3.12) and (3.13) for higher degree polynomial $f(x)$ and $g(x)$: (a) when $f(x) = x^2, g(x) = x^5$ and (b) when $f(x) = x^3, g(x) = x^7$ showing the spiral nature of the trajectory for even f and the closed orbits for odd f.

3.3.2 Analytic results based on Chiellini integrability condition

It is interesting to observe that invocation of the Chiellini condition for integrability allows us to determine analytically the maximum amplitudes. This may be accomplished by noting that as

$$V^{\pm}(x_i) = \int_{x_0}^{x_i} e^{\pm 2F(s)} g(s) ds = \int_{x_0}^{x_i} e^{\pm 2F(s)} \frac{g(s)}{f(s)} f(s) ds$$

where $F(x) = \int_{x_0}^{x} f(s) ds \Longleftrightarrow F'(x) = f(x)$, we have after integrating by parts and using the Chiellini integrability condition,

$$\frac{d}{dx}\left(\frac{g}{f}\right) = \mu f(x), \quad \mu = const.(\neq 0), \tag{3.17}$$

$$V^{\pm}(x_i) = \frac{1}{(\pm 2)} e^{\pm 2F(s)} \left(\frac{g(s)}{f(s)} - \frac{\mu}{(\pm 2)}\right)\Big|_{x_0}^{x_i}. \tag{3.18}$$

The Chiellini integrability condition was derived in the context of exact integrability of the Abel equation of first kind [14, 15]

$$\frac{dv}{dx} = f(x)v^2 + g(x)v^3.$$

A second-order ODE of the Liénard type, $\ddot{x} + f(x)\dot{x} + g(x) = 0$, may be transformed to the first-order Abel equation of the above type by the transformation $\dot{x} = 1/v$. A proof of the exact integrability of the Abel equation using the Chiellini condition is given in [16] and the class of exact solutions of the Liénard equation in parametric form is derived. Extension of the Chiellini integrability condition to the general Abel equation is also dealt with in [16].

Recently it has been demonstrated in [32] that the Liénard equation, $y''(z) + f(y)y'(z) + g(y) = 0$, can be mapped to the linear equation $\omega_{\zeta\zeta} + \sigma\omega_{\zeta} + \omega = 0$ by the transformation $\omega = F(y), d\zeta = G(y)dz$ where $G(y) = f(y)/\sigma$ and $F(y) = \lambda(\int f(y)dy + \kappa)$ provided the Chiellini condition namely $d/dy(f/g) = const.f$ is satisfied. The condition (3.17) implies that $g/f = \mu F(x) + \nu$ where ν is an arbitrary constant of integration. Clearly the functions f and g are no longer functionally independent. This severely restricts the class of equations of the Liénard type that can be analytically solved in parametric form. Nonetheless if f and g are certain prescribed functions which do satisfy the Chiellini condition then it is a straightforward matter to read off the values of the constants μ and ν from the aforementioned ratio.

Now by defining $\eta_{\pm} = (\pm 2\nu - \mu)/\mu$ and introducing the function $G_{\pm}(x) = \pm 2F(x) + \eta_{\pm}$, the expression for the potential in (3.18) can be put into the form

$$V^{\pm}(x_i) = \frac{\mu}{4} e^{-\eta_{\pm}} \left[e^{G_{\pm}(x_i)} G_{\pm}(x_i) - e^{G_{\pm}(x_0)} G_{\pm}(x_0)\right]. \tag{3.19}$$

As mentioned in (3.4) the first turning point is given by a solution of $V^+(x_1) = y_0^2/2$ which is positive or more explicitly by a positive solution of

$$e^{G_+(x_1)}G_+(x_1) = e^{G_+(x_0)}G_+(x_0) + \frac{2y_0^2}{\mu}e^{\eta_+}. \tag{3.20}$$

In general it is possible to find recursively the subsequent turning points which are the solutions with proper signs of the equation

$$e^{G_\pm(x_{i+1})}G_\pm(x_{i+1}) = e^{G_\pm(x_i)}G_\pm(x_i), \quad +(-) \text{ for } i = \text{even(odd)}. \tag{3.21}$$

Eqn.(3.21) has the appearance $e^X X = Y$ which is the the standard form of the Lambert equation and its solutions are given by the Lambert W function, i.e, $X = W(Y)$. Hence it follows that

$$G_\pm(x_{i+1}) = W\left(e^{G_\pm(x_i)}G_\pm(x_i)\right), \tag{3.22}$$

from which we can formally determine

$$x_{i+1} = G_\pm^{-1}\left(W\left(e^{G_\pm(x_i)}G_\pm(x_i)\right)\right), \quad +(-) \text{ for } i = \text{even(odd)} \tag{3.23}$$

if the function $G_\pm$ is invertible. Therefore we conclude that if the Chiellini condition is fulfilled by the functions f and g then the maximum amplitudes can be determined recursively in terms of the Lambert W function.

3.3.3 Analysis of the period function

Starting from the initial point (x_0, y_0) if the first intersection with the x-axis is at $x = x_1(> 0)$ then subsequently the trajectory is determined by the condition

$$\frac{1}{2}e^{-2F(x)}y^2 + V^-(x) = V^-(x_1).$$

If the next turning point, i.e., the next intersection with the negative x-axis is at $x = x_2$ then the time for the transit of the half-cycle from x_1 to x_2 is given by

$$\tau_{12} = \frac{1}{\sqrt{2}}\int_{x_2}^{x_1}\frac{e^{-F(x)}dx}{\sqrt{V^-(x_1) - V^-(x)}}. \tag{3.24}$$

Similarly the time taken for the transit of the next-half cycle from x_2 on the negative x-axis to x_3 on the positive x-axis is given by

$$\tau_{23} = \frac{1}{\sqrt{2}}\int_{x_2}^{x_3}\frac{e^{F(x)}dx}{\sqrt{V^+(x_2) - V^+(x)}}. \tag{3.25}$$

Cycle(n^{th})	T_n	ΔE_n
1	6.360502498547287	0.08805266518005395
2	6.308066845017076	0.01833863366586541
3	6.295534499523865	0.006618943128696708
4	6.29057350609154	0.0031022724220284292
5	6.288104015677968	0.0016959179654737477
6	6.286695917618085	0.0010263408918240735
7	6.285816631877343	0.0006676772782294726
8	6.285230961390923	0.0004584700142998832
9	6.284821348882355	0.0003283012470082225

Table 3.2: Time periods and the corresponding changes in the energy in each cycle when $f(x) = 0.5$.

(x_0, y_0)	T
$(0, 0.2)$	6.197928744154146
$(0, 0.3)$	6.111126244536706
$(0, 0.4)$	6.014565567199962
$(0, 0.5)$	5.918345639978987

Table 3.3: Time periods of the cycles when $f(x) = 3x$ for different initial conditions.

Thus the time taken for the completion of the first cycle is $T_1 = \tau_{12} + \tau_{23}$, viz

$$T_1 = \frac{1}{\sqrt{2}} \left[-\int_{x_1}^{x_2} \frac{e^{-F(x)}dx}{\sqrt{V^-(x_1) - V^-(x)}} + \int_{x_2}^{x_3} \frac{e^{F(x)}dx}{\sqrt{V^+(x_2) - V^+(x)}} \right]. \tag{3.26}$$

In fact it is straightforward to generalize this formula for the n-th cycle which is given by

$$T_n = \frac{1}{\sqrt{2}} \left[-\int_{x_{2n-1}}^{x_{2n}} \frac{e^{-F(x)}dx}{\sqrt{V^-(x_{2n-1}) - V^-(x)}} + \int_{x_{2n}}^{x_{2n+1}} \frac{e^{F(x)}dx}{\sqrt{V^+(x_{2n}) - V^+(x)}} \right]. \tag{3.27}$$

The energy dissipated in the n-th cycle is given by

$$\Delta E_n = V^-(x_{2n-1}) - V^+(x_{2n}). \tag{3.28}$$

Table 3.2 gives the values of the time periods and the changes in the energy for the case $f(x) = 0.5$ while Table 3.3 shows the time periods of the closed orbits for three different initial conditions when $f(x) = 3x$. Note that we have assumed that the energy of the system is given by the Hamiltonian, which is a constant of motion, and differs therefore from the mechanical energy used by other authors [7].

3.3.4 Analytic Solutions

As for the solution of (3.12) and/or (3.13) it will be observed that as $H^{\pm}$ in (3.14) is a constant of motion therefore on the level curves, $H^{\pm} = E^{\pm}$, one has

$$\dot{x} = \pm\sqrt{2(E^{\pm} - V^{\pm}(x))}e^{\mp F(x)}, \tag{3.29}$$

where

$$V^{\pm}(x) = \int_{x_0}^{x} e^{\pm 2F(s)} \frac{g(s)}{f(s)} f(s)ds.$$

Upon imposing the Chiellini integrability condition it follows from (3.7) that the potential is given by

$$V^{\pm}(x) = \frac{\mu}{4} e^{-\eta_{\pm}} \left[e^{G_{\pm}(x)} G_{\pm}(x) - e^{G_{\pm}(x_0)} G_{\pm}(x_0) \right].$$

Substituting this into (3.29) we have

$$\frac{dx}{dt} = \pm\sqrt{\frac{\mu}{2}} e^{-\eta_{\pm}/2} \sqrt{K^{\pm} - e^{G_{\pm}(x)} G_{\pm}(x)} e^{\mp F(x)},$$

where $K^{\pm}$ is a constant. Hence it follows that the solution is reducible to quadrature

$$t = \pm\sqrt{\frac{2}{\mu}} \int_{x_0}^{x} \frac{e^{G_{\pm}(s)/2} ds}{\sqrt{K^{\pm} - e^{G_{\pm}(s)} G_{\pm}(s)}}.$$

3.4 Conclusion

In this work, a Liénard type equation with quadratic damping has been considered. It is observed that in order to incorporate damping it is first of all necessary to introduce a discontinuity in the equation depending upon the sign of the velocity. We observe further that if the function $f(x)$ is even then the motion is damped with the amplitudes decreasing in each cycle. However, when $f(x)$ is an odd function then the effects of the damping and the change in the sign of the velocity when taken together no longer lead to damped motion but instead give rise to closed orbits with fixed amplitudes. We have shown that by imposing the Chiellini condition of integrability on the functions f and g one can subsume many of the previous examples into a compact scheme. Incidentally the Chiellini condition is typically encountered in the context of integrability of the standard Liénard equation in course of its transformation to the first-order Abel equation of the first kind and also while finding a Lagrangian/Hamiltonian description of the Liénard equation. But its appearance in the analytical determination of the the amplitudes of motion via the Lambert W function certainly seems to be new. Finally using the Chiellini integrability condition it is possible to obtain the solutions of (3.12) and (3.13) up to a quadrature.

Clearly it would be interesting to generalize the present results to the situation where the nonlinear restoring force is of the form $\mathcal{F}(x) = ksgn(x)|x|^{\alpha}$; such a model has been investigated by Kovacic et al. [11].

Bibliography

[1] José P Baltanás, José L Trueba, and Miguel AF Sanjuán. Energy dissipation in a nonlinearly damped duffing oscillator. *Physica D: Nonlinear Phenomena*, 159(1-2):22–34, 2001.

[2] C Beards. *Engineering vibration analysis with application to control systems*. Elsevier, 1995.

[3] Yun Fong Lim and Kan Chen. Dynamics of dry friction: A numerical investigation. *Physical Review E*, 58(5):5637, 1998.

[4] Jeffrey M Falzarano, Steven W Shaw, and Armin W Troesch. Application of global methods for analyzing dynamical systems to ship rolling motion and capsizing. *International journal of bifurcation and chaos*, 2(01):101–115, 1992.

[5] Yongjun Shen, Shaopu Yang, Haijun Xing, and Guosheng Gao. Primary resonance of duffing oscillator with fractional-order derivative. *Communications in Nonlinear Science and Numerical Simulation*, 17(7):3092–3100, 2012.

[6] Marek Borowiec, Grzegorz Litak, and Arkadiusz Syta. Vibration of the duffing oscillator: effect of fractional damping. *Shock and Vibration*, 14(1):29–36, 2007.

[7] Livija Cvetićanin. Oscillator with strong quadratic damping force. *Publications de l'Institut Mathématique*, (99), 2009.

[8] Livija Cveticanin. Analysis techniques for the various forms of the duffing equation. *The Duffing Equation: Nonlinear Oscillators and their Behaviour [Internet]. Chichester, UK: John Wiley & Sons, Ltd*, pages 81–137, 2011.

[9] Temple H Fay. Quadratic damping. *International Journal of Mathematical Education in Science and Technology*, 43(6):789–803, 2012.

[10] Karl Klotter. Free oscillations of systems having quadratic damping and arbitrary restoring forces. *J. appl. Mech*, 22(4):493–499, 1955.

[11] Ivana Kovacic and Zvonko Rakaric. Study of oscillators with a non-negative real-power restoring force and quadratic damping. *Nonlinear Dynamics*, 64(3):293–304, 2011.

[12] Steven H Strogatz. *Nonlinear dynamics and chaos with student solutions manual: With applications to physics, biology, chemistry, and engineering*. CRC press, 2018.

[13] Ali H Nayfeh and Dean T Mook. *Nonlinear oscillations*. John Wiley & Sons, 2008.

[14] A Chiellini. Sullintegrazione dellequazione differenziale y'+ py2+ qy3= 0. *Bollettino dell Unione Matematica Italiana*, 10:301–307, 1931.

[15] Tiberiu Harko, Francisco SN Lobo, and MK Mak. A chiellini type integrability condition for the generalized first kind abel differential equation. *arXiv preprint arXiv:1310.1508*, 2013.

[16] Tiberiu Harko, Francisco SN Lobo, and MK Mak. A class of exact solutions of the liénard-type ordinary nonlinear differential equation. *Journal of Engineering Mathematics*, 89(1):193–205, 2014.

[17] M Robert, GH Corless, DEG Gonnet, DJ Hare, and DEK Jeffrey. On the lambert w function. *Advances in Computational Mathematics*, 5(4):329–359, 1996.

[18] Johann Heinrich Lambert. Observationes variae in mathesin puram. *Acta Helvetica*, 3(1):128–168, 1758.

[19] Carl Gustav Jakob Jacobi. *Sul principio dellultimo moltiplicatore e suo uso come nuovo principio generale di meccanica*. 1844.

[20] CGJ Jacobi. Theoria novi multiplicatoris systemati aequationum differentialium vulgarium applicandi. *Journal fúr die reine und angewandte Mathematik*, 1844(27):199–268, 1844.

[21] S Lie. Veralgemeinerung und neue verwerthung der jacobischen multiplicator-theorie. *Christ. Forh*, 255274, 1874.

[22] Sophus Lie. Vorlesungen über differentialgleichungen mit bekannten infinitesimalen transformationen. *Bull. Amer. Math. Soc*, 4:155–167, 1898.

[23] MC Nucci and PGL Leach. Jacobi's last multiplier and symmetries for the kepler problem plus a lineal story. *Journal of Physics A: Mathematical and General*, 37(31):7743, 2004.

[24] MC Nucci and KM Tamizhmani. Lagrangians for dissipative nonlinear oscillators: the method of jacobi last multiplier. *Journal of Nonlinear Mathematical Physics*, 17(2):167–178, 2010.

[25] Edmund Taylor Whittaker. *A treatise on the analytical dynamics of particles and rigid bodies*. Cambridge university press, 1988.

[26] BS Madhava Rao. On the reduction of dynamical equations to the lagrangian form. *Proc. Benaras Math. Soc.(NS)*, 2:53–59, 1940.

[27] MC Nucci and PGL Leach. The jacobi last multiplier and its applications in mechanics. *Physica Scripta*, 78(6):065011, 2008.

[28] A Ghose Choudhury, Partha Guha, and Barun Khanra. On the jacobi last multiplier, integrating factors and the lagrangian formulation of differential equations of the painlevé–gambier classification. *Journal of Mathematical Analysis and Applications*, 360(2):651–664, 2009.

[29] M Sabatini. On the period function of liénard systems. *journal of differential equations*, 152(2):467–487, 1999.

[30] A Ghose Choudhury and Partha Guha. On isochronous cases of the cherkas system and jacobi's last multiplier. *Journal of Physics A: Mathematical and Theoretical*, 43(12):125202, 2010.

[31] Partha Guha and A Ghose Choudhury. The jacobi last multiplier and isochronicity of liénard type systems. *Reviews in Mathematical Physics*, 25(06):1330009, 2013.

[32] Nikolay A Kudryashov and Dmitry I Sinelshchikov. On the criteria for integrability of the liénard equation. *Applied Mathematics Letters*, 57:114–120, 2016.

Chapter 4

Strongly Nonlinear Oscillators

Nonlinearities make differential equations difficult to solve and, in general, prohibit them to obtain explicit solutions expressible in finite terms. For this, dynamical system theory allows linear approximations of such systems through the method of *linearisation* (explained in second chapter). This simplification permits an approximation of the solution, and further analysis of the system. However, there are dynamical systems for which such linearisation methods does not work. Such systems either have nonlinear terms which strong in comparison to the linear term or there are no linear terms present in the equation. These are referred to as strongly nonlinear systems, defined in [1]. For these systems the linear approximation of the nonlinearity around the origin is not possible which restricts to study the dynamical features of the system..

Strong nonlinearity appears quite naturally in physical systems, especially in engineering sciences. In many experimental studies it is found that various materials such as aircraft materials, [2, 3], ceramic materials, [4], alloys, [5, 6], polymers, [7, 8], etc,. show strongly nonlinear behaviours in their stress-strain relations. The stress-strain relations determine restoring forces on the material which, in turn, defines the amplitude and frequency profile of the oscillation dynamics. In the linear regime, the stress-strain relationship is given by Hooke's law. For Hooke's systems, the potential is of quadratic form and the restoring force is linearly proportional to the displacement. However, this law is valid for small displacements only and as the displacement of the material is increased beyond a limit the material starts to behave in nonlinear manner. This linear approximation is sometimes called *harmonic approximation* and the deviation from the linear regime is termed *anharmonic* effects.

The various applications of strongly nonlinear systems demands persistent theoretical developments. Concerned with such problems, nonlinear dynamics practitioners have shown much interest in recent decades, [9, 10, 11, 12]. A very prominent text would be the book by *Livija Cveticanin*, [1], which inspired the studies in this chapter as well as the title. Another eminent book about this subject is by *Ronald E Mickens*, [13], where various analytical methods for the treatment of such systems are compiled. To deal with such problems there are various approximation techniques developed over the course of time, some notable methods includes the harmonic balance method, [14, 15], asymptotic methods, [16, 17, 18], modified Lindstedt-Poincaré method, [19, 20], variational methods,

[21] and others. These methods provide good insights into the working of the system and helps in understanding the form of the solution. However, because of the approximation, and lack of tools inhibits the approaches to appreciate the dynamical aspects of such systems.

In this chapter, I considered two studies consisting of strongly nonlinear oscillators. In the first study, I have considered purely nonlinear potential systems which are of the form $sgn(x)|x|^{\alpha}$, where $sgn(x)$ is signum function which return the sign of the argument, and α is the order of nonlinearity. In experiments it was found that α can be an integer or non-integer, [22, 23, 24, 25, 26]. Strong nonlinearities need not come from the potential part of the system. In the next study, I considered a system with quadratic damping experiencing a strongly nonlinear restoring force of generalised nature.

4.1 Nonlinear Oscillator: $\ddot{x} + c_{\alpha}^2 sgn(x)|x|^{\alpha} = 0$ [1]

From a theoretical point of view it is always desirable to have exact or accurate analytical approximations for the solutions of such equations. Lyapunov showed that when restoring force is proportional to an odd integer power of the displacement then the solution can be expressed in terms of the generalised cosine and sine functions denoted by cn and sn respectively.

On the other hand for the systems of the form

$$\ddot{x} + c_{\alpha}^2 sign(x)|x|^{\alpha} = 0, \tag{4.1}$$

or the allied system

$$\ddot{x} + c_{\alpha}^2 x|x|^{\alpha-1} = 0,$$

where α is not necessarily a positive integer and the solutions are described by Ateb functions (see appendix) which are the inverses of the incomplete Beta function.
As a generalisation of the potential $x^{4/3}$ an exact formula for the time period of the oscillation of the system (4.1) subject to the initial conditions $x(0) = A$ and $\dot{x}(0) = 0$ is given in [28],

$$T = \sqrt{\frac{8\pi}{c_{\alpha}^2(\alpha+1)}} \frac{\Gamma\left(\frac{1}{\alpha+1}\right)}{\Gamma\left(\frac{\alpha+3}{2(\alpha+1)}\right)} |A|^{\frac{1-\alpha}{2}}, \tag{4.2}$$

where Γ represents Euler Gamma function. The formula reduces to $\frac{2\pi}{c_{\alpha}}$ when $\alpha = 1$ which corresponds to linear harmonic oscillator. The solution may be expressed by the three argument Ateb function

$$x = A\, ca(\alpha, 1, \omega_{ca} t),$$

[1] This is part of published work, [27]

with frequency given by

$$\omega_{ca} = |A|^{\frac{\alpha-1}{2}} \sqrt{\frac{c_\alpha^2(\alpha+1)}{2}}.$$

It is evident that the frequency is in general amplitude dependent, unless $\alpha = 1$, which is the linear case.

4.1.1 Time period using Symmetrization Procedure

In this section we will explain the potential Symmetrization procedure given by Mañosas and Torres in [29]. In the process we consider the potential function of purely nonlinear oscillator. The expression for the potential energy of the system govern by (4.26) is given by

$$U(x) = \frac{c_\alpha^2}{\alpha+1}|x|^{\alpha+1}, \tag{4.3}$$

where it is clear that $U(0) = U'(0) = 0$ such that $U(x)$ has a local minima at origin, then we can define an involution by

$$U(\sigma(x)) = U(x), \quad \& \quad x\sigma \leq 0. \tag{4.4}$$

Now, let us define

$$g(x) = sign(x)\sqrt{V(x)}. \tag{4.5}$$

Combining this with the involution (4.4), we have

$$\begin{aligned} g(\sigma(x)) &= sign(\sigma(x))\sqrt{U(\sigma(x))}, \\ or \quad g(\sigma(x)) &= -sign(x)\sqrt{U(x)}, \\ or \quad g(\sigma(x)) &= -g(x), \\ or \quad \sigma(x) &= g^{-1}(-g(x)). \end{aligned} \tag{4.6}$$

For our potential

$$g(x) = sign(x)\frac{c_\alpha}{\sqrt{\alpha+1}}|x|^{\frac{\alpha+1}{2}}. \tag{4.7}$$

Also

$$g^{-1}(x) = sign(x)\left(\frac{\sqrt{\alpha+1}}{c_\alpha}|x|^{\frac{2}{\alpha+1}}\right). \tag{4.8}$$

Now set $h(x) = \frac{x-\sigma(x)}{2}$, and define the symmetrized potential as $\tilde{U} = U \circ h^{-1}$. The basic properties of h and $\tilde{U}$ are

Lemma 4.1.1 *The following assertions hold:*

- $h(\sigma(x)) = -h(x)$;
- $U(x) = \tilde{U}(h(x))$ *and* $\tilde{U}$ *is an even function;*
- $h^{-1}(x) - h^{-1}(-x) = 2x$.

The lemma is part of [29] and the proof could be found there. Now, for the symmetric potential, we define

$$\tilde{g}(x) = sign(x)\sqrt{\tilde{U}(x)},$$

which is an analytic odd diffeomorphism defined in $h(P)$ and $g = \tilde{g} \circ h$. For our case, $h(x) = x$, therefore we have

$$g(x) = \tilde{g}(h(x)) = \tilde{x}(x).$$

Consequently from (4.8) we have

$$\tilde{g}(x) = sign(x)\frac{c_\alpha}{\sqrt{\alpha+1}}|x|^{\frac{\alpha+1}{2}}, \tag{4.9}$$

and

$$\tilde{g}^{-1}(x) = sign(x)\left(\frac{\sqrt{\alpha+1}}{c_\alpha}|x|^{\frac{2}{\alpha+1}}\right). \tag{4.10}$$

Now if $T_{V(x)}$ and $T_{\tilde{V}}(y)$ denotes time period corresponding to the potentials $V(x)$ and $\tilde{V}(y)$, respectively and $x \in P$, $y \in h(P)$, then we have the following theorem,

Theorem 4.1.1

$$T_U(x) = 2\sqrt{2}\int_0^{\frac{x}{2}} (\tilde{g}^{-1})'(\tilde{g}(h(x))sin(\theta))d\theta = T_{\tilde{U}}(h(x)).$$

The proof of the theorem in given in [29]. The theorem shows that using the above construction any potential can be transformed to a symmetric potential keeping the time-period invariant. Now using the result from the theorem the time-period for our case is given as,

$$T_U(x_0) = \frac{4\sqrt{2}}{c_\alpha\sqrt{\alpha+1}}|x_0|^{\frac{1-\alpha}{2}}\int_0^{\frac{\pi}{2}} (\sin\theta)^{\frac{1-\alpha}{1+\alpha}}d\theta,$$

or

$$T_U(x_0) = \sqrt{\frac{8\pi}{c_\alpha^2(\alpha+1)}} \frac{\Gamma\left(\frac{1}{\alpha+1}\right)}{\Gamma\left(\frac{\alpha+3}{2(\alpha+1)}\right)} |x_0|^{\frac{1-\alpha}{2}}, \tag{4.11}$$

which exactly matches with the results obtained in [30].

The construction done in this section transform an asymmetric potential into a symmetric potential keeping the time-period in the process invariant. Although the case considered is already symmetric, the recipe is applicable in general. For purely nonlinear oscillators calculation of frequency is not straightforward, however, the method described here is helpful for such purposes. This will be more clear in the next section where we consider isotonic and generalised isotonic potential systems and obtain the corresponding time-periods using the symmetrization arguments.

4.2 On Generalised Isotonic Potential [2]

The potential of linear harmonic oscillator (LHO) given by, $\omega^2 x^2/2$,is a rational function having a minimum at the origin $x = 0$ and is symmetric. The LHO is characterized by the fact that its time period is independent of the amplitude. Although there are several instances of differential equations exhibiting periodic motion, it is indeed rare to find systems displaying periodic motions with an amplitude independent time period. Such systems are said to be *isochronous* and apart from the LHO there is only one isochronous system with a rational potential namely the isotonic oscillator [31]. The equation of motion, given by $\ddot{x} + \omega^2 x = l^2/x^3$, is nonlinear and derived from the isotonic potential, $V(x) = \omega^2 x^2 + l^2/x^2$. The potential consists of two branches separated by the asymptote $x = 0$ with each branch being as asymmetric curve displaying a minima. Physically a system governed by the isotonic potential corresponds to a simplest two-body case of the N-body translational invariant Calogero model [32] and is of great interest in quantum optics [33] and in the theory of coherent states [34, 35].

In this study we will consider isotonic potential system and, utilising the symmetrization arguments from previous section, an analytical expression for system will be obtained. Later, we generalise the isotonic potential and calculate the generalise time period expression.

4.2.1 Isotonic Potential: A brief recap and time-period calculation

Consider an isotonic potential given by

$$V(\zeta) = a\zeta^2 + \frac{b}{\zeta^2}, \ -\infty < \zeta < \infty. \tag{4.12}$$

[2] This is part of published work, [27]

It has two branches with minima at $\zeta = \pm\zeta_0$, where $V'(\zeta_0) = 0$, from which we have

$$2a\zeta_0 - \frac{2b}{\zeta_0^3} = 0 \quad \text{or} \quad \zeta_0 = \left(\frac{b}{a}\right)^{1/4},$$

and

$$V(\zeta_0) = a\left(\frac{b}{a}\right)^{1/2} + b\left(\frac{b}{a}\right)^{1/2} = 2\sqrt{ab}.$$

We consider only the branch for which $0 < \zeta < \infty$ and introduce a transformation of coordinates such that

$$\zeta \to \tilde{x} = \zeta - \zeta_0, \;\; V(\zeta) \to V(\tilde{x}) = V(\zeta) - 2\sqrt{ab}, \quad -\zeta_0 < \tilde{x} < \infty. \tag{4.13}$$

Consequently we find that

$$\begin{aligned} V(\tilde{x}) &= a\left(\frac{b}{a}\right)^{1/2}\left(\frac{\tilde{x}}{\zeta_0} + 1\right)^2 + \left(\frac{a}{b}\right)^{1/2}\frac{b}{\left(\frac{\tilde{x}}{\zeta_0} + 1\right)^2} - 2\sqrt{ab} \\ &= \sqrt{ab}\left[\left(\frac{\tilde{x}}{\zeta_0} + 1\right)^2 + \frac{1}{\left(\frac{\tilde{x}}{\zeta_0} + 1\right)^2} - 2\right]. \end{aligned} \tag{4.14}$$

Upon introduction of the scaling transformations
$x = \tilde{x}/\zeta_0, \;\; V(\tilde{x}) \to U(x) = \frac{k}{2}\frac{V(\tilde{x})}{\sqrt{ab}}$, it follows that

$$U(x) = \frac{k}{2}\left((x+1) - \frac{1}{(x+1)}\right)^2, \;\; -1 < x < \infty, \tag{4.15}$$

and the corresponding equation of motion is therefore given by

$$\begin{aligned} \ddot{x} &= -\frac{dU}{dx} \\ &= -k(x+1) + \frac{k}{(x+1)^3}, \end{aligned} \tag{4.16}$$

which may be more neatly expressed in terms of, $q = x + 1$, as

$$\ddot{q} + kq - \frac{k}{q^3} = 0, \quad 0 < q < \infty.$$

It will be observed that $U(x)$ is an asymmetric potential and for every $x \in (-1, \infty) \quad \exists \quad \sigma(x) \in (-1, \infty)$ such that $U(\sigma(x)) = U(x)$ with $x\sigma(x) < 0$. We define a function $g(x)$ by

$$g(x) = sgn(x)\sqrt{U(x)} = sgn(x)\frac{\sqrt{k}}{\sqrt{2}}\left(x + 1 - \frac{1}{x+1}\right).$$

It follows that

$$\begin{aligned} g(\sigma(x)) &= sgn(\sigma(x))\sqrt{U(\sigma(x))} \\ &= -sgn(x)\sqrt{U(x)} = -g(x), \end{aligned}$$

which clearly gives $\sigma(x) = g^{-1}(-g(x))$. However, *the bijectivity of* $g(x)$ *must be established.*
In general, for $x > 0$

$$\begin{aligned} & g(x) = \sqrt{U(x)} = \sqrt{\frac{k}{2}}\left(x + 1 - \frac{1}{x+1}\right) = y, \\ \Longrightarrow \quad & (x+1)^2 - \sqrt{\frac{2}{k}}(x+1)y - 1 = 0, \\ \Longrightarrow \quad & x + 1 = \frac{1}{2}\left[\frac{2}{k}y + \sqrt{\frac{2}{k}y^2 + 4}\right], \\ \Longrightarrow \quad & x = -1 + \frac{1}{\sqrt{2k}}y + \sqrt{\frac{1}{2k}y^2 + 1} = g^{-1}(y). \end{aligned}$$

Hence

$$\sigma(x) = g^{-1}(-g(x)) = -1 + \frac{1}{\sqrt{2k}}(-g(x)) + \sqrt{\frac{1}{2k}(-g(x))^2 + 1},$$

which simplifies to

$$\sigma(x) = -1 + \frac{1}{x+1}, \ -1 < x < \infty.$$

Next we define a variable $h(x) := \frac{x-\sigma(x)}{2}$,

$$\Longrightarrow \ h(x) = \frac{1}{2}\left(x + 1 - \frac{1}{x+1}\right).$$

Mañosas and Torres have shown that there exists a symmetric potential $\tilde{U}$ such that the period function in the potential $U(x)$ and $\widetilde{U}(h(x))$ is the same. The form of $\tilde{U}$ is to be found from the relation

$$\widetilde{U}(h(x)) = U(x).$$

In the present case this implies

$$\tilde{U}(h(x)) = \frac{k}{2}\left(x+1-\frac{1}{x+1}\right)^2 = \frac{k}{2}(2h(x))^2 = 2kh^2(x),$$

$$\therefore \quad \tilde{U}(\xi) = 2k\xi^2,$$

and upon setting $k = 1/4$, it reduces to

$$\widetilde{U}(\xi) = \frac{1}{2}\xi^2 \tag{4.17}$$

which is just the linear harmonic oscillator potential. Such a choice renders $U(x)$ and the function $g(x)$ to have the following explicit forms, *viz*

$$U(x) = \frac{1}{8}\left(x+1=\frac{1}{x+1}\right)^2,$$

$$g(x) = sgn(x)\frac{1}{2\sqrt{2}}\left(x+1=\frac{1}{x+1}\right).$$

This symmetrization of the isotonic potential and its subsequent reduction to the potential of a linear harmonic oscillator is the precisely the reason for these two systems to have identical time periods of 2π and hence become isochronous. Below we consider a generalization of the isotonic oscillator potential in the spirit of the opening paragraph of this article where the parameter α is any positive real number.

4.2.2 Generalised Isotonic potential

Our main result in this context may be stated as follows:

Theorem 4.2.1 *For the purely nonlinear generalised isotonic oscillator governed by a potential*

$$U(q) = \frac{c_\alpha}{8}\left(|q|^{\frac{\alpha+1}{2}} - \frac{1}{|q|^{\frac{\alpha+1}{2}}}\right)^2,$$

with α being positive real number, with equation of motion given by

$$\ddot{q} + \frac{c_\alpha}{8}(\alpha+1)q^\alpha = \frac{c_\alpha(\alpha+1)}{8\,q^{\alpha+2}}, \quad 0 < q < \infty,$$

subject to initial conditions $q(0) = q_0$ and $\dot{q}(0) = 0$, the time period, T, is given by

$$T = \frac{4}{\sqrt{c_\alpha}(\alpha+1)}\sum_{m=0}^{\infty}\sum_{n=0}^{\infty}\binom{\frac{2}{\alpha+1}}{m}\binom{\frac{1}{\alpha+1}-\frac{1}{2}-m}{n}k_\alpha^{2(m+n)}B(m+n+1/2,1/2),$$

where $k_\alpha = \sqrt{\frac{2\tilde{U}}{c_\alpha}}$ and $\tilde{U}$ is the symmetrised potential.

We begin our analysis by considering the potential

$$U(x) = \frac{c_\alpha}{8}\left(|x+1|^{\frac{\alpha+1}{2}} - \frac{1}{|x+1|^{\frac{\alpha+1}{2}}}\right)^2, \tag{4.18}$$

with α being a positive real number. The potential is asymmetric vanishing at $x = 0$ where it has a minimum. The corresponding equation of motion is given by

$$\ddot{x} + \frac{c_\alpha}{8}(\alpha+1)(x+1)^\alpha = \frac{c_\alpha(\alpha+1)}{8(x+1)^{\alpha+2}}, \quad -1 < x < \infty$$

In terms of the variable $q = x+1$ and with $c_\alpha = 8/(\alpha+1)$ this may be succinctly expressed in the form

$$\ddot{q} + q^\alpha = \frac{1}{q^{\alpha+2}}, \quad 0 < q < \infty$$

As before, define $g(x) = sgn(x)\sqrt{U(x)}$ which for $x > 0$ yields

$$g(x) = \sqrt{\frac{c_\alpha}{8}}\left(|x+1|^{\frac{\alpha+1}{2}} - \frac{1}{|x+1|^{\frac{\alpha+1}{2}}}\right) = y,$$

$$\implies |x+1|^{\alpha+1} - \sqrt{\frac{8}{c_\alpha}}y|x+1|^{\frac{\alpha+1}{2}} - 1 = 0,$$

It now follows that

$$g^{-1}(x) = -1 + \left(\sqrt{\frac{2}{c_\alpha}}x + \sqrt{\frac{2}{c_\alpha}x^2+1}\right)^{\frac{2}{\alpha+1}}. \tag{4.19}$$

Consequently

$$\sigma(x) = g^{-1}(-g(x)) = -1 + \frac{1}{x+1},$$

as before.

Furthermore $h(x)$ also has the same form namely,

$$h(x) = \frac{1}{2}\left(x+1-\frac{1}{x+1}\right).$$

Note that as $x \to -1$ the function $h(x) \to -\infty$ while as $x \to \infty$, $h(x)$ approaches $+\infty$, that is in other words $h(x) \in (-\infty, +\infty)$. Setting $\tilde{U}(h(x)) = U(x)$ we get

$$x + 1 = h + \sqrt{h^2+1},$$

and hence

$$\tilde{U}(h(x)) = \frac{c_\alpha}{8}\left((\sqrt{h^2(x)+1}+h(x))^{\frac{\alpha+1}{2}} - \frac{1}{(\sqrt{h^2(x)+1}+h(x))^{\frac{\alpha+1}{2}}}\right), \; h(x) \in (-\infty, \infty)$$

so that

$$\tilde{U}(\xi) = \frac{c_\alpha}{8}\left((\sqrt{\xi^2+1}+\xi)^{\frac{\alpha+1}{2}} - \frac{1}{(\sqrt{\xi^2+1}+\xi))^{\frac{\alpha+1}{2}}}\right). \tag{4.20}$$

It will be observed that $\tilde{U}(\xi)$ is symmetric along $\xi = 0$, i.e. $\tilde{U}(-\xi) = \tilde{U}(\xi)$, with a minima at $\xi = 0$.

Now, conservation of energy gives

$$\frac{1}{2}\dot{\xi}^2 + \tilde{U}(\xi) = c = \tilde{U}(\xi_0), \tag{4.21}$$

and equation of motion is given by

$$\ddot{\xi} = -\tilde{U}'(\xi),$$

which yields

$$\ddot{\xi} + \frac{c_\alpha(\alpha+1)}{8}(\sqrt{\xi^2+1})^\alpha\left(\left(1+\frac{\xi}{\sqrt{\xi^2+1}}\right)^{\alpha+1} - \left(1-\frac{\xi}{\sqrt{\xi^2+1}}\right)^{\alpha+1}\right) = 0. \tag{4.22}$$

Calculation of the Time period

The time period of the above the motion satisfies

$$\frac{T}{4} = \int_0^{\xi_0} \frac{d\xi}{|\dot{\xi}|},$$

$$\implies T = 2\sqrt{2}\int_0^{\xi_0} \frac{d\xi}{\sqrt{\tilde{U}(\xi_0) - \tilde{U}(\xi)}} = \frac{2\sqrt{2}}{\sqrt{\tilde{U}(\xi_0)}}\int_0^{\xi_0} \frac{d\xi}{\sqrt{1-\frac{\tilde{U}(\xi)}{\tilde{U}(\xi_0)}}}$$

Introducing a change of variable

$$u^{\frac{\alpha+1}{2}} = \sqrt{\frac{\tilde{U}(\xi)}{\tilde{U}(\xi_0)}} = \sqrt{\frac{c_\alpha}{8\tilde{U}(\xi_0)}}\left[(\sqrt{\xi^2+1}+\xi)^{\frac{\alpha+1}{2}} - (\sqrt{\xi^2+1}-\xi)^{\frac{\alpha+1}{2}}\right].$$

The time period in the transformed system is given as

$$T = \frac{2\sqrt{2}}{\sqrt{\tilde{U}(\xi_0)}}\int_0^1 \frac{|\frac{d\xi}{du}|du}{\sqrt{1-u^{\alpha+1}}}.$$

Now, the calculation of $|\frac{d\xi}{du}|$ gives the expression

$$\frac{d\xi}{du} = \frac{k_\alpha}{2\sqrt{t^2+1}}\left[(\sqrt{t^2+1}+t)^{\frac{2}{\alpha+1}} + (\sqrt{t^2+1}-t)^{\frac{2}{\alpha+1}}\right]u^{\frac{\alpha-1}{2}},$$

where $k_\alpha = \sqrt{\frac{2\tilde{U}(\xi_0)}{c_\alpha}}$, and $t = k_\alpha u^{\frac{\alpha+1}{2}}$. Further, using series expansion,

$$\frac{(\sqrt{t^2+1}+t)^{\frac{2}{\alpha+1}} + (\sqrt{t^2+1}-t)^{\frac{2}{\alpha+1}}}{\sqrt{t^2+1}} = 2\sum_{m=0}^{\infty}\sum_{n=0}^{\infty}\binom{\frac{2}{\alpha+1}}{m}\binom{\frac{1}{\alpha+1}-\frac{1}{2}-m}{n}(k_\alpha^2 u^{\alpha+1})^{m+n}$$

.

Hence the time period becomes

$$T = \frac{4}{\sqrt{c_\alpha}}\int_0^1 \frac{u^{\frac{\alpha-1}{2}}}{\sqrt{1-u^{\alpha+1}}}\sum_{m=0}^{\infty}\sum_{n=0}^{\infty}\binom{\frac{2}{\alpha+1}}{m}\binom{\frac{1}{\alpha+1}-\frac{1}{2}-m}{n}(k_\alpha^2 u^{\alpha+1})^{m+n}du, \tag{4.23}$$

or

$$T = \frac{4}{\sqrt{c_\alpha}}\sum_{m=0}^{\infty}\sum_{n=0}^{\infty}\binom{\frac{2}{\alpha+1}}{m}\binom{\frac{1}{\alpha+1}-\frac{1}{2}-m}{n}k_\alpha^{2(m+n)}\int_0^1 \frac{u^{\frac{\alpha-1}{2}}}{\sqrt{1-u^{\alpha+1}}}(u^{(\alpha+1)(m+n)})du.$$

The integral in the above expression is given as

$$\int_0^1 \frac{u^{\frac{\alpha-1}{2}}}{\sqrt{1-u^{\alpha+1}}}(u^{(\alpha+1)(m+n)})du = \frac{\Gamma(m+n+1/2)\Gamma(1)}{(\alpha+1)\Gamma(m+n+3/2)}\,{}_2F_1\left(\frac{1}{2}, m+n+\frac{1}{2}, m+n+\frac{3}{2}; 1\right),$$

putting it in the time period expression and simplifying gives

$$T = \frac{4}{\sqrt{c_\alpha}(\alpha+1)}\sum_{m=0}^{\infty}\sum_{n=0}^{\infty}\binom{\frac{2}{\alpha+1}}{m}\binom{\frac{1}{\alpha+1}-\frac{1}{2}-m}{n}k_\alpha^{2(m+n)}\frac{\Gamma(m+n+1/2)\Gamma(1/2)}{(m+n)!}.$$

Observing that

$$\frac{\Gamma(m+n+1/2)\Gamma(1/2)}{(m+n)!} = B(m+n+1/2, 1/2),$$

we have

$$T = \frac{4}{\sqrt{c_\alpha}(\alpha+1)}\sum_{m=0}^{\infty}\sum_{n=0}^{\infty}\binom{\frac{2}{\alpha+1}}{m}\binom{\frac{1}{\alpha+1}-\frac{1}{2}-m}{n}k_\alpha^{2(m+n)}B(m+n+1/2, 1/2). \tag{4.24}$$

It is an amplitude dependent time period with the amplitude dependence resulting from the expression k_α, given by

$$k_\alpha = \sqrt{\frac{2\tilde{U}(\xi_0)}{c_\alpha}}$$

Notice further that when $\alpha = 1$ and $c_\alpha = 1$, the time period is

$$T = 2\sum_{m=0}^{\infty}\sum_{n=0}^{\infty}\binom{1}{m}\binom{-m}{n}(2\tilde{U}(\xi_0))^{(m+n)}B(m+n+\frac{1}{2};\frac{1}{2}) = 2\pi.$$

Thus we recover the standard result for the isotonic potential. In general (4.24) is an amplitude dependent expression and therefore one can rule out the possibility for general values of parameter α. While the isotonic oscillator can be viewed as a quantum harmonic oscillator with a centrifugal barrier the generalised version presented here may be looked upon as a purely nonlinear oscillator with a higher order barrier potential. To the best of our knowledge quantization of such a potential has not yet attempted yet. For the isotonic oscillator it is known that at the quantum level the energy spectrum is equispaced with the energy difference being twice that of the quantum LHO. The presence of the centrifugal barrier term appears to cause half of the energy levels of the LHO to disappear. Whether any similar feature can exists for a generalised isotonic potential appears to be an open question at the present juncture.

4.2.3 Conclusion

In this study, first we considered symmetrization procedures from [29] to obtain time-period of strongly nonlinear potential of the form $sgn(x)|x|^\alpha$. Second, we discussed the isotonic potential and its time-period and later, we generalised the isotonic potential to obtain a strongly nonlinear potential system. For such systems usual linearisation and perturbation methods do not allow to procure any qualitative information about the system. We utilised symmetrization procedures to attain an expression for time-period for the generalised isotonic potential in terms of known functions.

4.3 Oscillators with non-negative real-power restoring force and quadratic damping [3].

Oscillators with quadratic damping together with nonlinear nonnegative real-power restoring force are interesting problems and were well studied by I. Kovacic and Z. Rakaric in [37], they consider a second-order differential equation of the form

$$x'' + \mu\, sgn(x')x'^2 + sgn(x)|x|^\alpha = 0, \tag{4.25}$$

where the prime denotes differentiation with respect to t, μ denotes the damping coefficient and $\alpha \in \mathbb{R}^+$.

In this work, we consider a strongly nonlinear system with quadratic damping of the form

$$x'' + sgn(x')f(x)x'^2 + sgn(x)|g(x)| = 0, \tag{4.26}$$

[3]This is part of published work, [36]

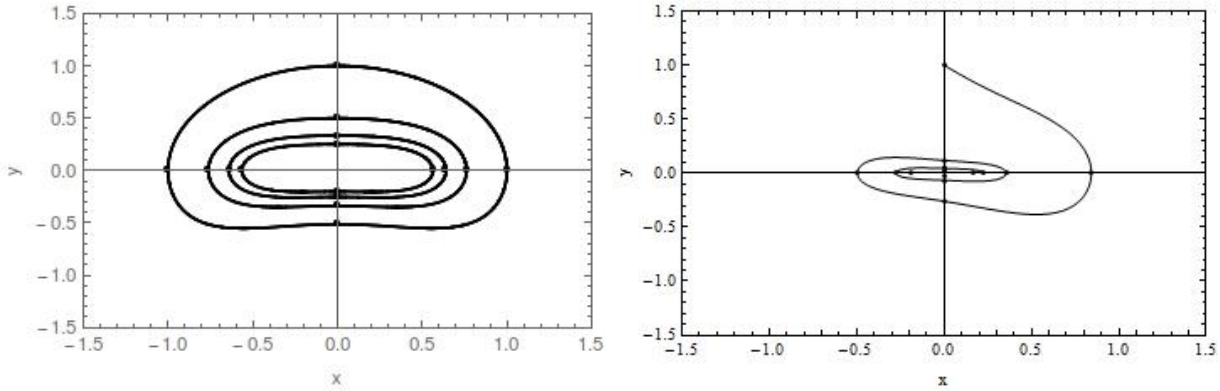

(a) $f(x) = x,\ g(x) = x^3$. (b) $f(x) = 1,\ g(x) = x^3$.

Figure 4.1: Phase space plots for odd-power restoring force ($g(x) = x^3$) with a) odd damping coefficient, $f(x) = x$, showing closed orbits for different initial conditions, and b) even damping coefficient, $f(x) = 1$, showing damp orbit.

where the damping coefficient is a function of the displacement and study it for different cases using different instances of $f(x)$ and $g(x)$. We formulate a generalised scheme for the calculation of the mechanical energy defined as that of an undamped oscillator. We also derive a piecewise Hamiltonian description for the system in different quadrants.

To start with consider the following expression derived from (4.26),

$$\frac{d}{dt}\left[\frac{1}{2}(x')^2 + \int_0^x |g(s)|\, ds\right] = -sgn(x')f(x)x'^3. \tag{4.27}$$

Let $T = \frac{1}{2}(x')^2$, and,$V = \int_0^x |g(s)|\, ds$, then $E = T + V$. Now, from (4.27) we can have

$$\frac{dT}{dx} + 2\, sgn(x')f(x)\, T = -sgn(x)|g(x)|. \tag{4.28}$$

In order to understand the qualitative features of the system, we consider the following two cases depending on the whether the forcing term is even or odd.

Case 1: odd-power restoring forces

In this situation (4.26) can be written as

$$x'' + sgn(x')f(x)x'^2 + g(x) = 0, \tag{4.29}$$

which is the same system considered in [38]. As shown in [38] for even damping coefficient, we have a damped orbit figure4.1b and for odd damping we have a closed orbit figure4.1a. This is a consequence of the Hamiltonian structure of (4.29).

Example 1 When $f(x) = 1$, $g(x) = x^3$, the system is given as

$$x'' + sgn(x')x'^2 + x^3 = 0 \tag{4.30}$$

Then from (4.28) we have

$$\frac{dT}{dx} + 2T = -x^3 \quad x' > 0, \tag{4.31}$$

$$\frac{dT}{dx} - 2T = -x^3 \quad x' < 0. \tag{4.32}$$

Solution to the above equations are given as

$$T = \frac{1}{8}\left(3 - 6x + 6x^2 - 4x^3\right) + c_+ e^{-2x} \quad x' > 0,$$

$$T = \frac{1}{8}\left(3 + 6x + 6x^2 + 4x^3\right) + c_- e^{2x} \quad x' < 0,$$

where $c_\pm$ are constants of integration and are fixed using the initial conditions. The corresponding energies are

$$E = T + V = \frac{1}{8}\left(3 - 6x + 6x^2 - 4x^3\right) + c_+ e^{-2x} + \frac{x^4}{4}, \quad x' > 0,$$

$$E = T + V = \frac{1}{8}\left(3 + 6x + 6x^2 + 4x^3\right) + c_- e^{2x} + \frac{x^4}{4}, \quad x' < 0.$$

Now consider another example with odd damping coefficient, $f(x) = x$.
Example 2 In this setting, (4.29) becomes

$$x'' + sgn(x')xx'^2 + x^3 = 0$$

and (4.28) takes the form

$$\frac{dT}{dx} + 2xT = -x^3 \quad x' > 0, \tag{4.33}$$

$$\frac{dT}{dx} - 2xT = -x^3 \quad x' < 0. \tag{4.34}$$

The final energy is given as

$$E = T + V = \frac{1}{2}\left(1 - x^2\right) + c_+ e^{-x^2} + \frac{x^4}{4}, \quad x' > 0,$$

$$E = T + V = \frac{1}{2}\left(1 + x^2\right) + c_- e^{x^2} + \frac{x^4}{4}, \quad x' < 0,$$

where $c_\pm$ are constants of integration. Figure 4.2a, 4.2b shows the energy-displacement curve for the above considered examples, and the corresponding phase space orbits are shown in figure 4.1a, 4.1b.

Case 2: even-power restoring forces

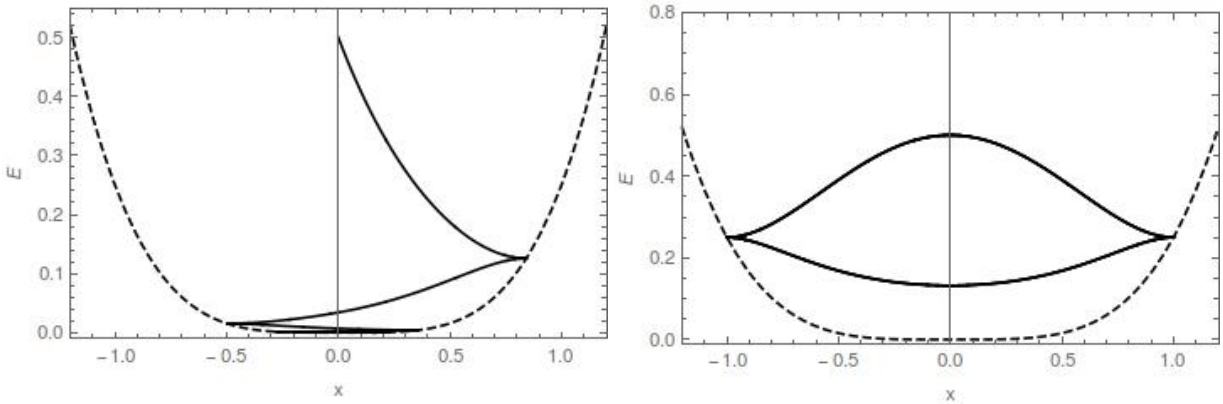

(a) $f(x) = 1$, $g(x) = x^3$.

(b) $f(x) = x$, $g(x) = x^3$.

Figure 4.2: Energy variation with displacement for odd-power restoring forces, $g(x) = x^3$ with a) even damping coefficient, $f(x) = 1$), and b) odd damping coefficient, $f(x) = x$.

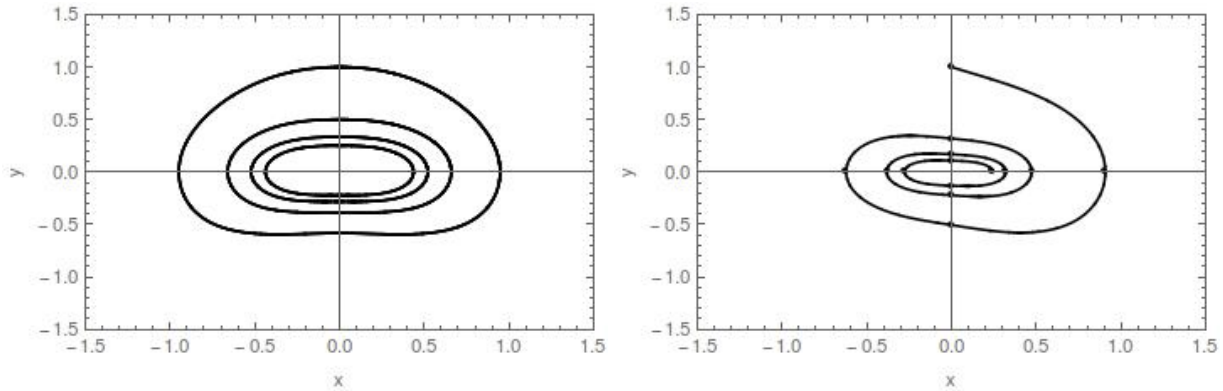

(a) $f(x) = x,\ g(x) = x^2$.

(b) $f(x) = 1,\ g(x) = x^2$.

Figure 4.3: Phase-space plots for even-power restoring force, $g(x) = x^2$ with a) odd damping coefficient function, $f(x) = x$, showing center orbits, and b) even damping coefficient function, $f(x) = 1$, showing damped orbits.

In the case of even-power restoring force, the forcing term is again an odd function and behaves qualitatively in the same manner as in the odd-power case. However, the damping and the period will vary depending upon α. Figure 4.3 shows the orbits for even and odd damping coefficients.

The equations for this case are given as

$$\begin{aligned} x'' + sgn(x')f(x)x'^2 + g(x) &= 0, \quad x > 0, && (4.35)\\ x'' + sgn(x')f(x)x'^2 - g(x) &= 0, \quad x < 0. && (4.36) \end{aligned}$$

The dynamics in this case varies in each quadrants of the phase plane. We illustrate this below.

Example 3 Suppose $f(x) = 1$, and $g(x) = x^2$. The system is then

$$x'' + sgn(x')x'^2 + sign(x)x^2 = 0.$$

The dependence of energy on displacement can be computed using (4.28) and $E = T + V$ and leads to the following expressions

$$\begin{aligned} E &= \frac{1}{4}\left(-1 + 2x - 2x^2\right) + c_{++}e^{-2x} + \frac{x^3}{3}, \quad x > 0,\ x' > 0\\ E &= \frac{1}{4}\left(1 + 2x + 2x^2\right) + c_{-+}e^{2x} + \frac{x^3}{3}, \quad x < 0,\ x' > 0\\ E &= \frac{1}{4}\left(1 - 2x + 2x^2\right) + c_{+-}e^{-2x} + \left|\frac{x^3}{3}\right|, \quad x > 0,\ x' < 0\\ E &= \frac{1}{4}\left(-1 - 2x - 2x^2\right) + c_{--}e^{2x} + \left|\frac{x^3}{3}\right|, \quad x < 0,\ x' < 0 \end{aligned}$$

where $c_{\pm\pm}$ are constants of integration. Figure (4.4a) shows the energy variation with displacement with the dotted lines denoting the potential V.

Our next example displays closed orbits.

Example 4 Assume $f(x) = x$, then the system is given by

$$x'' + sgn(x')xx'^2 + sign(x)x^2 = 0.$$

By following a similar procedure as outlined before we find the energy dependence on displacement to be given by

$$\begin{aligned} E &= e^{-x^2}\left(-\frac{1}{2}e^{x^2}x + \frac{1}{4}\sqrt{\pi}\mathcal{E}rfi(x)\right) + c_{++}e^{-x^2} + \frac{x^3}{3}, \quad x > 0,\ x' > 0\\ E &= e^{x^2}\left(\frac{1}{2}e^{-x^2}x - \frac{1}{4}\sqrt{\pi}\mathcal{E}rf(x)\right) + c_{-+}e^{x^2} + \frac{x^3}{3}, \quad x < 0,\ x' > 0\\ E &= e^{-x^2}\left(\frac{1}{2}e^{x^2}x - \frac{1}{4}\sqrt{\pi}\mathcal{E}rfi(x)\right) + c_{+-}e^{-x^2} + \left|\frac{x^3}{3}\right|, \quad x > 0,\ x' < 0 \end{aligned}$$

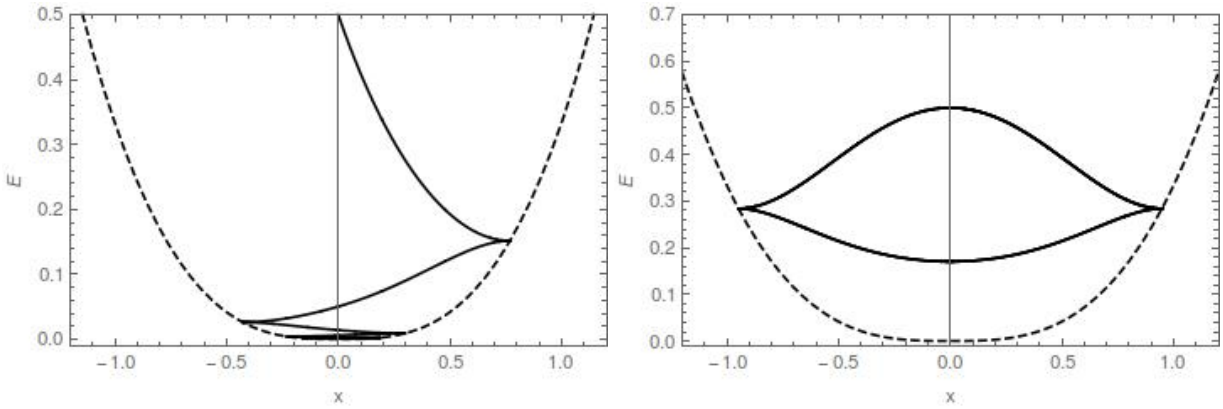

(a) $f(x) = 1,\ g(x) = x^2$. (b) $f(x) = x,\ g(x) = x^2$.

Figure 4.4: Energy-displacement curve for even-power restoring force ($g(x) = x^2$) with a) even damping coefficient function ($f(x) = 1$), and b) odd damping coefficient function ($f(x) = x$).

$$E = e^{x^2}\left(-\frac{1}{2}e^{-x^2}x + \frac{1}{4}\sqrt{\pi}\mathcal{E}rf(x)\right) + c_{--}e^{x^2} + \left|\frac{x^3}{3}\right|, \quad x < 0,\, x' < 0$$

where $c_{\pm\pm}$ are constants of integration and $\mathcal{E}rf\ and\ \mathcal{E}rfi$ are error functions and imaginary error functions. Figure 4.4b shows the energy variation with displacement with dotted lines denoting potential V.

4.3.1 The Hamiltonian structure of the system

In the above analysis the mechanical energy $E = T+V$ corresponds to that of a particle of unit mass moving in the potential V. Owing to the presence of the damping term it is quite natural that the mechanical energy is not conserved. However, it is interesting to note that in the case of ODEs of the form of (4.26) one can formulate an alternative description in terms of a variable mass. By borrowing the concepts of Jacobi Last Multiplier and construction of Hamiltonian from previous chapter, the Hamiltonian for system (4.25) can be written in the following form

$$H^{\pm\pm} = \frac{1}{2}e^{\pm 2F(x)}x'^2 \mp \int_0^x e^{\pm 2F(s)}g(s)\,ds, \tag{4.37}$$

where $F(x) = \int_0^x f(s)\,ds$ and the first $(\pm)$ in the superscript of H denotes $(\pm)$ in the power of exponential which basically comes from sign function in the coefficient of damping term while the second one denotes $(\pm)$ in the forcing term. It also needs to be mentioned that the expression of the Hamiltonian is written in terms of configuration space variables which can be easily transformed into momentum terms. It is done mainly to facilitate the calculation of the Hamiltonian values. It is also natural to define the potential function by

$$V_H^{\pm} = \int_0^x e^{\pm 2F(s)}g(s)\,ds. \tag{4.38}$$

n^{th} cycle	ΔH	ΔE
1	-0.493039	-0.493039
2	-0.00603154	-0.00603154
3	-0.000307447	-0.000684351
4	-0.0000497198	-0.000154833

Table 4.1: Change in Hamiltonian and Energy in each complete cycle in example 1 ($f(x) = 1,\ g(x) = x^3$).

n^{th} cycle	ΔH	ΔE
1	-0.486074	-0.486074
2	-0.011064	-0.0278193
3	-0.000956281	-0.000956281
4	-0.000216832	-0.000714582

Table 4.2: Change in Hamiltonian and energy in each complete cycle in example 2 ($f(x) = x,\ g(x) = x^3$).

In the following we provide explicit expressions for the Hamiltonian for our previous examples and also list the comparative changes in the values of H and E for each case. The Hamiltonian for example 1 when $f(x) = 1$, and $g(x) = x^3$, is

$$H^{\pm} = \frac{1}{2}e^{\pm 2x}x'^2 + \frac{(3 + e^{\pm 2x}\,(-3 \pm 2x\,(3 \pm x(-3 \pm 2x))))}{8},$$

and for example 2 when $f(x) = x$, and $g(x) = x^3$, is

$$H^{\pm} = \frac{1}{2}e^{\pm x^2}x'^2 + \frac{\left(1 + e^{\pm x^2}(-1 + \pm x^2)\right)}{2}.$$

The above Hamiltonians does not depend on the sign of displacement. This is evident from (4.29). Table 4.1 shows the changes in the values of the Hamiltonian and energy E in each complete cycle.

The Hamiltonian for the examples in even-power case are given as

$$H^{s\,w} = \frac{1}{2}e^{s\,x^2}x'^2 + \frac{w\left(2e^{s\,x^2}\sqrt{s}x - \sqrt{\pi}\mathcal{E}rfi(\sqrt{s}x)\right)}{4s^{3/2}},$$

where s, $w = \{\pm 1\}$ and denotes the sign of displacement x and velocity x', respectively. Table 4.2 shows the change in the values of Hamiltonian and energy in each cycle.

4.3.2 Conclusion

In this work, a general quadratically damped oscillator with purely non-linear force is studied. The associated mechanical energy of the general system has been calculated

and analytic expression for odd and even restoring forces are obtained. Further, the Hamiltonian description of the system is shown and analytic expression has been obtained for different cases.

4.4 Summary

Nonlinearities in equations are hard to deal with and there is no "one-method-to-rule-them-all". Systems with weak nonlinearities or systems with some linear parts allows methods like linearisation or perturbation techniques to tackle the problem in an approximate manner. However, with strongly nonlinear systems the life of a dynamicist becomes worse. This chapter concerned itself with strongly nonlinear systems by considering two case studies regarding such potentials.

In the first study a generalised isotonic potential is considered. Given the conservative nature of the system it is possible to formulate the hamiltonian structure for it. This allows to write the solution of the system but only upto quadrature. Although, this could be numerically solved, there is no known method to the author to obtain it in a closed function form. Further, due to unavailability of linearisation schemes it is not possible to attain some idea of its dynamical features. To this end, a symmetrisation scheme provided in [29] was employed where a time-period preserving transformation transforms the general potential in symmetric form. This allows the time-period to be obtained in terms of closed function form. Such information is very crucial, particularly, in modelling engineering systems.

In the second study, a strongly nonlinear system is considered experiencing damping of quadratic form. For this work the damping characteristics in a purely nonlinear potential well were profiled in terms of energy for multiple cases. Further, Hamiltonian description of quadratic damping from previous chapter is also given and compared with energy profiles.

Bibliography

[1] Livija Cveticanin. *Strong Nonlinear Oscillators*. Springer, 2018.

[2] G Prathap and TK Varadan. The inelastic large deformation of beams. *Journal of Applied Mechanics*, 1976.

[3] Stephen P Timoshenko and James M Gere. *Theory of elastic stability*. Courier Corporation, 2009.

[4] Ian J McColm and NJ Clark. Forming, shaping, and working of high-performance ceramics. *Blackie and Son Ltd., 1988,*, page 345, 1988.

[5] CC Lo and S Das Gupta. Bending of a nonlinear rectangular beam in large deflection. *Journal of Applied Mechanics*, 1978.

[6] Gilbert Lewis and Frank Monasa. Large deflections of cantilever beams of non-linear materials of the ludwick type subjected to an end moment. *International Journal of Non-Linear Mechanics*, 17(1):1–6, 1982.

[7] Henry W Haslach Jr. Influence of adsorbed moisture on the elastic post-buckling behavior of columns made of non-linear hydrophilic polymers. *International journal of non-linear mechanics*, 27(4):527–546, 1992.

[8] Ian M Ward and John Sweeney. *Mechanical properties of solid polymers*. John Wiley & Sons, 2012.

[9] Ivana Kovacic. Four types of strongly nonlinear oscillators: Generalization of a perturbation procedure. *Procedia IUTAM*, 19:101–109, 2016.

[10] Md Abdur Razzak. A new analytical approach to investigate the strongly nonlinear oscillators. *Alexandria Engineering Journal*, 55(2):1827–1834, 2016.

[11] Wang Shimin and Yang Lechang. An analytical approximation method for strongly nonlinear oscillators. *Journal of Applied Mathematics*, 2012.

[12] Akuro Big-Alabo, Emmanuel Ogheneochuko Ekpruke, and Chiwunba Victor Ossia. Quasi-static quintication method for periodic solution of strong nonlinear oscillators. *Scientific African*, 11:e00704, 2021.

[13] Ronald E Mickens. *Truly nonlinear oscillations: harmonic balance, parameter expansions, iteration, and averaging methods*. World Scientific, 2010.

[14] H Hu. Solution of a mixed parity nonlinear oscillator: Harmonic balance. *Journal of Sound and Vibration*, 299(1-2):331–338, 2007.

[15] Md Abdur Razzak. A simple harmonic balance method for solving strongly nonlinear oscillators. *Journal of the Association of Arab Universities for Basic and Applied Sciences*, 21:68–76, 2016.

[16] IV Andrianov. Asymptotics of nonlinear dynamical systems with a high degree of nonlinearity. In *Doklady. Mathematics*, volume 66, pages 270–273, 2002.

[17] Igor Andrianov and Jan Awrejcewicz. Asymptotic approaches to strongly non-linear dynamical systems. *Systems Analysis Modelling Simulation*, 43(3):255–268, 2003.

[18] Ji-Huan He. Some asymptotic methods for strongly nonlinear equations. *International journal of Modern physics B*, 20(10):1141–1199, 2006.

[19] Turgut Öziş and Ahmet Yıldırım. Determination of periodic solution for a u1/3 force by he's modified lindstedt–poincaré method. *Journal of Sound and Vibration*, 301(1-2):415–419, 2007.

[20] Ji-Huan He. Modified lindstedt–poincare methods for some strongly non-linear oscillations: Part i: expansion of a constant. *International Journal of Non-Linear Mechanics*, 37(2):309–314, 2002.

[21] MK Yazdi and PH Tehrani. Rational variational approaches to strong nonlinear oscillations. *International Journal of Applied and Computational Mathematics*, 3(2):757–771, 2017.

[22] AYT Leung, Zhongjin Guo, and HX Yang. Residue harmonic balance analysis for the damped duffing resonator driven by a van der pol oscillator. *International Journal of Mechanical Sciences*, 63(1):59–65, 2012.

[23] RA Ibrahim. Recent advances in nonlinear passive vibration isolators. *Journal of sound and vibration*, 314(3-5):371–452, 2008.

[24] K Cooper and RE Mickens. Generalized harmonic balance/numerical method for determining analytical approximations to the periodic solutions of the x 4/3 potential. *JSV*, 250(5):951–954, 2002.

[25] YZ Chen. Evaluation of motion of the duffing equation from its general properties. *Journal of sound and vibration*, 264(2):491–497, 2003.

[26] Manuel F Pérez Polo, Manuel Pérez Molina, and Javier Gil Chica. Chaotic dynamic and control for micro-electro-mechanical systems of massive storage with harmonic base excitation. *Chaos, Solitons & Fractals*, 39(3):1356–1370, 2009.

[27] A Ghose-Choudhury, Aritra Ghosh, Partha Guha, and **Ankan Pandey**. On purely nonlinear oscillators generalizing an isotonic potential. *International Journal of Non-Linear Mechanics*, 106:55–59, 2018.

[28] Ivana Kovacic. On the response of purely nonlinear oscillators: An ateb-type solution for motion and an ateb-type external excitation. *International Journal of Non-Linear Mechanics*, 92:15–24, 2017.

[29] F Mañosas and Pedro J Torres. Two inverse problems for analytic potential systems. *Journal of Differential Equations*, 245(12):3664–3673, 2008.

[30] Livija Cveticanin, Ivana Kovacic, and Zvonko Rakaric. Asymptotic methods for vibrations of the pure non-integer order oscillator. *Computers & Mathematics with Applications*, 60(9):2616–2628, 2010.

[31] Oleg A Chalykh and Alexander P Veselov. A remark on rational isochronous potentials. *Journal of Nonlinear Mathematical Physics*, 12(sup1):179–183, 2005.

[32] Manuel F Rañada. A quantum quasi-harmonic nonlinear oscillator with an isotonic term. *Journal of Mathematical Physics*, 55(8):082108, 2014.

[33] Ji-Suo Wang, Tang-Kun Liu, and Ming-Sheng Zhan. Nonclassical properties of even and odd generalized coherent states for an isotonic oscillator. *Journal of Optics B: Quantum and Semiclassical Optics*, 2(6):758, 2000.

[34] K Thirulogasanthar and Nasser Saad. Coherent states associated with the wavefunctions and the spectrum of the isotonic oscillator. *Journal of Physics A: Mathematical and General*, 37(16):4567, 2004.

[35] M Roshanzamir-Nikou and H Goudarzi. The laplace transform approach for a dirac isotonic oscillator with a tensor potential in d-dimensions. *Physica Scripta*, 89(1):015001, 2013.

[36] **Ankan Pandey**, A Ghose Choudhury, and Partha Guha. Quadratically damped oscillators with non-linear restoring force. *arXiv preprint arXiv:1610.07821*, 2016.

[37] Ivana Kovacic and Zvonko Rakaric. Study of oscillators with a non-negative real-power restoring force and quadratic damping. *Nonlinear Dynamics*, 64(3):293–304, 2011.

[38] **Ankan Pandey**, A Ghose-Choudhury, and Partha Guha. Chiellini integrability and quadratically damped oscillators. *International Journal of Non-Linear Mechanics*, 92:153–159, 2017.

Appendix B

Ateb Functions

The term Ateb (Beta read backward) was coined by Rosenberg, [1], and he defined Ateb functions as half of the inverse of incomplete Beta functions. The inverse of the incomplete Beta function is defined by

$$B_t(a,b) = \int_0^{0\geq t\geq 1} z^{\alpha-1}(1-z)^{b-1}dz, \tag{B.1}$$

Senik, [2], in 1969 showed that the Ateb functions are actually the solutions of the differential equations

$$\dot{x} = y^{\alpha}, \qquad \dot{y} = -\frac{2}{\alpha+1}x, \tag{B.2}$$

namely $x(t) = sa(1,\alpha,t)$ and $y(t) = ca(1,\alpha,t)$ and that these may be expressed in terms of the three argument *ca* and *sa* functions. It may be verified that the inverse of the half of the Incomplete Beta function $\frac{1}{2}B_t\left(\frac{1}{2},\frac{1}{\alpha+1}\right)$ coincides with $x(t)$ on $\left[-\frac{1}{2}\Pi_\alpha, \frac{1}{2}\Pi_\alpha\right]$ where $\Pi_\alpha := B_t\left(\frac{1}{\alpha+1},\frac{1}{2}\right)$.

The Ateb functions are $2\Pi_\alpha$-periodic functions. Further, *sa* is an odd function called *sine Ateb* (*sa*), and *ca* is an even function called *cosine Ateb* (*ca*). The *ca* and *sa* functions satisfies following properties:

- Periodic relations:

$$sa(1,\alpha,z) = \begin{cases} -sa(1,\alpha,-z) \\ \pm sa(1,\alpha,\Pi_\alpha \pm z) \\ \mp sa(1,\alpha,2\Pi_\alpha \mp z) \\ \mp ca(\alpha,1,\frac{1}{2}\Pi_\alpha \pm z) \end{cases} \tag{B.3}$$

$$ca(\alpha,1,z) = \begin{cases} ca(\alpha,1,-z) \\ -ca(\alpha,1,\Pi_\alpha \pm z) \\ ca(\alpha,1,2\Pi_\alpha \pm z) \\ sa(1,\alpha,\frac{1}{2}\Pi_\alpha \pm z) \end{cases} \quad ; \tag{B.4}$$

- Relation between sa and ca:

$$sa^2(1,\alpha,z) + ca^{\alpha+1}(\alpha,1,z) = 1; \tag{B.5}$$

- Derivative:

$$\begin{aligned} \frac{d}{dz}ca(\alpha,1,z) &= -\frac{2}{1+\alpha}sa(1,\alpha,z), \\ \frac{d}{dz}sa(1,\alpha,z) &= ca^{\alpha}(\alpha,1,z); \end{aligned} \tag{B.6}$$

In addition to these two functions, Rosenberg defined the hyperbolic counterparts of these, [1].

The values of theses functions can be approximated from their fourier series representation which are discussed in [3]. Another way to approximate the numerical values is through Taylor series which given in [4]. Apart from these various other applications and utilities of these functions could be found in [5].

Bibliography

[1] RM Rosenberg. *The Ateb(h)*- functions and their properties. Quarterly of Applied Mathematics, 21(1):37-47, 1963.

[2] PM Senik. Inversion of the incomplete beta function. Ukrainian Mathematical Journal, 21(3):271-278, 1969.

[3] Ivanna Droniuk and M Nazarkevich. Modeling nonlinear oscillatory system under disturbance by means of ateb-functions for the internet. In *Proceeding of the 6th International Working Conference on Performance Modeling and Evaluation of Heterogeneous Networks (HET-NETs' 10)*, pages 325-334, 2010.

[4] VV Gricik and MA Nazarkevich. Mathematical models algorythms and computation of ateb-functions. *Dopovidi NAN Ukraini Seriji A*, 12:37-43, 2007.

[5] Livija Cveticanin. *Strong Nonlinear Oscillators*. Springer, 2018.

Chapter 5

History Dependent Nonlinearities

In the modeling of blood cell production process, the production rate depends on the current levels of the blood cells in the system. However, various models failed to explain important phenomenons in the process which was later corrected using the fact that there is a time lag between the initiation of new cells and production of mature cells and hence the rate of change of blood cells depends on the current state as well as on a previous state. In certain materials, the stress-strain response show viscoelastic behavior, a combination of viscosity and elastic response, whose modeling shows a memory effect in the material.

In the above examples the common theme is the modeling of the respective nonlinearities were done by utilising the state at an earlier time. So far, we have considered nonlinearities which are functions of the current states of the system variables. However, there are certain dynamical systems where governing equations depends on previous states of the system. This dependence on the history of the system evolution revamps the qualitative and quantitative properties of the system in non-trivial manner.

In this chapter, two classes of nonlinearities will be considered which depends on the history of the dynamical process. In the first study, we will look into fractional dynamical systems where dependence of state variables is upon both ODEs and fractional derivatives. For this a basic understanding will be presented along with a case study of fractional coupled oscillators. In the second study, we will consider the class of delay dynamical systems and examine its role in the dynamics through a case study.

5.1 Fractional Dynamical System

The history of fractional derivatives starts in 1695, when *1'Hopital* suggested to *Leibniz* the possibility of taking a derivative of order 1/2, to which Leibniz replied: "You can see by that, sir, that one can express by an infinite series a quantity such as $d^{1/2}xy$ or $d^{1:2}xy$. Although infinite series and geometry are distant relations, infinite series admits only the use of exponents that are positive and negative integers, and does not, as yet, know the use of fractional exponents." Later, in the same letter, *Leibniz* continues prophetically: "Thus it follows that $d^{1/2}x$ will be equal to $x\sqrt{dx : x}$. This is an apparent paradox from which, one day, useful consequences will be drawn." *Leibniz*, in his correspondence to *Johann*

Bernoulli, he mentions the derivatives of "general order". The fractional derivatives also captures the attention of *Euler* when he wrote: "When n is a positive integer, and if p should be a function of x, the ratio $d^n p$ to dx^n can always be expressed algebraically, so that if $n = 2$ and $p = x^3$, then d^2x^3 to dx^2 is $6x$ to 1. Now it is asked what kind of ratio can then be made if n be a fraction. The difficulty in this case can easily be understood. For if n is a positive integer d^n can be found by continued differentiation. Such a way, however, is not evident if n is a fraction. But yet with the help of interpolation which I have already explained in this dissertation, one may be able to expedite the matter" [*Euler*, 1738]. This subject was also considered by *Laplace*, however, it did not appear in a text until 1819, when *Lacroix* expressed it as

$$\frac{d^n t^m}{dt^n} = \frac{m!}{(m-n)!} t^{m-n}, \tag{5.1}$$

where n is an integer. Such definitions goes on for a long time until *Fourier* used his integral representation and *Abel* solutions of integral equations of *Tautochrone* problem to define it in a more general setting. Later *Liouville* extended their work and published three long memoirs in 1832 and several more publications in rapid succession. *Liouville* was successful in applying his definitions to problems in potential theory. The theory of fractional derivative further went through lot of research which includes work of *Leibniz, Hargreave* etc. A more detailed and elaborate account of the events and development could be found in [1, 2, 3]. An interesting read on the early development of fractional calculus can be found in [4].

In the past few decades, many important developments took place to establish the subject in parallel with its regular derivative counterparts. The development of variational principle for fractional dynamical systems, [5, 6, 7], leads to the Hamiltonian formalism for fractional systems, [8, 9, 10], including Hamilton-Jacobi formalism, [11], Jacobi Last Multiplier (JLM) methods, [12]. Further, the progress leads to the development of fractional version of quantum mechanics, [13, 14]. Later developments includes fractional control system, [15, 16, 17], fractional conservation laws, [18], fractional wave phenomenons, [19] and, similarly, in many fields.

Apart from the mathematical interests, FDEs have numerous applications in science and engineering, and the theory of dynamical systems, in general. The FDEs with respect to spatial variables represents interactions across large distances and have been studied extensively in systems with long range interactions, [20, 21, 22]. FDEs have also been found quite effective in modelling the perplexing phenomenon of anomalous diffusion, [23, 24]. One of the very prominent application of FDEs are in viscoelastic materials, [2, 25]. Other applications of FDEs include dielectric modelling, [26, 27], relaxation processes, [28] and many more.

5.1.1 Fractional Oscillators

Fractional Harmonic Oscillator

The harmonic oscillator is the simplest oscillator equation. The direct transformation to the fractional system could be achieved by generalising the order of the derivative as

$$\frac{d}{dt} \to \frac{d^\gamma}{dt^\gamma},$$

where for simplicity $0 < \gamma < 1$. To adjust the dimensionality of the time in the derivative a coefficient is usually added which could be shifted to the non-derivative part. The transformed fractional harmonic oscillator is

$$\frac{d^{2\gamma}}{dt^{2\gamma}} x(t) + w^2\, x(t) = 0, \tag{5.2}$$

where $w \in \mathcal{R}$. The solution of (5.2) is

$$x(t) = x(0) E_{2\gamma}[-w^2 t^{2\gamma}], \tag{5.3}$$

where $E_a[t]$ is *Mittag-Leffler* function, [29], defined as

$$E_a[t] = \sum_{m=0}^{\infty} \frac{t^m}{\Gamma(am+1)}. \tag{5.4}$$

Mittag-Leffler function is a generalisation of exponential function and reduce to it for $a = 1$, [29, 30, 31]. Further, for $\gamma = 1$ solution becomes

$$x(t) = x(0) E_2[-w^2 t^2] = x(0) \cos wt.$$

The numerical simulation is shown in figure 5.1. The simulation is done for $w = \sqrt{2}$ and $\gamma = \{1, 0.9, 0.45\}$. Figure 5.1 clearly shows the damping aspect of the fractional system, however one further interesting thing is that the damping for $\gamma < 0.5$ shows smooth approach of the trajectory towards the origin without any oscillatory behaviour but for $\gamma > 0.5$ the trajectories are oscillatory but with continuously decreasing amplitude. The damping for $\gamma < 0.5$ is called critical damping and for $\gamma > 0.5$ is under-damping. The damp structure exists for $\gamma < 1$, for $\gamma > 1$ the system shows diverging trajectories. This suggests the capabilities of FDEs to represent different classes of dynamics, namely underdamp, overdamp, oscillatory, and diverging, through just one equation and a single parameter, order of the derivative.

Exploration of Limit cycles

It is clear form the previous section that fractional-order derivatives have damping character, therefore, in order to achieve periodic oscillatory solution there must be a forcing

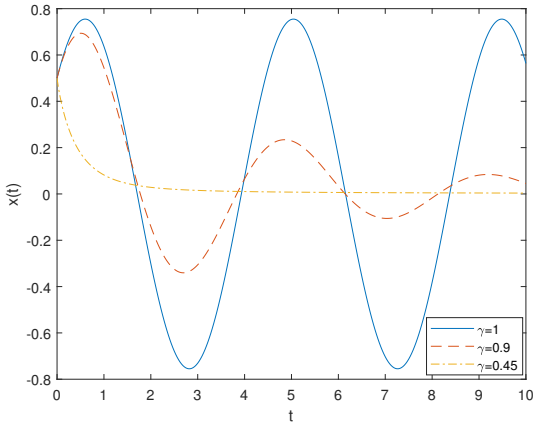

Figure 5.1: Numerical simulation of Fractional Harmonic Oscillator (5.2) for $w = \sqrt{2}$ and $\gamma = \{1, 0.9, 0.45\}$. The figure shows contrasting behaviour of the oscillator for different order of derivatives: oscillation for $\gamma = 1.0$ (solid line); underdamped oscillation for $\gamma = 0.9$ (dashed line); overdamping for $\gamma = 0.45$ (dot dashed line).

term present in the system. From an dynamical perspective, this competition between damping and forcing term will result in a equilibrium solution where both the terms balance each other. In this section, I will explore the dynamical aspects of Fractional dynamical systems-equilibrium points, stability of equilibrium points and bifurcations. Further conditions for Hopf bifurcation will be established and will be implemented in case studies of modified van der Pol oscillator.

Stability of Fractional dynamical systems

Consider the fractional order autonomous dynamical system with parameter $\mu \in \mathcal{R}^m$

$$D_t^\alpha x(t) = f(x, \mu), \quad x \in \mathcal{R}^n. \tag{5.5}$$

Also $x(0) = x_0$.

Definition 5.1.1 *A point $x_e \in \mathcal{R}^n$ is an equilibrium point of (5.5) if $f(x_e) = 0$.*

The linearisation around the equilibria point is given as

$$D_t^\alpha x(t) = Jx(t), \tag{5.6}$$

where $J_{ij} = \frac{\partial f^i}{\partial x^j}(x_e)$ is the jacobian at $x = x_e$.

Theorem 5.1.1 *The linearised system (5.6) is locally stable if for each eigenvalue λ of J, $|arg(\lambda)| > \frac{\pi\alpha}{2}$, and linearly unstable if $|arg(\lambda)| < \frac{\pi\alpha}{2}$ for atleast one eigenvalue, and non-hyperbolic if $|arg(\lambda)| = \frac{\pi\alpha}{2}$.*

The stability criteria is due to Matignon [32].

Fractional Van der Pol Oscillator

Consider the fractional Van der Pol oscillator

$$\begin{aligned} D^{\alpha}x &= y \\ D^{\alpha}y &= -\epsilon(x^2-1)y - w^2x, \end{aligned} \tag{5.7}$$

where $\epsilon, w \in \mathcal{R}$ are parameters and $0 < \alpha < 1$ be the order the derivative. The equation equivalently can be written as

$$D^{2\alpha}x + \epsilon(x^2-1)D^{\alpha}x + w^2x = 0. \tag{5.8}$$

The equilibrium point is $(x, y) = (0, 0)$ and the corresponding jacobian is given as

$$J = \begin{pmatrix} 0 & 1 \\ -w^2 & \epsilon \end{pmatrix}$$

and the characteristic equation is

$$\lambda^2 - \epsilon\lambda + w^2 = 0. \tag{5.9}$$

Let $\lambda = Re^{i\theta}$ and separately equating the real and imaginary part to zero, we get

$$\begin{aligned} R^2\cos 2\theta - \epsilon R\cos\theta + w^2 &= 0, \\ R\sin 2\theta - \epsilon\sin\theta &= 0. \end{aligned} \tag{5.10}$$

Eliminating R from the equation gives

$$\cos\theta = \frac{\epsilon}{2w}. \tag{5.11}$$

From the stability criteria in theorem 5.1.1 the equilibrium is stable for $\cos^{-1}\frac{\epsilon}{2w} > \frac{\pi\alpha}{2}$ and unstable for $\cos^{-1}\frac{\epsilon}{2w} < \frac{\pi\alpha}{2}$.
For numerical simulation I consider $\alpha = 0.5$, $w = 1.0$, for which the stability criteria becomes $\epsilon < \sqrt{2}$. Hence the simulation is done for $\epsilon = 1.3$ and $\epsilon = 1.5$ for stable equilibrium and unstable equilibrium, respectively. The instability coincides with hopf bifurcation and hence gives birth to the limit cycle which is shown in figure 5.2.

Fractional Coupled van der pol-Duffing oscillators

The fractional van der pol oscillator showed the dependence of stability region on the order of derivative. This involvement of the order is quite obvious given the forcing nature of it. In the case of coupled oscillators, the position and velocity or combined coupling are extensively studied. Fractional derivatives provide a more general coupling between two oscillators. In this section, I will consider two van der pol-Duffing oscillators coupled with fractional coupling, given as

$$\begin{aligned} \ddot{x} + x + \epsilon(x^2-1)\dot{x} + \epsilon\, b\, x^3 &= \epsilon\gamma D^{\alpha}(y-x) \\ \ddot{y} + y + \epsilon(y^2-1)\dot{y} + \epsilon\, b\, y^3 &= \epsilon\gamma D^{\alpha}(x-y), \end{aligned} \tag{5.12}$$

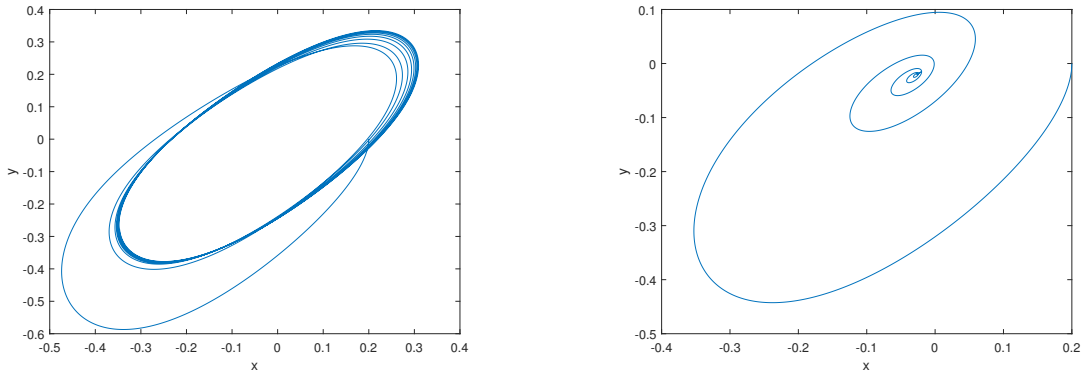

(a) $\epsilon = 1.5$ (b) $\epsilon = 1.3$

Figure 5.2: Phase portrait of Fractional Van der Pol (5.7) for $w = 1.0$, $\alpha = 0.5$. The subplots a) $\epsilon = 1.5$, showing limit cycle corresponding to the unstable origin, and b) $\epsilon = 1.3$, showing stable origin.

where ϵ, γ are regular van der pol parameters, b is coefficient of cubic nonlinearity and α is the order of the fractional derivative. The in-phase solution could be found by eliminating the coupling which leave what is basically the regular van der pol equation. Let the in-phase solution be denoted by $u(t)$ for which let the approximate form is given as

$$u(t) = 2\cos t + O(\epsilon). \tag{5.13}$$

To study the stability of in-phase solution consider $\phi = x - u$, and $\psi = y - u$ as small deviations from the in-phase solution. Putting it in (5.12) and ignoring the nonlinear terms gives

$$\begin{aligned} \ddot{\phi} + \epsilon(u^2 - 1)\dot{\phi} + (1 + 2\epsilon u\dot{u} + 3\epsilon\, bu^2)\phi &= \epsilon\gamma D^\alpha(\psi - \phi) \\ \ddot{\psi} + \epsilon(u^2 - 1)\dot{\psi} + (1 + 2\epsilon u\dot{u} + 3\epsilon\, bu^2)\psi &= \epsilon\gamma D^\alpha(\phi - \psi). \end{aligned} \tag{5.14}$$

These equations of motion of the deviations decouple by defining $w = \phi + \psi$ and $v = \phi - \psi$. The corresponding equations are

$$\ddot{w} + \epsilon(u^2 - 1)\dot{w} + (1 + 2\epsilon u\dot{u} + 3\epsilon\, bu^2)w = 0 \tag{5.15}$$

$$\ddot{v} + \epsilon(u^2 - 1)\dot{v} + (1 + 2\epsilon u\dot{u} + 3\epsilon\, bu^2)v = -2\epsilon\gamma D^\alpha v. \tag{5.16}$$

Now the first equation is basically the variational equation for the single van der pol oscillator for which the solution is known to be a stable limit cycle. Hence the stability structure is determined by the second equation alone.

The presence of ϵ parameter demands two time scale perturbation approach. Therefore, consider $\zeta = \omega t$ and $\eta = \epsilon t$, where w is the frequency of the limit cycle and is assumed to have a power series representation in ϵ as

$$\omega = 1 + O(\epsilon^2). \tag{5.17}$$

Under the two time scale $\dot{v}, \ddot{v}$ becomes

$$\begin{aligned} \dot{v} &= \omega v_\zeta + \epsilon v_\eta \\ \ddot{v} &= \omega^2 v_{\zeta\zeta} + 2\omega\epsilon v_{\zeta\eta} + \epsilon^2 v_{\eta\eta}. \end{aligned} \tag{5.18}$$

The fractional derivative could be transformed as

$$\begin{aligned} D^\alpha = D_t^\alpha v &= \frac{1}{\Gamma(1-\alpha)} \int_0^t z^{-\alpha} \dot{v}(t-z) dz \\ consider\ z \to \frac{k}{\omega}, &\qquad \frac{d}{dt} \to \frac{d}{d\zeta}\omega \\ D_t^\alpha v(\zeta) &= \frac{1}{\Gamma(1-\alpha)} \int_0^\zeta (\frac{k}{\omega})^{-\alpha} v'(\zeta - k)\omega \frac{dk}{\omega}, \quad where\ v'(\zeta) = \frac{dv}{d\zeta} \\ D_t^\alpha v(\zeta) &= \omega^\alpha D_\zeta^\alpha v(\zeta) \end{aligned} \tag{5.19}$$

Now putting all these expressions in (5.18) we have

$$\omega^2 v_{\zeta\zeta} + 2\omega\epsilon v_{\zeta\eta} + \epsilon^2 v_{\eta\eta} + \epsilon(u^2 - 1)(\omega v_\zeta + \epsilon v_\eta) + (1 + 2\epsilon u\dot{u} + 3\epsilon\, b u^2)v = -2\epsilon\gamma D_\zeta^\alpha v(\zeta,\, \eta) \tag{5.20}$$

Further I seek a solution $v(t)$ in terms of a power series as

$$v(\zeta, \eta) = v_0(\zeta, \eta) + \epsilon v_1(\zeta, \eta) + O(\epsilon^2). \tag{5.21}$$

Putting the expansion in (5.20) and equating the terms for each order of ϵ to zero, we get

- $O(1)$**:** $v_{0\zeta\zeta} + v_0 = 0.$

(5.22)

- $O(\epsilon)$**:** $v_{1\zeta\zeta} + v_1 = -2v_{0\zeta\eta} - (1 + 2\cos 2\zeta)v_{0\zeta} + (4sin2\zeta + 6\, b(1 + \cos 2\zeta))v_0 - 2\gamma D_\zeta^\alpha v_0.$

(5.23)

The general solution of $O(1)$ is

$$v_0(\zeta, \eta) = A(\eta)\cos\zeta + B(\eta)\sin\zeta. \tag{5.24}$$

Replacing v_0 with above expression in (5.23) involves fractional derivative of v_0 which needs special attention. To resolve the derivative consider first

$$\begin{aligned} D^{\alpha}\cos\zeta &= \frac{1}{\Gamma(1-\alpha)}\int_0^{\zeta} -z^{-\alpha}\sin\zeta - z dz, \\ &= -\frac{1}{\Gamma(1-\alpha)}\int_0^{\zeta} z^{-\alpha}(\sin\zeta\cos z - \cos\zeta\sin z)dz, \\ &= -\frac{\sin\zeta}{\Gamma(1-\alpha)}\int_0^{\zeta} z^{-\alpha}\cos z dz + \frac{\cos\zeta}{\Gamma(1-\alpha)}\int_0^{\zeta} z^{-\alpha}\sin z dz. \qquad (5.25) \\ & \qquad (5.26) \end{aligned}$$

Now the last integral converges only in the limit $\zeta \to \infty$, therefore, I evaluate the integral for the steady states. Now using

$$\int_0^{\infty} z^{-\alpha}\cos z dz = \Gamma(1-\alpha)\sin\frac{\alpha\pi}{2}, \quad \int_0^{\infty} z^{-\alpha}\sin z dz = \Gamma(1-\alpha)\cos\frac{\alpha\pi}{2}, \qquad (5.27)$$

we have

$$D^{\alpha}cos\zeta = \cos\zeta\cos\frac{\alpha\pi}{2} - \sin\zeta\sin\frac{\alpha\pi}{2}. \qquad (5.28)$$

Similarly,

$$D^{\alpha}sin\zeta = \sin\zeta\cos\frac{\alpha\pi}{2} + \cos\zeta\sin\frac{\alpha\pi}{2}. \qquad (5.29)$$

Using the above derived expressions and solution of v_0, equation (5.23) gives

$$\begin{aligned} \ddot{v_1} + v_1 = \quad & -2(-A'\sin\zeta + B'\cos\zeta) - (1+2\cos 2\zeta)(-A\sin\zeta + B\cos\zeta) \\ & +(4\sin 2\zeta + 6\,b(1+\cos 2\zeta))(A\cos\zeta + B\sin\zeta) \\ & -2\gamma\bigg(A\bigg(\cos\zeta\cos\frac{\alpha\pi}{2} - \sin\zeta\sin\frac{\alpha\pi}{2}\bigg) \\ & +B\bigg(\sin\zeta\cos\frac{\alpha\pi}{2} + \cos\zeta\sin\frac{\alpha\pi}{2}\bigg)\bigg). \qquad (5.30) \end{aligned}$$

Collecting the resonant terms, we have

$$\begin{aligned} \ddot{v_1} + v_1 = \quad & \bigg(2A' + 2A + 2\gamma A\sin\frac{\alpha\pi}{2} - 2\gamma B\cos\frac{\alpha\pi}{2} - 3\,b\,B\bigg)\sin\zeta \\ & \bigg(-2B' - 2\gamma A\cos\frac{\alpha\pi}{2} - 2\gamma B\sin\frac{\alpha\pi}{2} - 9\,b\,A\bigg)\cos\zeta + NRT. \qquad (5.31) \end{aligned}$$

By eliminating the secular terms, we have the slow flow equations

$$\begin{aligned} A' &= -A - \gamma\bigg(A\sin\frac{\alpha\pi}{2} - B\cos\frac{\alpha\pi}{2}\bigg) - 3\,b\,B \qquad (5.32) \\ B' &= -\gamma\bigg(A\cos\frac{\alpha\pi}{2} + B\sin\frac{\alpha\pi}{2}\bigg) - 9\,b\,A. \qquad (5.33) \end{aligned}$$

The slow flow equations are linear with the coefficient matrix given as

$$M = \begin{pmatrix} -1 - \gamma \sin\frac{\alpha\pi}{2} & \gamma \cos\frac{\alpha\pi}{2} - 3\,b \\ -\gamma \cos\frac{\alpha\pi}{2} - 9\,b & -\gamma \sin\frac{\alpha\pi}{2} \end{pmatrix}. \tag{5.34}$$

Based on the eigenvalues of M matrix the stability region in $\alpha - \gamma$ parameter plot is given in figure 5.3.

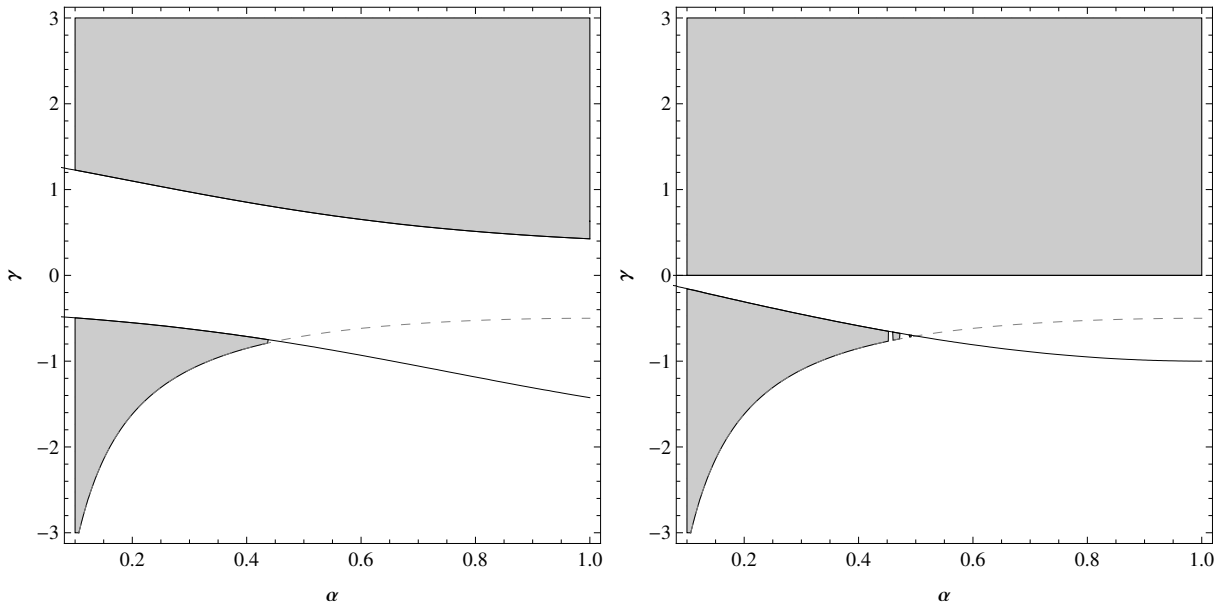

(a) $b = -0.15$ (b) $b = 0$

Figure 5.3: Stability region of in-phase solution $u(t)$ in $\alpha - \gamma$ parameter space. The shaded parts are stable regions of the limit cycle for a) $b = -0.15$, and b) $b = 0$. Dashed line represents the condition $tr(M) = 0$ which denoted the critical line of Hopf bifurcation and solid lines represents $det(M) = 0$.

In the figure 5.3, the shaded regions are stable and plain regions are unstable. The stability of the origin of 5.32 and 5.33 denotes the stability of in-phase solution $u(t)$.

The important insight is that of dependence of stability on the order of fractional derivative. When the cubic nonlinearity is absent ($b = 0.0$), figure 5.3 shows negative γ values favours lower orders of the derivative, and it is stable and independent of the order for positive γ values. This exactly matches with the results from [33]. When the cubic nonlinearity is switched on ($b = -0.15$), there is a erosion of stability regions for negative γ values in addition to some parts of positive γ values being unstable which were earlier stable.

5.1.2 Conclusion

In this work, we first showed that trajectories of fractional harmonic oscillator are oscillatory when order, $\gamma = 1$, under-damp, when $0.5 \geq \gamma < 1.0$, and over-damp for $\gamma < 0.5$. The corresponding solutions are presented in terms of *Mittag-Leffler* functions. Next, we

considered the fractional van der pol oscillator system where the concept of the stability of the origin, and conditions for Hopf bifurcation were obtained and its dependence on the order of the fractional derivative were established. Lastly, we considered fractional coupled VDP-D oscillator where we employed perturbation scheme to obtain the stability of the in-phase solution of the system. Further, we analysed the how the cubic nonlinearity couples with the fractional derivatives and effects the stability of the solution. This work helps us establish the role of order of the fractional derivative, the dual nature of the fractional derivative as both forcing and damping characteristics.

5.2 Delay Dynamical System

In the dynamical processes consisting of feedbacks or which have multiple dynamical units, there usually is a signal delay which changes the dynamical landscape unexpectedly. This dynamics, governed by *Delay Differential Equations* (DDE), depends on an earlier state of the system usually incorporated in the equation as, $x(t-\tau)$, where $x(t)$ represents the current state and τ is the delay in the system.

The introduction of delays has been a major breakthrough in accurate modelling of physical processes which leads to many applications in science and engineering. The application of delays appears very prominently in traffic dynamics, [34, 35], population dynamics, [36, 37], chemical kinetics, [38], biological systems, [39, 40], economic models, [41, 42]. Delays play major role in control of chaotic systems, [43, 44, 45, 46], signal processing in robotics, [47, 48]. Applications of delay dynamical systems cut across fields and has varied degree of utilities like in modelling musical instruments, [49], laser dynamics, [50].

DDEs belongs to a class of functional differential equations (FDE) instead of ODEs. As it is explained in the first chapter, in ODEs the input or initial values of variables and its derivatives are defined at the same instant, while, for FDEs the initial values for the variables and its derivatives are defined at different instances of the independent variable. DDEs are a type of FDEs which contain functions dependent on present as well as past values of the dependent variables. This dependence makes DDEs, and FDEs in general, an infinite-dimensional system which is in contrast with ODEs which are finite-dimensional systems.

To illustrate, consider a linear first-order DDE of the form,

$$\dot{x}(t) = x(t-\tau), \tag{5.35}$$

where τ is the delay. Let the initial value problem (IVP) associated with (5.35) is defined on $[t_0, t_0+T]$, then initial values for $[t_0-\tau, t_0]$ are not discrete values but a function, $\phi(t)$ of time and is usually called history function. In solving DDE IVP the continuity of the solutions is a crucial step as the history function and the solution need to be continuous at $t = t_0$. This discontinuity can persist over time through the order of derivatives. For example, if there is a discontinuity in first derivative at $t = t_0$, then second order will be discontinuous at $t = 2\,t_0$ and so on. This is known as propagation of discontinuity. Further, there can be multiple delays, [51, 52], in an equation, $\{\tau_1, \tau_2, ..\}$, or even a

distribution of delay terms, [53], based on some function. For such equations the history function must be appropriately defined. Fractional derivatives in FrDE in the previous sections can be considered a form weighted distribution of delays.

It is not, in general, possible to find a closed-form exact solution of DDEs. For linear cases there are few prescriptions in literature [54, 55] which helps in analysing such problems. *Laplace transformation* technique is a natural contender for a linear DDEs with constant coefficient, [56]. *Method of steps*, [57], is another of method for general linear DDEs. In *Method of steps* the DDE is reduce to ODEs over successive intervals and the existence of the solution depends on ODEs in each interval. This process is tedious in practice and often carried out with numerical algorithms.

Another way to analyse DDEs is through *characteristic equation*. As in the case of linear ODEs, the solution of linear homogeneous DDEs are in the form of exponentials. Therefore, by assuming a solution of exponential form and placing it in the equation we get a *characteristic equation*. Solutions of the *characteristic equation* determines the linear behaviour of the system and the stability profile. For nonlinear DDEs, the system could be linearised and then the corresponding *characteristic equation* could be utilised to determine the stability of the system. However, unlike ODEs where the *characteristic equation* is a polynomial, in DDEs the *characteristic equations* are transcendental. This transcendental nature results in infinite number of roots and hence infinite family of independent solutions.

For weakly nonlinear DDEs, multiscale perturbation techniques are most commonly employed, [58, 59]. In this section, we considered two van der pol-Duffing oscillators with delay coupling and analysed them using slow flow methods.

5.2.1 Delay Coupled van der pol-Duffing (VDP-D) Oscillators [1]

In this work we study the dynamics of coupled VDP-D oscillators with delay coupling. The problem of two van der pol oscillators with the delay coupling was investigated by Rand and Wirkus in [58] who chose the delay coupling in the damping terms because this form of coupling occurs in radioactively coupled microwave oscillator arrays. The coupling of microwave oscillators via delayed velocity coupling has been extensively studied by electrical engineers [61, 62, 63, 64]. The two principal features of microwave oscillators are negative resistance and gain saturation. The former one causes the amplitude of the oscillations to grow while the latter limits the amplitude of the oscillations. A similar phenomenon also occurs in laser physics and is manifested in the form of relaxation oscillations [65]. As a consequence the van der pol oscillator is often considered as a generic microwave oscillator.

The present work introduces a cubic nonlinearity effect into the coupled delayed Van Der Pol system considered in [66]. This leads to a VDP-D equation and provides an important mathematical model for dynamical systems having a single unstable fixed point, along with a stable limit cycle. Examples of such phenomena arise quite naturally in engineering problems.

[1] This is part of a published work, [60]

Specifically we analyse two coupled VDP-D oscillators with delayed velocity coupling. The work is in the spirit of Rand and his collaborators. Time delay is included explicitly in the differential equations rather than the delay in the averaged equations. In the study of two weakly delayed coupled van der pol oscillators Wirkus and Rand [58] found that both the in-phase and out of phase modes were stable for delays of about a quarter of the uncoupled period of the oscillators. In this work we generalize the result of R. Rand to two weakly coupled VDP-D oscillators in which the coupling term involves a time delay τ. We use the method of averaging to obtain the approximate simplified system and then investigate the stability and bifurcation of their equilibria which correspond to periodic motions in the original system.

The system of coupled delayed VDP-D oscillators we consider are given by

$$\ddot{x}_1 + \epsilon(x_1^2 - 1)\dot{x}_1 + x_1 - \epsilon x_1^3 = \alpha\epsilon\dot{x}_2(t - T), \tag{5.36}$$

$$\ddot{x}_2 + \epsilon(x_2^2 - 1)\dot{x}_1 + x_2 - \epsilon x_2^3 = \alpha\epsilon\dot{x}_1(t - T). \tag{5.37}$$

The in-phase mode of this coupled system occurs when $x_1 = x_2$ for which we have the common equation

$$\ddot{y} + \epsilon(y^2 - 1)\dot{y} + y - \epsilon y^3 = \alpha\epsilon\dot{y}(t - T). \tag{5.38}$$

To find a periodic solution of this equation we use the Lindstetd-Poincarè perturbation technique and set $\tau = \omega t$ where $\omega = 1 + \epsilon k + O(\epsilon^2)$. This gives the equation

$$\omega^2 y'' + \epsilon\omega(y^2 - 1)y' + y - \epsilon y^3 = \alpha\epsilon\omega y'(\tau - \omega T), \tag{5.39}$$

where the primes denote differentiation with respect to the variable τ. Next we expand y is a power series in ϵ i.e., set

$$y = y_0 + \epsilon y_1 + \cdots$$

and equate the coefficients of various powers of ϵ to get

$$y_0'' + y_0 = 0 \tag{5.40}$$

$$y_1'' + y_1 = -2ky_0'' - (y_0^2 - 1)y_0' + y_0^3 + \alpha y_0'(\tau - T). \tag{5.41}$$

Assuming a solution of the form $y_0 = R\cos\tau$ of (5.40) we substitute this into (5.41) to obtain

$$y_1'' + y_1 = (2kR + \alpha R\sin T + \frac{3}{4}R^3)\cos\tau - (R + \alpha R\cos\tau - \frac{1}{4}R^3)\sin\tau + \frac{R^3}{4}\cos 3\tau + \frac{R^3}{4}\sin 3\tau \tag{5.42}$$

By demanding the secular terms to vanish we obtain the solutions for the amplitude R and k as given below

$$R = 2\sqrt{1+\alpha\cos T}, \quad k = -\frac{1}{2}(\alpha\sin T + 3(1+\alpha\cos T). \tag{5.43}$$

Consequently for the in-phase mode we have

$$y \approx y_0 = 2\sqrt{1+\alpha\cos T}\cos\{1 - \frac{\epsilon}{2}(\alpha\sin T + 3(1+\alpha\cos T))t\}. \tag{5.44}$$

Stability of the in-phase mode

In order to study the stability of the in-phase mode we set

$$x_1 = y(t) + w_1, \quad x_2 = y(t) + w_2,$$

and linearise the system (5.36)-(5.37) about $w_1 = w_2 = 0$. This leads to the following system of coupled linear delayed differential equations (DDE), namely

$$\ddot{w}_1 + \epsilon(y^2-1)\dot{w}_1 + (1+\epsilon(2y\dot{y}-3y))w_1 = \alpha\epsilon\dot{w}_2(t-T), \tag{5.45}$$
$$\ddot{w}_2 + \epsilon(y^2-1)\dot{w}_2 + (1+\epsilon(2y\dot{y}-3y))w_2 = \alpha\epsilon\dot{w}_1(t-T). \tag{5.46}$$

The above system is easily decoupled by the transformation

$$z_1 = w_1 + w_2, \quad z_2 = w_1 - w_2,$$

whence they become

$$\ddot{z}_1 + \epsilon(y^2-1)\dot{z}_1 + (1+\epsilon(2y\dot{y}-3y))z_1 = \alpha\epsilon\dot{z}_1(t-T), \tag{5.47}$$
$$\ddot{z}_2 + \epsilon(y^2-1)\dot{z}_2 + (1+\epsilon(2y\dot{y}-3y))z_2 = -\alpha\epsilon\dot{z}_2(t-T). \tag{5.48}$$

The decoupled system given in the last two equations have the generic form

$$\ddot{u} + \epsilon(y^2-1)\dot{u} + (1+\epsilon(2y\dot{y}-3y))u = \beta\alpha\epsilon\dot{u}(t-T), \tag{5.49}$$

where $u = z_1$ for $\beta = 1$ and $u = z_2$ for $\beta = -1$.

Two variable perturbation method for Eqn (5.49)

To investigate the presence of different time scales in the delayed equation (5.49) we take recourse to the two variable perturbation method involving the times scales $\tau = \omega t$ and $\eta = \epsilon t$. It follows that

$$\frac{du}{dt} = \omega u_\tau + \epsilon u_\eta$$

$$\frac{d^2u}{dt^2} = \omega^2 u_{\tau\tau} + 2\omega\epsilon u_{\tau\eta} + \epsilon^2 u_{\eta\eta}$$

Inserting these expressions into (5.49) we obtain

$$(\omega^2 u_{\tau\tau}+2\omega\epsilon u_{\tau\eta}+\epsilon^2 u_{\eta\eta})+\epsilon(y^2-1)(\omega u_\tau+\epsilon u_\eta)+(1+\epsilon(2yy_\tau-3y))u = \epsilon\alpha\beta(\omega u_\tau+\epsilon u_\eta)(\tau-\omega T,\eta-\epsilon T). \tag{5.50}$$

Expanding u and ω in a power series in ϵ, *viz*

$$u = u_0 + \epsilon u_1 + O(\epsilon^2), \quad \omega = 1 + \epsilon k + O(\epsilon^2)$$

we have upon inserting the expression for k using (5.43) and (5.44) and retaining terms up to the first-order in ϵ:

$$u_{0\tau\tau} + u_0 = 0 \tag{5.51}$$

$$\begin{aligned} u_{1\tau\tau} + u_1 &= -2u_{0\tau\eta} + (\alpha\sin T + 3(1+\alpha\cos T))u_{0\tau\tau} + (1-4(1+\alpha\cos T)\cos^2\tau)u_{0\tau} \\ &+[8(1+\alpha\cos T)\cos\tau\sin\tau + 6\sqrt{1+\alpha\cos T}\cos\tau]u_0 + \alpha\beta u_{0\tau}(\tau-T,\eta-\epsilon T) \end{aligned} \tag{5.52}$$

Next assume that (5.51) has the solution of the form

$$u_0(\tau,\eta) = A(\eta)\cos\tau + B(\eta)\sin\tau$$

so that the delayed term has the form

$$u_0(\tau-T,\eta-\epsilon T) = A_d\cos\tau - T + B_d\sin\tau - T$$

where $A_d = A(\eta-\epsilon T)$ and $B_d = B(\eta-\epsilon T)$ respectively. Inserting the above solution into (5.52) and requiring that the secular terms vanish gives the following system of equations for the amplitudes *viz*

$$\frac{dA}{d\eta} = -\left(1+\frac{3\alpha\cos T}{2}\right)A + \frac{\alpha\sin T}{2}B + \frac{\alpha\beta\cos T}{2}A_d - \frac{\alpha\beta\sin T}{2}B_d, \tag{5.53}$$

$$\frac{dB}{d\eta} = \left(3(1+\alpha\cos T) - \frac{\alpha\sin T}{2}\right)A - \frac{\alpha\cos T}{2}B + \frac{\alpha\beta\sin T}{2}A_d + \frac{\alpha\beta\cos T}{2}B_d. \tag{5.54}$$

The last two equations represent the *slow flow* system of delay differential equations. The first step to analysing the system (5.53)-(5.54) consists in setting $A = Pe^{\lambda\eta}, B = Qe^{\lambda\eta}$ and $A_d = Pe^{\lambda(\eta-\epsilon T)}, B_d = Qe^{\lambda(\eta-\epsilon T)}$ in (5.53) and (5.54) which gives

$$\lambda A = -A\left(1+\frac{3\alpha\cos T}{2}\right)A + \frac{\alpha\sin T}{2}B + \frac{\alpha\beta\cos T}{2}Ae^{-\lambda\epsilon T} - \frac{\alpha\beta\sin T}{2}Be^{-\lambda\epsilon T},$$

$$\lambda B = \left(3(1+\alpha\cos T) - \frac{\alpha\sin T}{2}\right)A - \frac{\alpha\cos T}{2}B + \frac{\alpha\beta\sin T}{2}e^{-\lambda\epsilon T}A + \frac{\alpha\beta\cos T}{2}e^{-\lambda\epsilon T}B.$$

Considering the case $\beta = -1$ we are led therefore to the homogeneous system of equations:

$$\begin{pmatrix} -\lambda - 1 - \frac{\alpha\cos t}{2}(3 + e^{-\lambda\epsilon T}) & \frac{\alpha\sin T}{2}(1 + e^{-\lambda\epsilon T}) \\ 3(1 + \alpha\cos T) - \frac{\alpha\sin T}{2}(1 + e^{-\lambda\epsilon T}) & -\lambda - \frac{\alpha\cos T}{2}(1 + e^{-\lambda\epsilon T}) \end{pmatrix} \begin{pmatrix} A \\ B \end{pmatrix} = \begin{pmatrix} 0 \\ 0 \end{pmatrix}$$

For non-trivial solutions it is necessary that the determinant vanishes. We set $\lambda = i\Omega$ and equate the determinant to zero to obtain

$$-\Omega^2 + i\Omega\Big(1 + \alpha\cos T(2 + e^{-i\epsilon\Omega T})\Big) + \frac{\alpha^2\cos^2 T}{4}(3 + 4e^{-i\epsilon\Omega T} + e^{-2i\epsilon\Omega T})$$

$$+\frac{\alpha^2\sin^2 T}{4}(1 + 2e^{-i\epsilon\Omega T} + e^{-2i\epsilon\Omega T}) + \frac{\alpha\cos T}{2}(1 + e^{-i\epsilon\Omega T}) - \frac{3}{2}\alpha\sin T(1 + \alpha\cos T)e^{-i\epsilon\Omega T} = 0$$

We separate the real and imaginary parts of the last equation to get

Real Part:

$$-\Omega^2 + \frac{\Omega\alpha\cos T}{2}\sin\Omega\epsilon T + \frac{\alpha\cos T}{2} + \frac{3\alpha^2}{4}\cos^2 T + \frac{\alpha^2\cos^2 T}{4}\cos\Omega\epsilon T$$

$$+\frac{\alpha\cos T}{2}\cos\Omega\epsilon T + \frac{\alpha\cos T}{2}\Omega\sin\Omega\epsilon T + \frac{3\alpha^2\cos^2 T}{4}\cos\Omega\epsilon T + \frac{\alpha^2\cos^2 T}{4}\cos 2\Omega\epsilon T$$

$$+\frac{\alpha^2\sin^2 T}{4}(1 + \cos 2\Omega\epsilon T + 2\cos\Omega\epsilon T) - 3(1 + \alpha\cos T)\frac{\alpha\sin T}{2}(1 + \cos\Omega\epsilon T) = 0. \quad (5.55)$$

Imaginary Part:

$$\Omega + \frac{\Omega 3\alpha}{2}\cos T + \frac{\Omega\alpha\cos T}{2}\cos\Omega\epsilon T + \frac{\alpha\cos T}{2}\Omega - \frac{\alpha^2\cos^2 T}{4}\sin\Omega\epsilon T$$

$$+\frac{\alpha\Omega\cos T}{2}\cos\Omega\epsilon T - \frac{\alpha\cos T}{2}\sin\Omega\epsilon T - \frac{3\alpha^2\cos^2 T}{4}\sin\Omega\epsilon T - \frac{\alpha^2\cos^2 T}{4}\sin 2\Omega\epsilon T$$

$$-\frac{\alpha^2\sin^2 T}{4}\sin 2\Omega\epsilon T + \frac{\alpha^2\sin^2 T}{4}(-2\sin\Omega\epsilon T) + 3(1 + \alpha\cos T)\frac{\alpha\sin T}{2}\sin\Omega\epsilon T = 0. \quad (5.56)$$

We expand T and Ω in a power series in ϵ, viz,

$$T = T_0 + \epsilon T_1 + \epsilon^2 T_2 + \cdots$$

$$\Omega = \Omega_0 + \epsilon\Omega_1 + \epsilon^2\Omega_2 + \cdots$$

Substituting these expansions into the equations (5.58) and (5.59) and equating terms of the various orders of ϵ we obtain,

Coefficient of ϵ^0:

$$\Omega_0(1 + 3\alpha \cos T_0) = 0 \Longrightarrow \quad \cos T_0 = -\frac{1}{3\alpha} \tag{5.57}$$

$$\Omega_0 = \frac{1}{3}\sqrt{p^2 - 6p - 1}, \quad p = \sqrt{9\alpha^2 - 1} \tag{5.58}$$

Coefficient of ϵ^1:

$$T_1 = \frac{T_0}{3}\left(1 - \frac{p}{3}\right) \qquad or \qquad T_1 = -\frac{T_0}{9}(p - 3) \tag{5.59}$$

$$\Omega_1 = -\frac{T_0}{54}\left[\frac{3p^3 - 7p^2 - 9p - 21}{\sqrt{p^2 - 6p - 1}}\right]. \tag{5.60}$$

The higher order terms can also be found in a similar manner. The expressions for Ω and T gives the conditions for the Hopf bifurcation of the solution $y(t)$. If consider only the first order then the condition is given as $\alpha = -\frac{1}{cosT_0}$. To check the stability of the limit cycle, originated out of this Hopf bifurcation, let $\lambda = R + i\,\Omega$ and expand λ in the neighbourhood of the limit cycle. As the real part R would be zero at the cycle, The stability could be checked by noticing the sign of the first derivative. From the calculations, it was found that the first order term is given as $R = \frac{1}{2}(-1 - 3\,\alpha\, cosT)$. This expression is expected as it reduces to the Hopf condition for $R = 0$. However, one point to keep in mind is that these conditions are not exact and true only for first order and with higher orders, corrections will be added to the expressions and more precise conditions could be obtain as shown by Gluzman and Rand in [66].

The saddle-node condition could be obtain by assuming $\lambda = 0$ and the determinant vanishes. For $\beta = -1$ the conditions are

$$\alpha = 0, \ \& \ \alpha = -\frac{2(cosT - 3\, sinT)}{3 + cos2T - sin2T}.$$

The $\beta = 1$ case gives the conditions for the birth of in-phase periodic mode , corresponding to the independence of A and B on η. The condition is given as

$$\alpha = \frac{-1}{\cos T}.$$

There are no correction terms involved in this expression as we considered the case for $\lambda = 0$. Also, there is no ϵ dependence, which is evident as these are slow flow equations and only dependence on ϵ is in the delay. In the next section, we will see that this condition corresponds to the change in stability of the origin itself.

Stability analysis of velocity delay coupling

The Duffing-Van der Pol oscillator defined in (5.36), (5.37) possesses an unstable fixed point at origin and a stable limit cycle around it in uncoupled case. Coupling the system without delay does not affect the limit cycle and it continue to exist for all parameter values. However, with delay coupling, the stability of the origin changes for some parameter arrangements. To study the stability of origin, assume the variation of the coordinates in the neighbourhood of the origin proportional to $e^{m\,t}$ which gives the characteristic equation for the stability of origin as

$$m^2 + \epsilon m + 1 = \alpha\epsilon\, m\, e^{-mT}. \tag{5.61}$$

The characteristic equation is transcendental in nature and could not have closed form solutions. To analyse it for periodic orbit, consider the $\lambda = i\, m_I$ which on solving gives the delay curves as

$$m_{I\pm} = \left[\frac{1}{2}(\epsilon^2(\alpha^2-1)+2) \pm \frac{1}{2}((\epsilon^2(\alpha^2-1)+2)^2-4)^{1/2}\right]^{1/2}.$$

and satisfies

$$\cos m_{\pm} T_{\pm} = \frac{-1}{\alpha}, \tag{5.62}$$

Condition in (5.62) gives the condition for Hopf Bifurcation of the origin. The delay curves could be expanded for small ϵ and approximated as

$$m_{I\pm} = 1 + \frac{1}{2}\sqrt{\alpha^2-1}\,\epsilon + O(\epsilon^2), \tag{5.63}$$

which, for the first order, gives $\alpha = -\frac{1}{cosT}$. This is what we got from the slow flow analysis of the periodic solution. The higher order corrections were not present in the slow flow, however the stability analysis of the origin provides some higher order corrections.
Now, the characteristic equation (5.61), in a more general form, had been studied and analysed before and given the conditions

$$\alpha < 1 \;\;\&\;\; \alpha^2 > 1,$$

the conclusions of the studies are given in the following theorem

Theorem 5.2.1 *For $T_{\pm}(n)$ defined as (5.62), there is a positive integer n such that there are n switches from stability to instability to stability, i.e., when*

$$T \in [0, T_+(0)] \cup (T_-(0), T_+(1)) \cup ... \cup (T_-(n-1), T_+(n))$$

all roots of (5.61) have negative real parts.

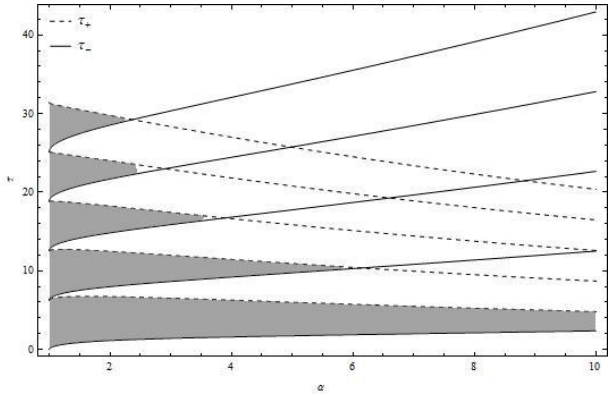

Figure 5.4: The plot shows the variation of delay with coupling coefficient for values $\omega = 1.0$, $k = 0.1$, with $n = \{1, 2, 3, 4\}$ for T_+ and $n = \{1, 2, 3\}$ for T_-.

The theorem is part of [67] and the proof is straightforward, for which please refer to [68]. The theorem provides the conditions for the real part of the roots of (5.61) to be negative which denotes the stability of the origin. The origin is a stable focus for $\alpha < -1$ for some sets of delay values as specified in theorem 5.2.1. For $-1 < \alpha < 1$ the eigenvalues are purely real and the upper bound of its values is obtain as the roots of the characteristic equation for $T = 0$, given as

$$m_{\pm} = -\frac{1}{2}\epsilon(1-\alpha) \pm \frac{1}{2}\sqrt{\epsilon^2(1-\alpha)^2 - 4}. \tag{5.64}$$

The upper boundedness could be proven by Rouche's theorem. Clearly, the origin is unstable in this region.

The origin for $\alpha > 1$ shows transition as in the case for $\alpha < -1$. It is stable for some sets of delay values and unstable for other. The unstable phases corresponds with the stable limit cycle. Figure 5.4 shows the stability regions (shaded) for $\alpha > 1$ case.

Numerical Simulation

In previous sections, we derived the conditions for the Hopf bifurcation of the origin which corresponds with the birth of in-phase periodic solution. Further, we have seen that the origin is stable for $\alpha^2 > 1$ which corresponds to the case of amplitude death of the oscillator. In this section, we numerically simulate the coupled system.

From theorem 4.1 we have conditions for the stability of the origin. We simulated the system for $\alpha = 1.5$, & $\epsilon = 0.1$ with initial conditions $x(0) = 0.5$, $y(0) = 0.5$, $\dot{x}(0) = 0.5$, $\dot{y}(0) = 0.5$. The corresponding critical delay values are $T \in [0, 0.7953] \cup [0.8894, 6.7371] \cup [7.5336, 12.6789]$. The resultant plots are shown in figure 5.5 which clearly shows the expected behaviour and in line with analytical calculations.

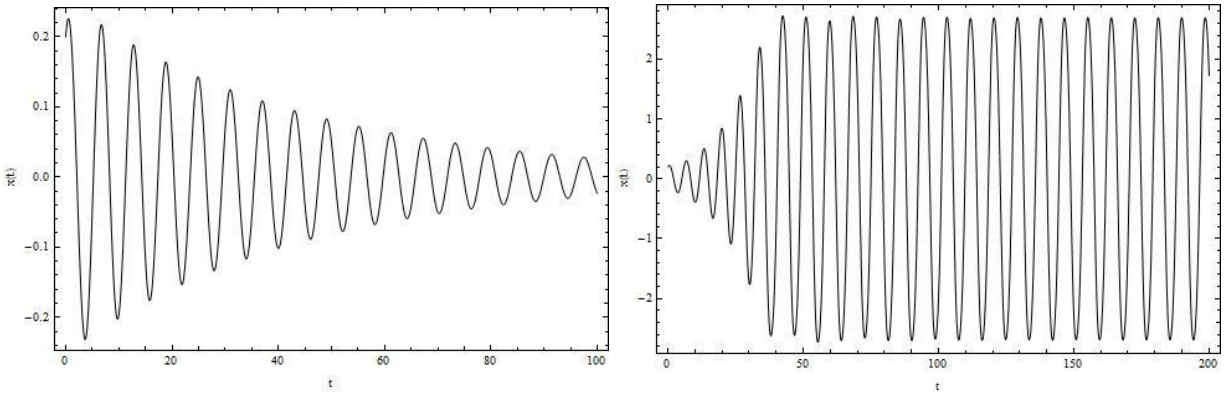

(a) $T = 2.7,\ \alpha = 1.5$ (b) $T = 7.2,\ \alpha = 1.5$

Figure 5.5: The plot shows time series of system (5.36,5.37) for parameters $\omega = 1.0$, $k = 0.1$, $\lambda = -0.1,\ \alpha = 1.5$ and $T = 2.7,\ \&\ T = 7.2$ denoting the stability of origin and limit cycle, respectively.

Conclusion

In this paper we studied coupled Duffing-Van der Pol oscillators by velocity delay terms. At first we used Lindstedt-Poincaré method to obtain an approximate expression for the in-phase mode. Then we studied the stability of the in-phase mode by applying the two variable perturbation method to

$$\ddot{u} + \epsilon(y^2 - 1)\dot{u} + (1 + \epsilon(2y\dot{y} - 3y))u = \beta\alpha\epsilon\dot{u}(t - T),$$

where $u = z_1$ for $\beta = 1$ and $u = z_2$ for $\beta = -1$. This resulted in the DDE slow flow. This resulted in a system of modified ODEs which possessed Hopf and saddle-node bifurcations. The vanishing of the determinant of the slow flow of DDE yields the nontrivial solution, but it is harder to solve. So, motivated from Gluzman-Rand work, we sought a series solution. Further, the stability of the in-phase mode was analysed. This stability corresponds to change in stability of the origin which was shown in section 4. The coupled system was also numerically studied and it was observed that numerical results are in sync with the analytical calculations.

5.3 Summary

In summary, through this work a basic understanding is developed for systems with dependence of current states on past/previous states. In delay system, this dependence is on a previous state and sometimes may be on multiple states. This is mostly in a discrete manner. For fractional dynamical system the dependence is in a weighted cumulative form. There are various weighted cumulative definition have been formed which are employed as per the application requirement. These nonlinearities show both forcing as well as damping components at the same time which allows manipulation of the energy through various terms of the system.

In the case study the role of fractional derivatives in the qualitative behaviours of the system, like stability, periodic solutions, and bifurcation of solution, is analysed. To begin with, fractional systems can show range of damping scenarios ranging underdamp to overdamp and everything in between, as well as oscillatory behaviours through a single term. These behaviours are basically parametrised by the order of the derivative involved. The stability conditions for FDEs are also different and depends on the order of derivative involved. Hence, it was observed that through the order of derivatives, a huge range of phenomenons can be explained. Next, the case study gives insight into the analytical treatment of coupled nonlinear oscillators and the influence of fractional derivative on the dynamics of the system. In particular, the effect of fractional derivative on the harmonics and the existence of the non-trivial steady states was profoundly analysed. Together with this, the order of the derivative destabilises the oscillations for some values of coupling parameter and stabilises the oscillations for some other values. These observations allow vast applications of models.

For the delay dynamical systems, an overview of the influence of delays in the dynamical processes in obtained. The case study, considered, assisted in developing the concepts of delay in coupled weakly nonlinear oscillators and the analytical techniques required for treating such systems.

Bibliography

[1] Vasily E Tarasov. *Fractional dynamics: applications of fractional calculus to dynamics of particles, fields and media*. Springer Science & Business Media, 2011.

[2] Francesco Mainardi. *Fractional calculus and waves in linear viscoelasticity: an introduction to mathematical models*. World Scientific, 2010.

[3] George M Zaslavsky and Georgij Moiseevič Zaslavskij. *Hamiltonian chaos and fractional dynamics*. Oxford University Press on Demand, 2005.

[4] Bertram Ross. The development of fractional calculus 1695–1900. *Historia Mathematica*, 4(1):75–89, 1977.

[5] Dumitru Baleanu and Sami I Muslih. On fractional variational principles. In *Advances in Fractional Calculus*, pages 115–126. Springer, 2007.

[6] Dumitru Baleanu. New applications of fractional variational principles. *Reports on Mathematical Physics*, 2(61):199–206, 2008.

[7] Tatiana Odzijewicz, Agnieszka B Malinowska, and Delfim FM Torres. A generalized fractional calculus of variations. *arXiv preprint arXiv:1304.5282*, 2013.

[8] Fred Riewe. Nonconservative lagrangian and hamiltonian mechanics. *Physical Review E*, 53(2):1890, 1996.

[9] Ali Khalili Golmankhaneh, Alireza Khalili Golmankhaneh, Dumitru Baleanu, and Mihaela Cristina Baleanu. Hamiltonian structure of fractional first order lagrangian. *International Journal of Theoretical Physics*, 49(2):365–375, 2010.

[10] Lin Li and Shao-Kai Luo. Fractional generalized hamiltonian mechanics. *Acta Mechanica*, 224(8):1757–1771, 2013.

[11] Fred Riewe. Mechanics with fractional derivatives. *Physical Review E*, 55(3):3581, 1997.

[12] Shao-Kai Luo, Xiao-Tian Zhang, and Jin-Man He. A general method of fractional dynamics, ie, fractional jacobi last multiplier method, and its applications. *Acta Mechanica*, 228(1):157–174, 2017.

[13] Nick Laskin. Fractional schrödinger equation. *Physical Review E*, 66(5):056108, 2002.

[14] Nick Laskin. Fractional quantum mechanics. *Physical Review E*, 62(3):3135, 2000.

[15] BM Vinagre, I Podlubny, A Hernandez, and V Feliu. Some approximations of fractional order operators used in control theory and applications. *Fractional calculus and applied analysis*, 3(3):231–248, 2000.

[16] Dingyü Xue. *Fractional-order control systems: fundamentals and numerical implementations*, volume 1. Walter de Gruyter GmbH & Co KG, 2017.

[17] Concepción A Monje, YangQuan Chen, Blas M Vinagre, Dingyu Xue, and Vicente Feliu-Batlle. *Fractional-order systems and controls: fundamentals and applications*. Springer Science & Business Media, 2010.

[18] Stephen W Wheatcraft and Mark M Meerschaert. Fractional conservation of mass. *Advances in Water Resources*, 31(10):1377–1381, 2008.

[19] Sverre Holm and Sven Peter Näsholm. Comparison of fractional wave equations for power law attenuation in ultrasound and elastography. *Ultrasound in medicine & biology*, 40(4):695–703, 2014.

[20] Albert CJ Luo and Valentin Afraimovich. *Long-range Interactions, Stochasticity and Fractional Dynamics: Dedicated to George M. Zaslavsky (1935—2008)*. Springer Science & Business Media, 2011.

[21] Nick Laskin and G Zaslavsky. Nonlinear fractional dynamics on a lattice with long range interactions. *Physica A: Statistical Mechanics and its Applications*, 368(1):38–54, 2006.

[22] GM Zaslavsky, M Edelman, and VE Tarasov. Dynamics of the chain of forced oscillators with long-range interaction: From synchronization to chaos. *Chaos: An Interdisciplinary Journal of Nonlinear Science*, 17(4):043124, 2007.

[23] Wen Chen, Hongguang Sun, Xiaodi Zhang, and Dean Korošak. Anomalous diffusion modeling by fractal and fractional derivatives. *Computers & Mathematics with Applications*, 59(5):1754–1758, 2010.

[24] Xiao-Jun Yang and JA Tenreiro Machado. A new fractional operator of variable order: application in the description of anomalous diffusion. *Physica A: Statistical Mechanics and its Applications*, 481:276–283, 2017.

[25] Ronald L Bagley and PJ Torvik. A theoretical basis for the application of fractional calculus to viscoelasticity. *Journal of Rheology*, 27(3):201–210, 1983.

[26] Vasily E Tarasov. Universal electromagnetic waves in dielectric. *Journal of Physics: condensed matter*, 20(17):175223, 2008.

[27] Vasily E Tarasov. Fractional integro-differential equations for electromagnetic waves in dielectric media. *Theoretical and Mathematical Physics*, 158(3):355–359, 2009.

[28] Francesco Mainardi and Rudolf Gorenflo. Time-fractional derivatives in relaxation processes: a tutorial survey. *arXiv preprint arXiv:0801.4914*, 2008.

[29] Gösta Magnus Mittag-Leffler. Sur la nouvelle fonction eα (x). *CR Acad. Sci. Paris*, 137(2):554–558, 1903.

[30] Hans J Haubold, Arak M Mathai, and Ram K Saxena. Mittag-leffler functions and their applications. *Journal of Applied Mathematics*, 2011, 2011.

[31] Rudolf Gorenflo, Anatoly A Kilbas, Francesco Mainardi, Sergei V Rogosin, et al. *Mittag-Leffler functions, related topics and applications*, volume 2. Springer, 2014.

[32] Denis Matignon. Stability results for fractional differential equations with applications to control processing. 2(1):963–968, 1996.

[33] MK Suchorsky and RH Rand. A pair of van der pol oscillators coupled by fractional derivatives. *Nonlinear Dynamics*, 69(1):313–324, 2012.

[34] Gábor Orosz, R Eddie Wilson, and Bernd Krauskopf. Global bifurcation investigation of an optimal velocity traffic model with driver reaction time. *Physical Review E*, 70(2):026207, 2004.

[35] Takashi Nagatani and Ken Nakanishi. Delay effect on phase transitions in traffic dynamics. *Physical Review E*, 57(6):6415, 1998.

[36] Kondalsamy Gopalsamy. *Stability and oscillations in delay differential equations of population dynamics*, volume 74. Springer Science & Business Media, 2013.

[37] Meng Liu, Chuanzhi Bai, and Yi Jin. Population dynamical behavior of a two-predator one-prey stochastic model with time delay. *Discrete & Continuous Dynamical Systems-A*, 37(5):2513, 2017.

[38] Irving R Epstein. Delay effects and differential delay equations in chemical kinetics. *International Reviews in Physical Chemistry*, 11(1):135–160, 1992.

[39] Jerry Joseph Batzel and Hien T Tran. Stability of the human respiratory control system i. analysis of a two-dimensional delay state-space model. *Journal of mathematical biology*, 41(1):45–79, 2000.

[40] Michael C Mackey and Leon Glass. Oscillation and chaos in physiological control systems. *Science*, 197(4300):287–289, 1977.

[41] Lujun Zhou and Yaqiong Li. A dynamic is-lm business cycle model with two time delays in capital accumulation equation. *Journal of Computational and Applied Mathematics*, 228(1):182–187, 2009.

[42] Marek Szydłowski and Adam Krawiec. The kaldor–kalecki model of business cycle as a two-dimensional dynamical system. *Journal of Nonlinear Mathematical Physics*, 8(sup1):266–271, 2001.

[43] JH Park and OM Kwon. A novel criterion for delayed feedback control of time-delay chaotic systems. *Chaos, Solitons & Fractals*, 23(2):495–501, 2005.

[44] B Rezaie, MR Jahed Motlagh, M Analoui, and S Khorsandi. Stabilizing fixed points of time-delay systems close to the hopf bifurcation using a dynamic delayed feedback control method. *Journal of Physics A: Mathematical and Theoretical*, 42(39):395102, 2009.

[45] Fadia Zouad, Nadia Machkour, Karim Kemih, Lazaros Moysis, Christos Volos, and Ioannis Stouboulos. Predictive control of a fractional order delayed chaotic system with circuit implementation. In *2019 Panhellenic Conference on Electronics & Telecommunications (PACET)*, pages 1–4. IEEE, 2019.

[46] Sanyan Chen, Yuchao Wang, Peng Huang, and Xiaoyan Chen. Adaptive robust output control of nonlinear delayed chaotic systems. In *2017 International Conference on Advanced Mechatronic Systems (ICAMechS)*, pages 30–35. IEEE, 2017.

[47] Thomas B Sheridan. Space teleoperation through time delay: Review and prognosis. *IEEE Transactions on robotics and Automation*, 9(5):592–606, 1993.

[48] V Sree Krishna Chaitanya. Stability analysis of structurally unstable man–machine system involving time delays. *Nonlinear analysis: real world applications*, 6(5):845–857, 2005.

[49] Xavier Rodet. Models of musical instruments from chua's circuit with time delay. *IEEE Transactions on Circuits and Systems II: Analog and Digital Signal Processing*, 40(10):696–701, 1993.

[50] Serhiy Yanchuk. Properties of stationary states of delay equations with large delay and applications to laser dynamics. *Mathematical methods in the applied sciences*, 28(3):363–377, 2005.

[51] Weihua Deng, Changpin Li, and Jinhu Lü. Stability analysis of linear fractional differential system with multiple time delays. *Nonlinear Dynamics*, 48(4):409–416, 2007.

[52] Wu-Hua Chen, Zhi-Hong Guan, and Xiaomei Lu. Delay-dependent exponential stability of uncertain stochastic systems with multiple delays: an lmi approach. *Systems & Control Letters*, 54(6):547–555, 2005.

[53] Wu-Hua Chen and Wei Xing Zheng. Delay-dependent robust stabilization for uncertain neutral systems with distributed delays. *Automatica*, 43(1):95–104, 2007.

[54] Fatihcan M Atay. *Complex time-delay systems: theory and applications*. Springer, 2010.

[55] Yang Kuang. *Delay differential equations: with applications in population dynamics*. Academic press, 1993.

[56] Si Mohamed Sah and Richard H Rand. Three ways of treating a linear delay differential equation. In *Recent Trends in Applied Nonlinear Mechanics and Physics*, pages 251–257. Springer, 2018.

[57] Robert J Bauer, Gary Mo, and Wojciech Krzyzanski. Solving delay differential equations in s-adapt by method of steps. *Computer methods and programs in biomedicine*, 111(3):715–734, 2013.

[58] Stephen Wirkus and Richard Rand. The dynamics of two coupled van der pol oscillators with delay coupling. *Nonlinear Dynamics*, 30(3):205–221, 2002.

[59] Si Mohamed Sah and Richard H Rand. Delay terms in the slow flow. *arXiv preprint arXiv:1601.01853*, 2016.

[60] **Ankan Pandey**, Mainak Mitra, A Ghose-Choudhury, and Partha Guha. On coupled delayed van der pol-duffing oscillators. *Journal of Applied Nonlinear Dynamics*, 9(4), 2020 (In press).

[61] Jonathan James Lynch. *Analysis and design of systems of coupled microwave oscillators*. PhD thesis, University of California, Santa Barbara, 1995.

[62] Jonathan J Lynch and Robert A York. Stability of mode locked states of coupled oscillator arrays. *IEEE Transactions on Circuits and Systems I: Fundamental Theory and Applications*, 42(8):413–418, 1995.

[63] Robert A York. Nonlinear analysis of phase relationships in quasi-optical oscillator arrays. *IEEE Transactions on Microwave Theory and Techniques*, 41(10):1799–1809, 1993.

[64] Robert A York and Richard C Compton. Quasi-optical power combining using mutually synchronized oscillator arrays. *IEEE Transactions on Microwave Theory and Techniques*, 39(6):1000–1009, 1991.

[65] Murray Sargent III, MO Scullyand Jr, and WE Lamb. Laser physics, chapter 8, 1974.

[66] Mark Gluzman and Richard Rand. Dynamics of two coupled van der pol oscillators with delay coupling revisited. *arXiv preprint arXiv:1705.03100*, 2017.

[67] Kenneth L Cooke and Zvi Grossman. Discrete delay, distributed delay and stability switches. *Journal of mathematical analysis and applications*, 86(2):592–627, 1982.

[68] SJ Bhatt and CS Hsu. Stability criteria for second-order dynamical systems with time lag. *Journal of Applied Mechanics*, 33(1):113–118, 1966.

Chapter 6

Damped Forced Nonlinear Oscillators

Physical systems are not isolated in nature and does not behave independently. This may results in dissipation of energy making the system non-conservative in operation. The system may also be subjected to external signals which may be desirable or undesirable depending on the system. Such influence are present in chemical, biological and other system as well. These external influences often becomes detrimental for the system. A very peculiar example would be shaking of skyscrapers during earthquakes. A more familiar example is of brownian particles which under the influence of surrounding noise shows random motion.

In dynamical processes, forcing injects energy into the system and damping dissipates energy. The dynamics is highly regulated by the balance between the two which results in a periodic steady state. The stability of periodic solutions depends on the external and internal parameters. Further, the nonlinearity in the system interacts with the external forcing which results in very contrasting dynamical behaviours. As we studied in previous chapters, nonlinear damping of the system alters the qualitative features of the dynamics. It is interesting from a theoretical as well as application point of view to understand the interaction between nonlinearity in damping and external forcing and its influence in the dynamical behaviour.

6.1 Forced Coupled Duffing Oscillators with Nonlinear Damping: Resonance and Antiresonance [1]

Duffing oscillator equation is one most important and extensively studied nonlinear system owing to the multitude of nonlinear phenomenon that it demonstrate given its simple form. Periodically forced Duffing oscillator shows jump phenomenon exhibiting a frequency hysteresis behaviour. The role of linear damping in the dynamics of Duffing oscillator has been studied widely and much literature exist about the subject, [2, 3, 4]. However,

[1] This is part of a published work, [1]

the effects of nonlinear damping is comparatively less studied, and hence invites for more research.

The effect of nonlinear damping terms on the dynamics has been studied for quite some time. In [5] Ravindra et. al. studied the stability of a nonlinearly damped hard Duffing oscillator. Furthermore in [6], they investigated the role of nonlinear damping on the onset of period-doubling chaos in soft Duffing oscillator. In [7], Sanjuàn et al. discussed the role of nonlinear damping on some properties of universal escape oscillator. Hamiltonian description of the quadratic damping has been discussed in [8].

A single degree of freedom nonlinear oscillator under periodic forcing shows single resonance peak in its amplitude frequency response when the forcing frequency matches the oscillator's frequency. This phenomenon occurs for linear oscillator under periodic forcing as well. When such oscillators are coupled with another oscillator without any forcing, the frequency response of the forced oscillator shows dips between two resonance, termed antiresonance. Such dips appears when the forcing action of the coupled oscillator cancels the external forcing on the driven oscillator, causing destructive interference. Antiresonance is an important phenomenon in the field of nonlinear dynamics and have been interest of many research topics, [9, 10, 11, 12, 13]. In [9], the significance of antiresonance frequencies in experimental structural analysis is studied. Antiresonance phase shift was observed in strongly coupled cavity QED, [10]. In [14], Jothimurugan et al. considered n-coupled Duffing oscillators with periodic forcing on one of them. They showed the presence of multiple resonance and antiresonance frequencies.

The resonance and antiresonance phenomenons in coupled Duffing oscillator have been well studied for systems with linear damping. However, the effect of nonlinear damping in such phenomenons have never been studied, in the best of author's knowledge. In this work, we will consider nonlinearly damped coupled Duffing oscillators with one of them being periodically forced and investigate for various effects of nonlinear damping on the resonance and antiresonance structures.

6.1.1 Periodically driven coupled Duffing oscillator

Let us consider the system of interest in the form

$$\ddot{x} + \epsilon d\dot{x}|\dot{x}|^p + x - \epsilon b x^3 = \epsilon\alpha y + \epsilon F\cos\omega t \tag{6.2}$$

$$\ddot{y} + \epsilon d\dot{y}|\dot{y}|^p + y - \epsilon b y^3 = \epsilon\alpha x. \tag{6.3}$$

The equation represents linearly coupled Duffing oscillators with one of them periodically forced. In the equation, α is coupling coefficient, F and ω are forcing amplitude and forcing frequency respectively, and rest of the parameters are usual system parameters. The exponent p provides nonlinearity in the damping and can take integer values, for the purpose of this work. For further references, oscillator with dynamics represented by $x(t)$ will be referred as oscillator-x and that by $y(t)$ as oscillator-y.

Theoretical analysis

In this section we will analyse (6.3) using multi-scale perturbation analysis and study frequency response of the solution.
Following the usual multi-scale perturbation procedure, the solution (zeroth order solution) is assumed to be of the form

$$\begin{aligned} x(t,t) &= A(\tau)\,\cos(\omega t + \phi_A(\tau)) \\ y(t,t) &= B(\tau)\,\cos(\omega t + \phi_B(\tau)), \end{aligned} \tag{6.4}$$

where $\tau = \epsilon t$ is the slow time scale, A and ϕ are amplitude and phase of the periodic solution, respectively.

The damping term in (6.3) with above solution can be difficult to handle given the non smooth nature of the term. Therefore, the damping term is approximated in the form of Fourier series as

$$(-A\omega\sin(\omega t+\phi))|A\omega\sin(\omega t+\phi)|^p = -C_p\,\omega\,A|A|^p|\omega|^p\,\sin(\omega t+\phi) + HHT, \tag{6.5}$$

where $C_p = \frac{2\Gamma(\frac{p+3}{2})}{\sqrt{\pi}\Gamma(\frac{p+4}{2})}$ and $\Gamma(x)$ is Gamma function. 'HHT' refers to higher harmonic terms which are going to be suppressed owing to rotating wave approximation. The modulus around A and ω could be dropped as they are assumed positive . Using the above approximation along with solution (6.4) in the first order correction equation and setting the secular terms to zero gives the slow flow equation

$$A' = -\frac{C_p}{2}\,d\,\omega^p A^{p+1} + \frac{\alpha\,B}{2\omega}\,\sin(\phi_A-\phi_B) + \frac{F}{2\,\omega}\,\sin\phi_A \tag{6.6a}$$

$$A\phi_A' = -\frac{\delta\,A}{2\omega} + \frac{3\,b\,A^3}{8\omega} + \frac{\alpha\,B}{2\omega}\,cos(\phi_A-\phi_B) + \frac{F}{2\,\omega}\,\cos\phi_A \tag{6.6b}$$

$$B' = -\frac{C_p}{2}\,d\,\omega^p B^{p+1} - \frac{\alpha\,A}{2\omega}\,\sin(\phi_A-\phi_B) \tag{6.6c}$$

$$B\phi_B' = -\frac{\delta\,B}{2\omega} + \frac{3\,b\,B^3}{8\omega} + \frac{\alpha\,A}{2\omega}\,\cos(\phi_A-\phi_B). \tag{6.6d}$$

The derivatives in (6.6) are with respect to slow time τ. The fixed points of amplitude-phase equations (6.6) corresponds to the amplitude and phase of the periodic solution of (6.3) and the stability of these points will determine the stability of the periodic solution. To calculate the fixed points, we set $A'=0$, $B'=0$, $\phi_A'=0$, $\phi_B'=0$, which, after some algebraic manipulations, gives the amplitude-frequency response equation,

$$\left(\frac{C_p d\omega^{p+1}B^{p+1}}{2}\right)^2 + \left(\frac{\delta B}{2} - \frac{3B^3 b}{8}\right)^2 = \frac{\alpha^2A^2}{4}, \tag{6.7a}$$

$$\left(\frac{C_p d\,\omega^{p+1}}{2A}(A^{p+2}+B^{p+2})\right)^2 + \left(\frac{\delta}{2A}(A^2-B^2) - \frac{3b}{8A}(A^4-B^4)\right)^2 = \frac{F^2}{4}, \tag{6.7b}$$

and phase-frequency response equation,

$$\phi = \phi_A - \phi_B = arctan\left(-4\frac{C_p d\omega^{p+1}B^p}{4\delta - 3bB^2}\right), \tag{6.8}$$

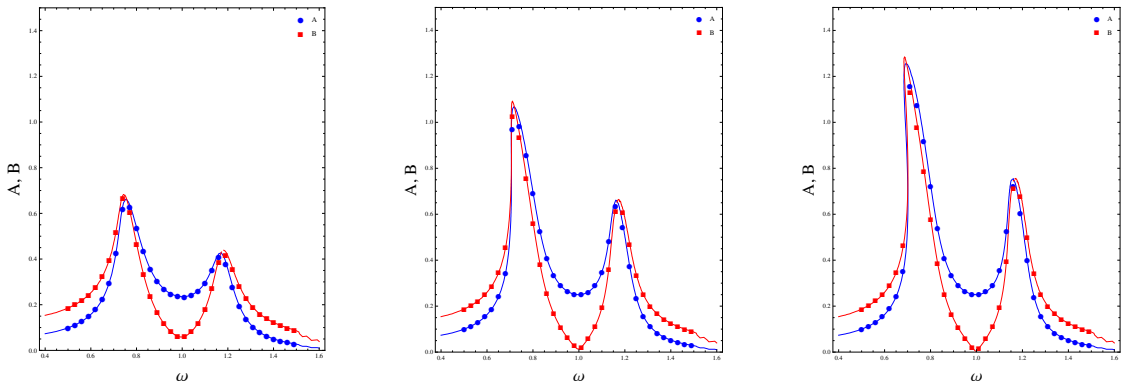

(a) $p = 0$ (b) $p = 1$ (c) $p = 2$

Figure 6.1: Amplitude Frequency Response of amplitudes A (of oscillator-x)(in blue) and B (of oscillator-y)(in red). Three sub-plots are for different damping exponents: a) $p = 0$; b) $p = 1$; c) $p = 2$. Continuous line represents theoretical predictions and solid circles and triangles are data points of numerically calculated amplitudes of A and B, respectively. The parameter settings are: $d = 1$, $b = 1$, $\alpha = 4$, $F = 1$, $\epsilon = 0.1$.

$$\phi_A = arctan\left(4\frac{C_p d\,\omega^{p+1}(A^{p+2} + B^{p+2})}{4\delta(A^2 - B^2) - 3\,b(A^4 - B^4)}\right). \tag{6.9}$$

The frequency response relations shows the dependence of amplitude/phase on the forcing frequency. The roots of these algebraic equations are fixed points of amplitude-phase equation which could solved algebraically. However, owing to complexity of the equation it is not practically possible to solve it analytically. To the rescue are numerical methods which are employed to obtain the roots for different parameter arrangements.

Figure 6.1 shows the amplitude-frequency response curve together with numerically obtained data points by solving (6.3) to show the authenticity of the theoretical results. The parameter values for the plot are: $d = 1.0$, $b = 1.0$, $F = 1.0$, $\epsilon = 0.1$, $\alpha = 4.0$. This parameter setting is applicable on all the plots in this work, unless otherwise specified. The figure presents theoretical approximations calculated using perturbation analysis and numerical simulation calculations of the response function directly from (6.3) which very verifies the theoretical predictions. The resonant peaks of individual oscillators will be refer to as A_r^1, A_r^2, and the corresponding frequency values, for resonance, as ω_r^{A1}, and ω_r^{A2} and same goes for the oscillator-y with amplitudes replaced by B. The resonance in figure (6.1) occurs at $\omega_r^{A1} = 0.74$, $\omega_r^{A2} = 1.19$ for $p = 0$, $\omega_r^{A1} = 0.71$, $\omega_r^{A2} = 1.16$ for $p = 1$, and $\omega_r^{A1} = 0.71$, $\omega_r^{A2} = 1.16$ for $p = 2$. For oscillator-y the resonances occur at $\omega_r^{B1} = 0.77$, $\omega_r^{B2} = 1.16$ for $p = 0$, $\omega_r^{B1} = 0.74$, $\omega_r^{B2} = 1.16$ for $p = 1$, and $\omega_r^{B1} = 0.71$, $\omega_r^{B2} = 1.16$ for $p = 2$. The resonance occurred at almost same frequencies regardless of the damping exponent. However, the calculations show that the amplitude value at resonance increases with the damping exponent as shown in the figure. This kind of increment in the maximum amplitude value is not expected and hence is non-trivial in nature.

The antiresonance dips occur at $\omega = 1.0$ in all the cases for both the oscillators. Also, the dips for $p = 1, 2$ are shorter for small α but becomes identical with $p = 0$ for larger values

of coupling parameter α. This dependence of antiresonance on α is shown in figure 6.2. The parameter setting is same as that of previous computation.

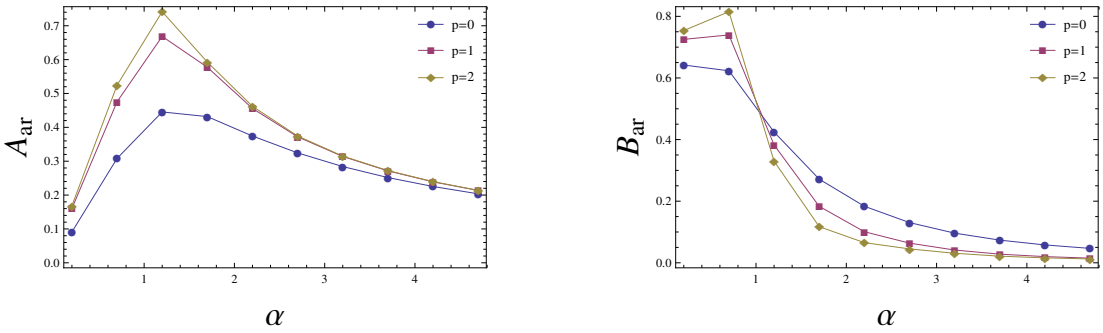

(a) A_{ar} vs α (b) B_{ar} vs α

Figure 6.2: The dependence of dips on coupling parameter α for damping exponents $p = 0, 1, 2$. Antiresonance values for a) oscillator-x (amplitude A); b) oscillator-y (amplitude B). The data points are numerically computed points and continuous lines are trend lines. Shows separation between the three exponents for small α and convergence for large α values. The parameter settings are: $d = 1$, $b = 1$, $\alpha = 4$, $F = 1$, $\epsilon = 0.1$.

The resonance values for both the oscillators also depend on the coupling parameter. This dependence is shown in figure6.3. The dependence is linear with respect to α and is same for all damping exponents.

The resonance peaks, as shown earlier, increase with the damping exponent as well as with coupling strength α. This dependence is shown in figure 6.4. The figure denotes a trend of saturation for large α for all the p values. This trend is also present in the theoretical predictions.

Stability Analysis

The stability of the periodic solutions corresponds to the stability of the fixed points of (6.6). For the stability analysis, we did linear stability analysis of amplitude-phase dynamics. The stability plot is shown in figure 6.5. From the analysis, it is evident that the unstable regions are increasing with damping exponent p.

Phase analysis

The phase dynamics is governed by (6.6c) and (6.6d) and the fixed points are given by (6.8) and (6.9). The phase response is given in figure 6.6. Oscillator-x shows an abrupt phase shift at antiresonance and resonance values for all the damping exponents. This is a characteristic of regular antiresonance in contrast to vibrational antiresonance where no such phase shift appears, [15]. For oscillator-y, there is no abrupt phase shift at antiresonance value for any p. The phase lag between the forcing and amplitude response decreases with damping exponent. This is evident from the phase response dependence on the C_p term which decreases for with higher p values.

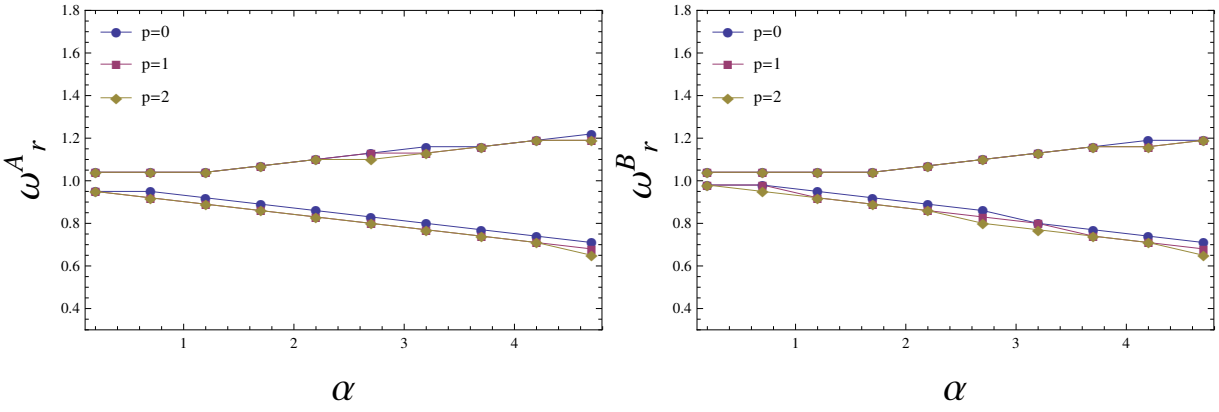

(a) ω_r^A vs α (b) ω_r^B vs α

Figure 6.3: The dependence of resonant frequencies on coupling parameter α for damping exponents $p = 0, 1, 2$. Resonance values for a) oscillator-x (amplitude A); b) oscillator-y (amplitude B). The data points are numerically computed points and continuous lines are trend lines. The two branches, below and above $\omega = 1$, belongs to two resonances for each oscillator. The parameter settings are: $d = 1$, $b = 1$, $\alpha = 4$, $F = 1$, $\epsilon = 0.1$.

6.1.2 Discussion and Conclusion

* The frequency response of both the oscillators are obtained and vindicated by numerical simulation results. The intensity of each oscillator seems to be enhanced with the damping exponent. This observation is shown in figure 6.1. This is attributed to the fact that the coefficient of the first harmonic of the Fourier series expansion of damping term decreases with the damping exponent. Hence with increasing damping exponents the contribution of the damping term decreases in the response function. This enhancement of amplitude denotes greater energy efficiency.

* Dependence of the response at resonant and antiresonant values on coupling is obtained. Higher damping exponents show similar trend as that of linear damping with higher values. For oscillator-x the dependence of antiresonance amplitudes A_{ar} take maxima at certain coupling and then amplitudes for all the exponents converge with increasing coupling. Oscillator-y amplitudes also converges for large coupling.

  Antiresonance appears after certain coupling value for each oscillator following a pitchfork bifurcation in the amplitude phase dynamics. Afterwards, the two resonant peaks move away from each other with increasing coupling values in a linear fashion. This dependence is same for all the exponents. The resonant values saturates for large values of coupling for all the exponents.

* Stability of the periodic solutions of (6.3) is obtained by analysing the stability of the fixed points of amplitude-phase equations (6.6). The stability is determined by using linear stability analysis and the fixed points are, basically, frequency response values.

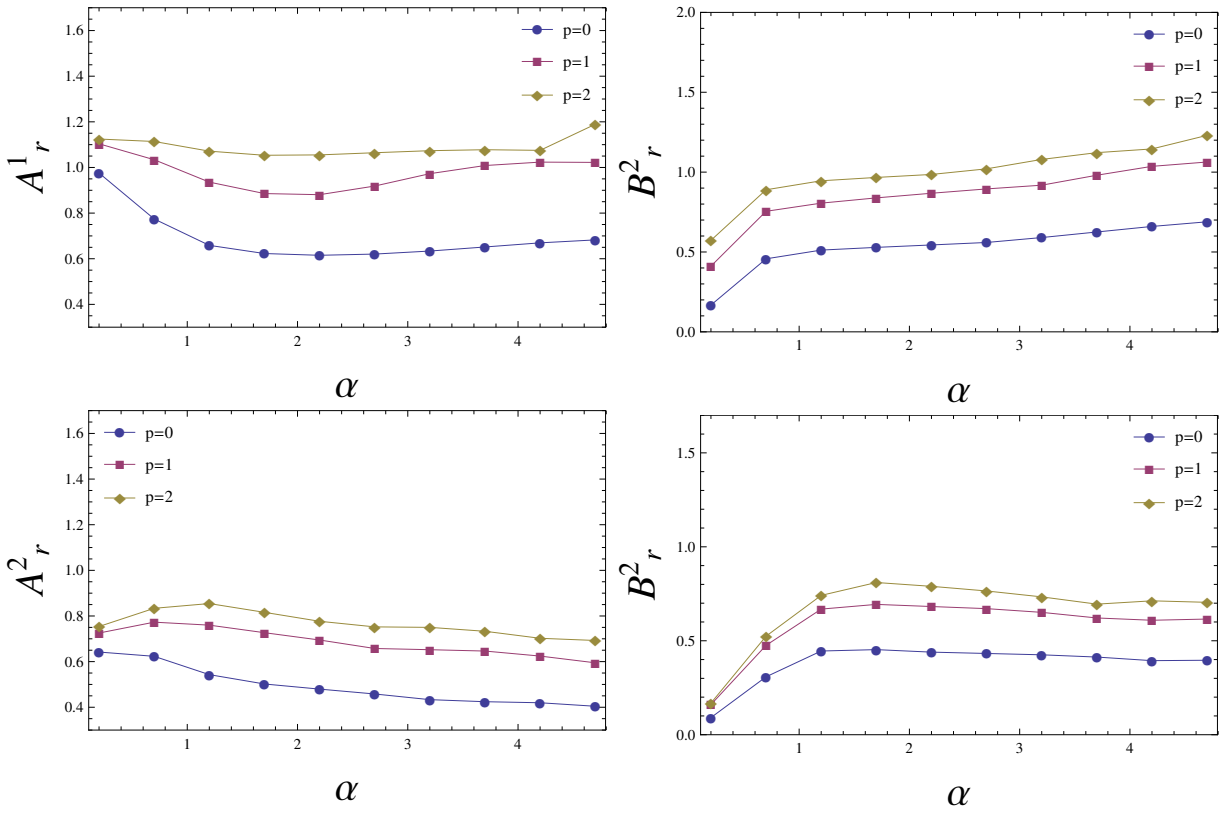

(a) A_r vs α (b) B_r vs α

Figure 6.4: The dependence of resonant peaks on coupling parameter α for damping exponents $p = 0, 1, 2$. Resonance values for a) oscillator-x (amplitude A); b) oscillator-y (amplitude B). The data points are numerically computed points and continuous lines are trend lines. The two branches, below and above $\omega = 1$, belongs to two resonances for each oscillator. The parameter settings are: $d = 1$, $b = 1$, $\alpha = 4$, $F = 1$, $\epsilon = 0.1$.

* Phase lag between the forcing and the response decreases with increasing damping exponent. Phase response shows a phase shift in oscillator-x while no abrupt phase shift oscillator-y. This is a signature of antiresonance phenomenon.

6.2 Nonlinear Systems Under Multiple Forcing - Vibrational Resonance

Nonlinear oscillators are often subjected to signals from surroundings some of which are important and some are unwanted and detrimental. The unwanted signals are termed as noise. However, it was shown that the noise could be useful in enhancing weak important signals and the phenomenon was called *stochastic resonance*, [16]. Later, similar effects were found using high-frequency harmonic signals instead of stochastic noise, [17], and the corresponding phenomenon was termed as *vibrational resonance* (VR).

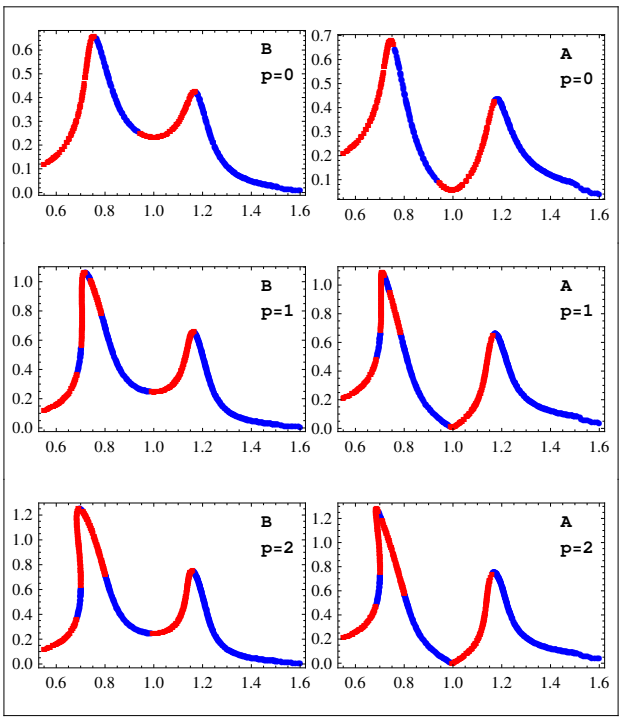

Figure 6.5: Stability analysis of amplitude-phase equation (6.6). The unstable values are shown in red and stable with blue. Each row corresponds to $p = 0$, $p = 1$, $p = 2$ and shows stability of amplitudes A and B. The parameter settings are: $d = 1$, $b = 1.5$, $\alpha = 4$, $F = 1$, $\epsilon = 0.1$.

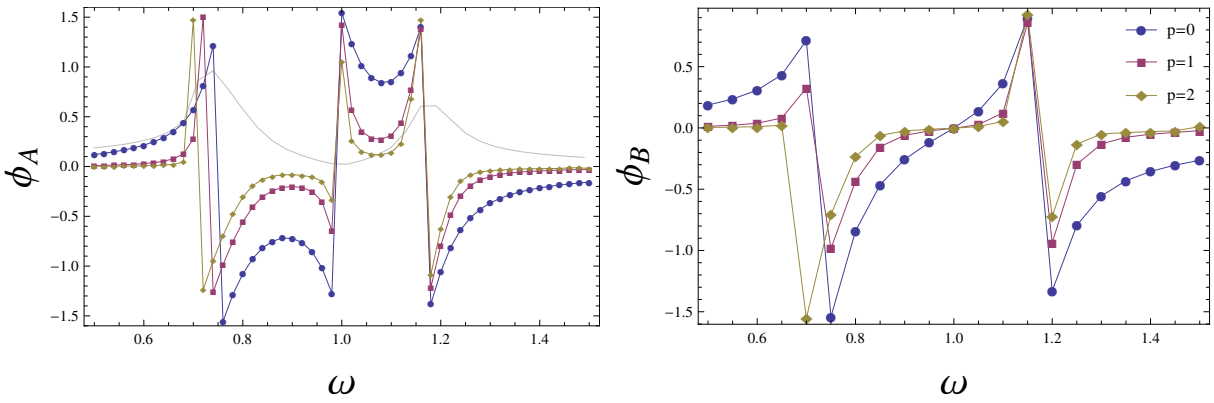

(a) (b)

Figure 6.6: Phase-frequency response of oscillator-x. a)The phase response of oscillator-x is given for all damping exponents. Amplitude response for $p = 1$ is given gray to correlate the response events. This response is given for $p = 2$. b) Phase response of oscillator-y for all the damping exponents. The parameter settings are: $d = 1$, $b = 1$, $\alpha = 4$, $F = 1$, $\epsilon = 0.1$.

There has been a lot of theoretical developments in VR from a nonlinear dynamics point of view since its inception. The first reporting of VR was done for overdamped bistable systems, [17]. Thereafter, huge interest was shown for investigation of VR in multistable systems, [18, 19], overdamped oscillators, [20], delayed systems, [21, 22], neuron models, [23], plasma, [24] and many more. Recently, Vibrational antiresonance was shown in [15] for coupled Duffing systems. The theoretical developments were followed by experimental investigations, [25, 26, 27].

Both *stochastic resonance* and *vibrational resonance* are nonlinear phenomenons and depends strictly on the form of the potential. In *vibrational resonance* a low-frequency signal is modulated with high-frequency periodic signals. The high-frequency periodic force regulates the fast scale dynamics whose average behaviour is perceived by the slow scale dynamics through modified stiffness of the system. The average behaviour also revise the damping in the system. The modified slow dynamics then shows linear response to the strength of high frequency signal force. The response amplitude is parametrised by characteristics of high-frequency force.

In this work, I have considered bistable Duffing oscillator subjected to low-frequency periodic forcing, modelling weak signals, and high-frequency periodic forcing. The system is further designed to experience nonlinear damping. This study is suppose to exhibit the contrasting behaviour of linear and nonlinear damping in the VR phenomenon and, in the process, develop the analytic understanding of VR.

6.2.1 The System

The system of interest is a Duffing system experiencing nonlinear damping driven by two external forcing. The damping is considered in a generalised form characterising the degree of nonlinearity by damping exponent p. The dynamics of the system is governed by

$$\ddot{x} + d\dot{x}|\dot{x}|^p - a^2x + bx^3 = F\cos\omega t + G\cos\Omega t, \tag{6.10}$$

where d is damping coefficient, a, b are Duffing parameters, F, G are forcing strengths of the external forcing, ω, Ω are frequencies of external forcing and p is the damping exponent. To investigate VR in the system we further consider $\Omega >> \omega$. The Duffing potential is bistable for $a^2 > 0$ resulting in steady states at $x = \pm(\frac{a}{\sqrt{b}})$ and is monostable for $a^2 < 0$ with steady state at $x = 0$.
The degree of nonlinearity in damping is given by the damping exponent (DE), p. In this work, we will consider integer values of the DE and study the cases $p \in \{0, 1\}$. In the following sections, to study the VR phenomenon, we will obtain the response amplitude of the system theoretically, and numerically, and study its dependence on system parameters for different values of damping exponent.

6.2.2 Theoretical Analysis

As the system is subjected to two external periodic forcing of frequencies of different scale, we will employ method of direct separation of slow and fast motions. To approach with

this, let us assume the solution of (6.10) be of the form

$$x(t,\tau) = X(t) + \Psi(t,\tau), \quad \tau = \Omega t. \tag{6.11}$$

Putting the above approximation in (6.10), we get

$$\ddot{X} + \ddot{\Psi} + d(\dot{X} + \dot{\Psi})|(\dot{X} + \dot{\Psi})|^p - a^2(X + \Psi) + b(X + \Psi)^3 = F\,\cos\omega t + G\,\cos\Omega t. \tag{6.12}$$

Variables X and Ψ represents the motion on slow, with frequency ω and fast, with frequency Ω, time scale respectively. As a consequence of this, $\ddot{\Psi}$, $\dot{\Psi} >> \ddot{X}$, $\dot{X}$. Taking advantage of this, the damping term could be simplified as

$$d(\dot{X} + \dot{\Psi})|(\dot{X} + \dot{\Psi})|^p \approx d\dot{X}|\dot{\Psi})|^p + d\dot{\Psi}|\dot{\Psi})|^p. \tag{6.13}$$

Further, as Ψ is a fast variable, it can be approximated as solution of the equation

$$\ddot{\Psi} + d\dot{\Psi}|\dot{\Psi}|^p = G\,\cos\Omega t. \tag{6.14}$$

Letting

$$\Psi = A\,cos(\Omega t + \phi), \tag{6.15}$$

and substituting in (6.14), we get

$$c_{p1}^2\,d^2\,\Omega^{2p+2}\,A^{2p+2} + \Omega^4 A^2 = G^2, \tag{6.16}$$

and

$$\phi = arctan(c_{p1} d\,\Omega^{p-1} A^p), \tag{6.17}$$

where $c_{p1} = \frac{2\Gamma(\frac{p+3}{2})}{\sqrt{\pi}\Gamma(\frac{p+4}{2})}$ is the coefficient in the harmonic approximation of the damping term expressed as

$$(-A\Omega\sin(\Omega t + \phi))|A\Omega\sin(\Omega t + \phi)|^p = -C_{p1}\,\Omega\,A|A|^p|\Omega|^p\,\sin(\Omega t + \phi). \tag{6.18}$$

The amplitude of the fast motion could be obtain by solving the algebraic equation (6.16) for each damping regime.
Notice that Ψ is 2π periodic in fast scale and therefore has zero mean as

$$< \Psi >= \frac{1}{2\pi}\int_0^{2\pi} \Psi(t,\tau)\,d\tau. \tag{6.19}$$

Now, substituting the solution of Ψ in (6.12) and averaging over the fast time $\tau = \Omega t$, considering the variables depending on slow time as constant, we obtain the slow dynamics equation as

$$\begin{aligned} \ddot{X} \;+\; d\dot{X} < |\dot{\Psi}|^p > \;-\, a^2(X + < \Psi >) \;\;&+\;\; b\,(X^3 + < \Psi^3 > \\ +\,3X^2 < \Psi > \,+\,3X < \Psi^2 >) \;\;&=\;\; F\,\cos\omega t. \end{aligned} \tag{6.20}$$

Averaging over odd powers of Ψ gives zero as Ψ is a cosine function. Rest of the averaging are given as

$$\begin{aligned} < |\dot{\Psi}|^p > &= A^p\,\Omega^p\,c_{p2}, \quad c_{p2} = \frac{\Gamma(\frac{p+1}{2})}{\sqrt{\pi}\Gamma(\frac{p+2}{2})}, \\ < \Psi^2 > &= \frac{A^2}{2}. \end{aligned} \tag{6.21}$$

The slow dynamics then becomes

$$\ddot{X} + \bar{d}\dot{X} + \bar{a}X + b\,X^3 = F\,\cos\omega t, \tag{6.22}$$

where

$$\bar{d} = d\,A^p\,\Omega^p\,c_{p2}, \quad \bar{a} = \frac{3\,b\,A^2}{2} - a^2. \tag{6.23}$$

The modified equation (6.22) governs the dynamics in effective potential $V_{eff} = \frac{\bar{a}}{2}\,X^2 + \frac{b}{4}X^4$ experiencing linear damping. The effective potential is also Duffing with coefficient of the linear term restructured under the influence of interaction between fast oscillating field and nonlinear damping. The effective potential can be bistable or monostable depending on the forcing amplitude G and the damping regime.

The equilibrium states of the unforced slow dynamics are $X_0 = 0$, $X_\pm = \pm\sqrt{\frac{-\bar{a}}{b}}$. The existence and position of latter ones depends on whether $\bar{a}$ is positive or negative which in turn is determined by the parameters of the high frequency field and the damping regime. In any case, the slow variable will oscillate around the stable equilibrium states which let us be denoted by X_s. To obtain the amplitudes and phase of the oscillating solution, linearise the motion around X_s for which consider the deviation $Y = X - X_s$, and substituting it in (6.22), we get

$$\ddot{Y} + \bar{d}\dot{Y} + (\bar{a} + 3bX_s^2)\,Y = F\,\cos\omega t. \tag{6.24}$$

Let the solution of the linear equation (6.24) be of the form

$$Y = B\,\cos(\omega t + \gamma), \tag{6.25}$$

and substitute in (6.24), which gives

$$B = \frac{F}{((\bar{d\omega})^2 + (\bar{a} + 3bX_s^2 - \omega^2)^2)^{1/2}}, \tag{6.26}$$

and

$$\gamma = arctan\left(\frac{\bar{d}\omega}{\omega^2 - \bar{a} - 3\,b\,X_s^2}\right). \tag{6.27}$$

Equations (6.26), and (6.27) gives the amplitude and phase expression for the slow dynamics. The expressions are obtain for general stable equilibrium points, X_s, which could be any of the three equilibrium states defined earlier. The resonance condition could be obtain by solving

$$\begin{aligned} \bar{a} - \omega^2 &= 0, \quad (X_s = X_0) \\ -2\,\bar{a} - \omega^2 &= 0, \quad (X_s = X_\pm) \end{aligned} \tag{6.28}$$

for G. The corresponding maximum amplitude is given as

$$B_{max} = \frac{F}{\bar{d}\omega}, \tag{6.29}$$

where

$$\bar{d} = \begin{cases} d\,\Omega^p\,c_{p2}\left(\frac{2(a^2+\omega^2)}{3\,b}\right)^{p/2} & X_s = X_0 \\ d\,\Omega^p\,c_{p2}\left(\frac{2a^2-\omega^2}{3\,b}\right)^{p/2} & X_s = X_\pm \end{cases} \tag{6.30}$$

For detailed analysis we will now consider each damping regime separately. Also for further calculations, consider the slow amplitude expression in the form $B = \frac{G}{\mu}$, with $\mu = ((\bar{d\omega})^2 + (\bar{a} + 3bX_s^2 - \omega^2)^2)^{1/2}$.

Case: $(p = 0)$

The $p = 0$ case is the linear case which has been studied before in great detail. Realisation of the desired results from the above analysis will vindicate the obtained results.
Substituting $p = 0$ in (6.16) the fast amplitude and phase are given as

$$A = \frac{G}{(d^2\,\Omega^2 + \Omega^4)^{1/2}}, \tag{6.31}$$

and

$$\phi = arctan\left(\frac{d}{\Omega}\right). \tag{6.32}$$

The effective potential has a critical value of the forcing amplitude $G_c = \sqrt{\frac{2\,a^2}{3\,b}}\eta$, with $\eta = (d^2\,\Omega^2 + \Omega^4)^{1/2}$, below $(G < G_c)$ which $\bar{a} < 0$ and potential is bistable with equilibrium points $X_s = X_\pm$ and above $(G > G_c)$ which $\bar{a} > 0$ and potential is monostable with equilibrium at $X_s = X_0$. The oscillation occurs around the stable equilibrium state X_0 for $G > G_c$ and around $X_\pm$ for $G < G_c$.
Now consider the slow amplitude. The maxima of B occurs at the minima of μ which corresponds to the condition

$$\bar{a} + 3bX_s^2 - \omega^2 = 0. \tag{6.33}$$

For $G > G_c$, the stable equilibrium point is $X_s = X_0$, which gives the minima condition

$$\frac{3\,b\,G_{max}^2}{2\,\eta^2} - a^2 - \omega^2 = 0, \tag{6.34}$$

or

$$G_{max} = \left(\frac{2\,\eta^2(a^2 + \omega^2)}{3\,b}\right)^{1/2}. \tag{6.35}$$

For $a^2 > 0$, the original system is monostable and the G_{max} condition exists for $\omega > 0$. However, for $a^2 < 0$, the original system is bistable and the G_{max} condition exists for

$\omega^2 \geq |a^2|$.
For $G < G_c$, the stable equilibrium points are $X_s = X_\pm$, which gives the minima condition

$$\frac{-3\,b\,G^2}{\eta^2} \;+\; 2\,a^2 \;-\; \omega^2 = 0, \tag{6.36}$$

or

$$G_{max} = \left(\frac{\eta^2(2\,a^2 \;-\; \omega^2)}{3\,b}\right)^{1/2}. \tag{6.37}$$

This maxima provides the second resonance in the amplitude response. This maxima exists when the original potential is bistable and for $\omega^2 \leq 2\,a^2$. The resonance amplitude for both the case is given as

$$B_{max} = \frac{F}{d\,\omega}. \tag{6.38}$$

The variation of G_{max} with ω is shown in figure 6.8. The corresponding parameter settings are $a = 1.0$, $b = 1.0$, $d = 0.05$, $F = 0.01$, $\Omega = 10.0$. The plot is based on theoretical predictions made above. From the plot it is observed that the slow dynamics undergoes subcritical pitchfork bifurcation at $\omega = \sqrt{2}$, below which system has two stable equilibrium $X_\pm$ and above which it has single equilibria X_0. Moreover, the plot shows two curves corresponding to resonance positions given by (6.35), and (6.37). The resonance position corresponding to the stable equilibrium $X_\pm$ decreases with ω and has a cutoff at $\omega = \sqrt{2}$ and the one for oscillation around the equilibria X_0 is increasing boundlessly. However, the amplitude at resonance decays with increasing ω and is same for both the resonance as is evident from the inverse dependence of the amplitude response on ω, (6.38). The variation of resonance amplitude is given in figure 6.9.

The theoretical plots of the amplitude response are shown in figure 6.7. The plots shows the amplitude response for $\omega = \{0.6,\ 1.0,\ 1.2,\ 1.45\}$. The two resonance separates out till the second resonance corresponding to $X_\pm$ ceases to exist at $\omega = \sqrt{2}$.

Case: $(p = 1)$

The $p = 1$ case corresponds to the quadratic damping and in this section we will investigate for VR phenomenon using the theoretical development done in *theoretical analysis* section. Using (6.16), the fast amplitude, and phase, for $p = 1$ case, are given as

$$A = \left(\left(\frac{3\pi}{128\,d^2\,\Omega^4}\right)(-3\pi\,\Omega^4 \;+\; (256\,d^2\,G^2\,\Omega^4 \;+\; 9\,\pi^2\,\Omega^8)^{1/2})\right)^{1/2}, \tag{6.39}$$

and

$$\phi = arctan\left(\frac{8\,d\,A}{3\pi}\right). \tag{6.40}$$

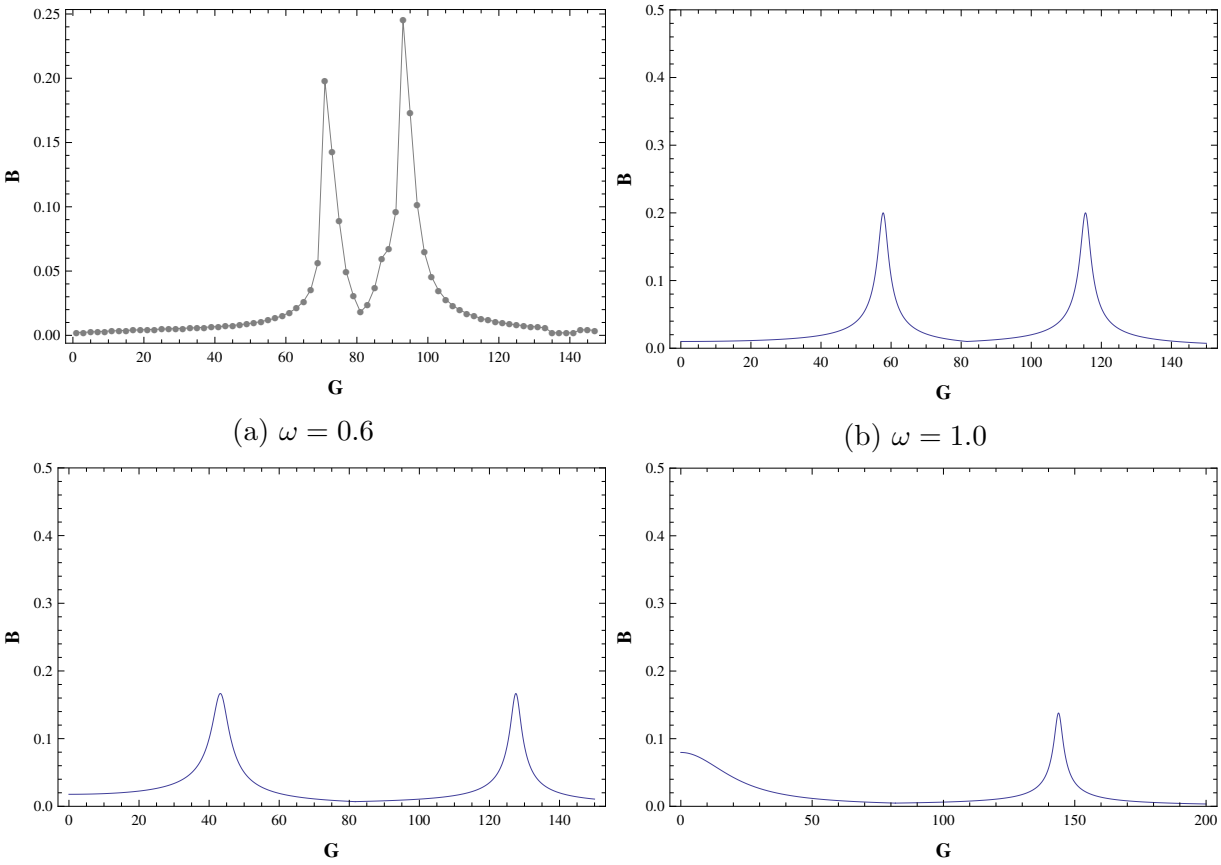

(a) $\omega = 0.6$

(b) $\omega = 1.0$

(c) $\omega = 1.2$

(d) $\omega = 1.45$

Figure 6.7: Amplitude response of (6.10) for damping exponent $p = 0$. The plots are obtained using theoretical predictions. The subplots shows the response for different values of ω mentioned in the caption of each subplot. The two resonance corresponds to equilibriums X_0, and $X_\pm$. The parameter settings are: $a = 1.0$, $b = 1.0$, $d = 0.05$, $F = 0.01$, $\Omega = 10.0$

The critical value of the forcing in the effective potential is

$$G_c = \frac{\sqrt{2}\sqrt{128a^4d^2\Omega^4 + 27\pi^2a^2b\Omega^4}}{9\pi b}. \tag{6.41}$$

The slow system has two stable equilibrium points $X_\pm$ for $G < G_c$ then it undergoes subcritical pitchfork bifurcation at $G = G_c$ resulting in a single stable equilibrium point X_0. The two regions characterised by G values are synonymous with consideration of oscillation around corresponding stable equilibriums and hence could be used interchangeably in further refrences.
The resonance condition (6.28) gives

$$G_{max} = \frac{(2(a^2 + w^2))^{1/2}(128a^2d^2 + 27b\pi^2 + 128d^2w^2)^{1/2}\Omega^2}{9b\pi} \tag{6.42}$$

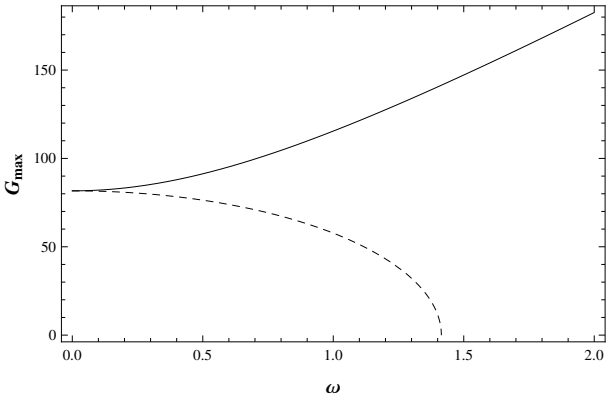

Figure 6.8: Vibrational Resonance position variation with respect to ω for $p = 0$. The plot is obtained using theoretical predictions. The continuous curve shows the variation of resonance position corresponding to the equilibrium state X_0 and dashed curve shows the variation corresponding to the equilibrium states $X_{\pm}$. The parameter settings are: $a = 1.0$, $b = 1.0$, $d = 0.05$, $F = 0.01$, $\Omega = 10.0$

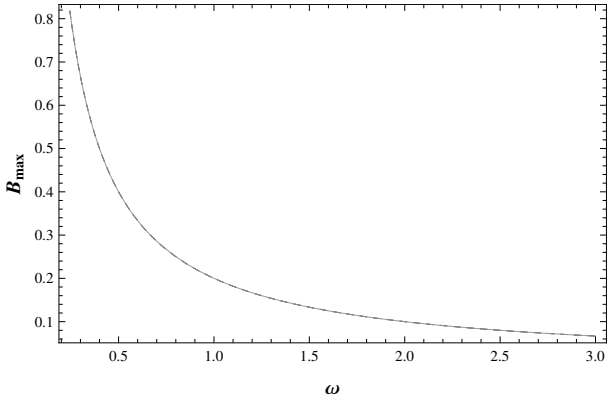

Figure 6.9: Variation of resonance value with respect to ω for $p = 0$. The plot is obtained using theoretical predictions. The continuous curve shows the variation of resonance value corresponding to the equilibrium state X_0 and dashed curve shows the variation corresponding to the equilibrium states $X_{\pm}$. The parameter settings are: $a = 1.0$, $b = 1.0$, $d = 0.05$, $F = 0.01$, $\Omega = 10.0$

for $G > G_c$, and

$$G_{max} = \frac{(2a^2 - w^2)^{1/2}(128a^2d^2 + 27b\pi^2 - 64d^2w^2)^{1/2}\Omega^2}{9b\pi}, \tag{6.43}$$

for $G < G_c$. The second resonance position has a cutoff frequency at $\omega = \sqrt{2}a$. It is similar to the linear damping case. The variation of the two resonance position with ω is shown in figure 6.11. From the plot it is clear that there are two resonance peaks for $\omega < \sqrt{2}a$ and single for higher values.

The corresponding resonance amplitude, obtained using (6.29), are given as

$$B_{max} = \frac{F}{\frac{2\,d\,\Omega\,\omega}{\pi}\left(\frac{2(a^2+\omega^2)}{3\,b}\right)^{1/2}}, \tag{6.44}$$

for $G > G_c$, and

$$B_{max} = \frac{F}{\frac{2\,d\,\Omega\,\omega}{\pi}\left(\frac{2\,a^2-\omega^2}{3\,b}\right)^{1/2}}, \tag{6.45}$$

for $G < G_c$. The second resonance amplitude around $X_{\pm}$ has a singularity at the cutoff frequency which results in a sudden spike in the amplitude as shown in figure 6.12. The spike indicate momentarily zero damping at cutoff. The first resonance decreases monotonically with ω but in a different functional manner than the linear damping case.

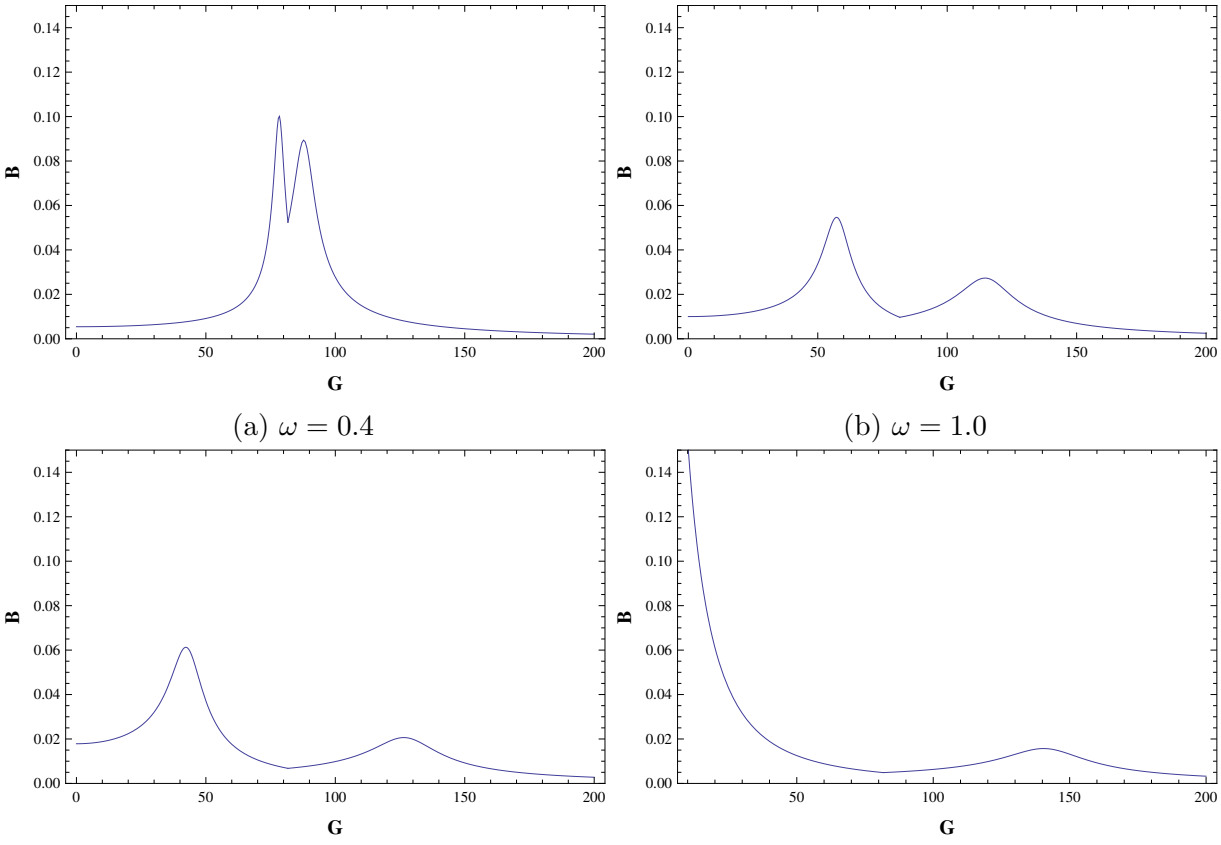

(a) $\omega = 0.4$ (b) $\omega = 1.0$

(c) $\omega = 1.2$ (d) $\omega = 1.42$

Figure 6.10: Amplitude response of (6.10) for damping exponent $p = 1$. The plots are obtained using theoretical predictions. The subplots shows the response for different values of ω mentioned in the caption of each subplot. The two resonance corresponds to equilibriums X_0, and $X_\pm$. The parameter settings are: $a = 1.0$, $b = 1.0$, $d = 0.05$, $F = 0.01$, $\Omega = 10.0$

The deviation in the behaviour the second resonance is because of the quadratic damping influence on the slow dynamics.

We also noted that, in figure 6.10, under similar parameter setting, the resonance amplitude is less for ($p = 1$) case than ($p = 0$). This is opposite to what is found in regular resonance where resonant amplitude increases with damping exponent, [1]. In regular resonance, the coefficient of harmonic equivalent decreases with damping exponent which leads to smaller effective damping coefficient and hence less effective damping. In the VR case, the damping coefficient becomes large because of inclusion of frequency Ω after averaging.

6.2.3 Conclusion

In this study, a nonlinearly damped bistable Duffing oscillator is considered which are subjected to two periodic signals of high and low frequencies. Utilising the separation of scales of the motion the frequency response was obtained for damping exponent, $p = 0$,

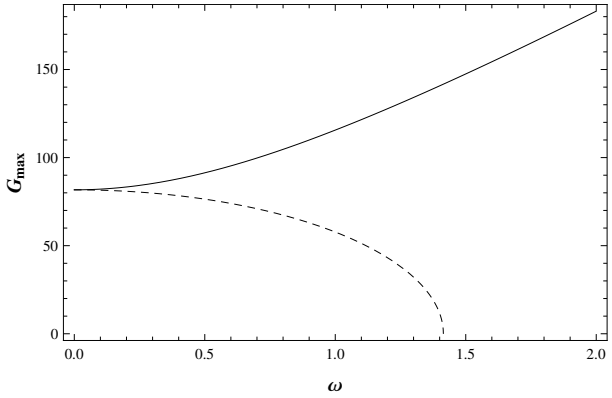

Figure 6.11: Vibrational Resonance position variation with respect to ω for $p = 1$. The plot is obtained using theoretical predictions. The continuous curve shows the variation of resonance position corresponding to the equilibrium state X_0 and dashed curve shows the variation corresponding to the equilibrium states $X_{\pm}$. The parameter settings are: $a = 1.0$, $b = 1.0$, $d = 0.05$, $F = 0.01$, $\Omega = 10.0$

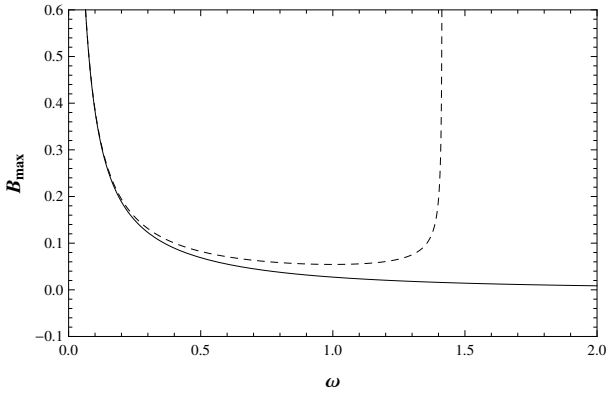

Figure 6.12: Variation of resonance value with respect to ω for $p = 1$. The plot is obtained using theoretical predictions. The continuous curve shows the variation of resonance value corresponding to the equilibrium state X_0 and dashed curve shows the variation corresponding to the equilibrium states $X_{\pm}$. The parameter settings are: $a = 1.0$, $b = 1.0$, $d = 0.05$, $F = 0.01$, $\Omega = 10.0$

linear damping, and $p = 1$, quadratic damping. For linear damping regime, the study vindicated the methodology employed when compared with existing results. The amplitude response shows two resonance peaks corresponding to two equilibrium in the slow dynamics. The two peaks cease to exist as ω is increased to a certain value because of a subcritical pitchfork bifurcation of the equilibrium.

In the quadratic damping regime there are also two resonance peaks till certain ω value. The resonance peaks were also observed to be smaller than the linear case. Moreover, the peak which cease to exist at the cutoff value of ω shows spike which indicates a momentarily zero damping for that peak.

6.3 Summary

Coupled oscillators interact with each other various ways, particularly, through its nonlinearity. Linear oscillators when coupled generate lissajuous figures, representing linear modes, which shows the different loops when the ratio of frequencies of the individual oscillators are integers. In nonlinear oscillators, the nonlinearity interacts with each other in complex manner where higher order interactions are possible. These produce multitude of phenomenons like internal resonance, nonlinear normal modes etc,. These effects are exacerbated when there is external force applied to any one of the oscillator.

These effects were studied in the context of contrasting behaviours of different nonlinear damping regimes. The amplitude phase response of the external force causes destructive

interference of oscillations which gives birth to the phenomenon of antiresonance. In the regular resonance, the amplitude gets peaked around the resonant frequencies. On the other hand, in antiresonance, this peak further go through a pitchfork bifurcation from which rises two peaks with a dip in between the peaks. From the analysis, it was found that the vibration amplitude peaks increases with the damping exponent. This is because the analysis was done with lower order approximation which reduces the effect of damping in the early harmonics terms. This change is accompanied by a reduction in the phase which shows better response of the system to the external force.

Another variant of resonance phenomenon was noticed when two external force with contrasting frequencies is applied to a single oscillator system. This variant is referred as vibrational resonance. In vibrational resonance the resonance is observed not as a function of the applied force frequency but rather as function of the amplitude of the external force. This phenomenon was studied in the context of different damping regimes, similar to the previous study, in a duffing system. The two external forces contains a fast moving force with high frequency and a slow moving force with very low frequency, comparatively. This difference in the motion scale plays a crucial role in the analysis of the system.

The two motion scale drives the system at two different speeds giving rise to high speed and low speed dynamics. For a same time period, the high speed dynamics moves a lot more than the low speed dynamics. Over a period, the slow dynamics perceives only the average behaviour of the fast dynamics. This average behaviour modifies the natural frequency and damping coefficient of the original system which in turn act as regular forced nonlinear oscillator. The modified system is parametrised by the amplitude of the fast moving force. This parametrisation can be seen in the resonance analysis for various damping regimes. The modifications make the damping in the original system vanish for certain parameters which has tremendous application opportunities. For different damping regimes these parameter values vary and also show contrasting behaviour in approaching such values.

These studies are introductory in nature and needs to be followed with more research within the context of various interacting nonlinearities. From the undertaken case studies two major outcomes are found. First is how the dynamics can be studied in multiple time scales which can be seen in both systems. Secondly, in how nonlinearites affects the harmonics of the vibrations.

Bibliography

[1] **Ankan Pandey**. Forced coupled duffing oscillators with nonlinear damping: Resonance and antiresonance. *arXiv preprint arXiv:1909.11390*, 2019.

[2] Ivana Kovacic and Michael J Brennan. *The Duffing equation: nonlinear oscillators and their behaviour*. John Wiley & Sons, 2011.

[3] MJ Brennan, I Kovacic, A Carrella, and TP Waters. On the jump-up and jump-down frequencies of the duffing oscillator. *Journal of Sound and Vibration*, 318(4-5):1250–1261, 2008.

[4] Tamás Kalmár-Nagy and Balakumar Balachandran. Forced harmonic vibration of a duffing oscillator with linear viscous damping. *The Duffing Equation*, 10:9780470977859, 2011.

[5] B Ravindra and AK Mallik. Stability analysis of a non-linearly damped duffing oscillator. *Journal of Sound Vibration*, 171:708–716, 1994.

[6] B Ravindra and AK Mallik. Role of nonlinear dissipation in soft duffing oscillators. *Physical review E*, 49(6):4950, 1994.

[7] Miguel AF Sanjuan. The effect of nonlinear damping on the universal escape oscillator. *International Journal of Bifurcation and Chaos*, 9(04):735–744, 1999.

[8] **Ankan Pandey**, A Ghose-Choudhury, and Partha Guha. Chiellini integrability and quadratically damped oscillators. *International Journal of Non-Linear Mechanics*, 92:153–159, 2017.

[9] F Wahl, G Schmidt, and L Forrai. On the significance of antiresonance frequencies in experimental structural analysis. *Journal of Sound and Vibration*, 219(3):379–394, 1999.

[10] Christian Sames, Haytham Chibani, Christoph Hamsen, Paul A Altin, Tatjana Wilk, and Gerhard Rempe. Antiresonance phase shift in strongly coupled cavity qed. *Physical review letters*, 112(4):043601, 2014.

[11] Borys Lysyansky, Oleksandr V Popovych, and Peter A Tass. Desynchronizing antiresonance effect of m: n on–off coordinated reset stimulation. *Journal of Neural Engineering*, 8(3):036019, 2011.

[12] D Hanson, TP Waters, DJ Thompson, RB Randall, and RAJ Ford. The role of anti-resonance frequencies from operational modal analysis in finite element model updating. *Mechanical Systems and Signal Processing*, 21(1):74–97, 2007.

[13] Walter D'AMBROGIO and A Fregolent. The use of antiresonances for robust model updating. *Journal of Sound and Vibration*, 236(2):227–243, 2000.

[14] R Jothimurugan, K Thamilmaran, S Rajasekar, and MAF Sanjuán. Multiple resonance and anti-resonance in coupled duffing oscillators. *Nonlinear Dynamics*, 83(4):1803–1814, 2016.

[15] Prasun Sarkar and Deb Shankar Ray. Vibrational antiresonance in nonlinear coupled systems. *Physical Review E*, 99(5):052221, 2019.

[16] Roberto Benzi, Alfonso Sutera, and Angelo Vulpiani. The mechanism of stochastic resonance. *Journal of Physics A: mathematical and general*, 14(11):L453, 1981.

[17] PS Landa and Peter VE McClintock. Vibrational resonance. *Journal of Physics A: Mathematical and general*, 33(45):L433, 2000.

[18] Shanmuganathan Rajasekar, K Abirami, and Miguel Angel Fernandez Sanjuan. Novel vibrational resonance in multistable systems. *Chaos: An Interdisciplinary Journal of Nonlinear Science*, 21(3):033106, 2011.

[19] Jesús Casado-Pascual and José Pablo Baltanás. Effects of additive noise on vibrational resonance in a bistable system. *Physical Review E*, 69(4):046108, 2004.

[20] Wang Can-Jun. Vibrational resonance in an overdamped system with a sextic double-well potential. *Chinese Physics Letters*, 28(9):090504, 2011.

[21] JH Yang and XB Liu. Controlling vibrational resonance in a multistable system by time delay. *Chaos: An Interdisciplinary Journal of Nonlinear Science*, 20(3):033124, 2010.

[22] C Jeevarathinam, S Rajasekar, and MAF Sanjuan. Theory and numerics of vibrational resonance in duffing oscillators with time-delayed feedback. *Physical Review E*, 83(6):066205, 2011.

[23] Bin Deng, Jiang Wang, Xile Wei, Haitao Yu, and Huiyan Li. Theoretical analysis of vibrational resonance in a neuron model near a bifurcation point. *Physical Review E*, 89(6):062916, 2014.

[24] TO Roy-Layinde, JA Laoye, OO Popoola, and Uchechukwu Enyim Vincent. Analysis of vibrational resonance in bi-harmonically driven plasma. *Chaos: An Interdisciplinary Journal of Nonlinear Science*, 26(9):093117, 2016.

[25] VN Chizhevsky and Giovanni Giacomelli. Experimental and theoretical study of vibrational resonance in a bistable system with asymmetry. *Physical Review E*, 73(2):022103, 2006.

[26] VN Chizhevsky, Emil Smeu, and G Giacomelli. Experimental evidence of "vibrational resonance" in an optical system. *Physical review letters*, 91(22):220602, 2003.

[27] JP Baltanás, L Lopez, II Blechman, PS Landa, A Zaikin, J Kurths, and MAF Sanjuán. Experimental evidence, numerics, and theory of vibrational resonance in bistable systems. *Physical Review E*, 67(6):066119, 2003.

List of Corrections

Page no.	Previously	Corrected	Remark
2	..newtonian mechanics..	..Newtonian mechanics..	Editing
14	.*flows*..	.*Flows*..	Typo
74	..Matignon [8].	..Matignon [32].	Reference number
75	..theorem(2)..	..theorem 5.1.1..	Theorem reference
Throughout	Functions used in equations as texts, example $cos(x)$	Functions changed to latex format, example $\cos x$	Latex formatting of mathematical functions

Table 6.1: List of corrections.

List of possible corrections has been given in table 6.1. Further remark is due on the styling of each chapter which shows variations across chapters. Chapters included in the thesis covers topics by considering different case studies and hence are subjected to different circumstances/arrangements in the explanation. However, a possible common theme has been tried to be implemented across the chapters.